Covalent Monolayers

DOI: 10.1002/anie.201306709

Covalent Surface Modification of Oxide Surfaces

*Sidharam P. Pujari, Luc Scheres, Antonius T. M. Marcelis, and Han Zuilhof**

Keywords:
covalent bonds · monolayers · oxides · reaction mechanisms · surface chemistry

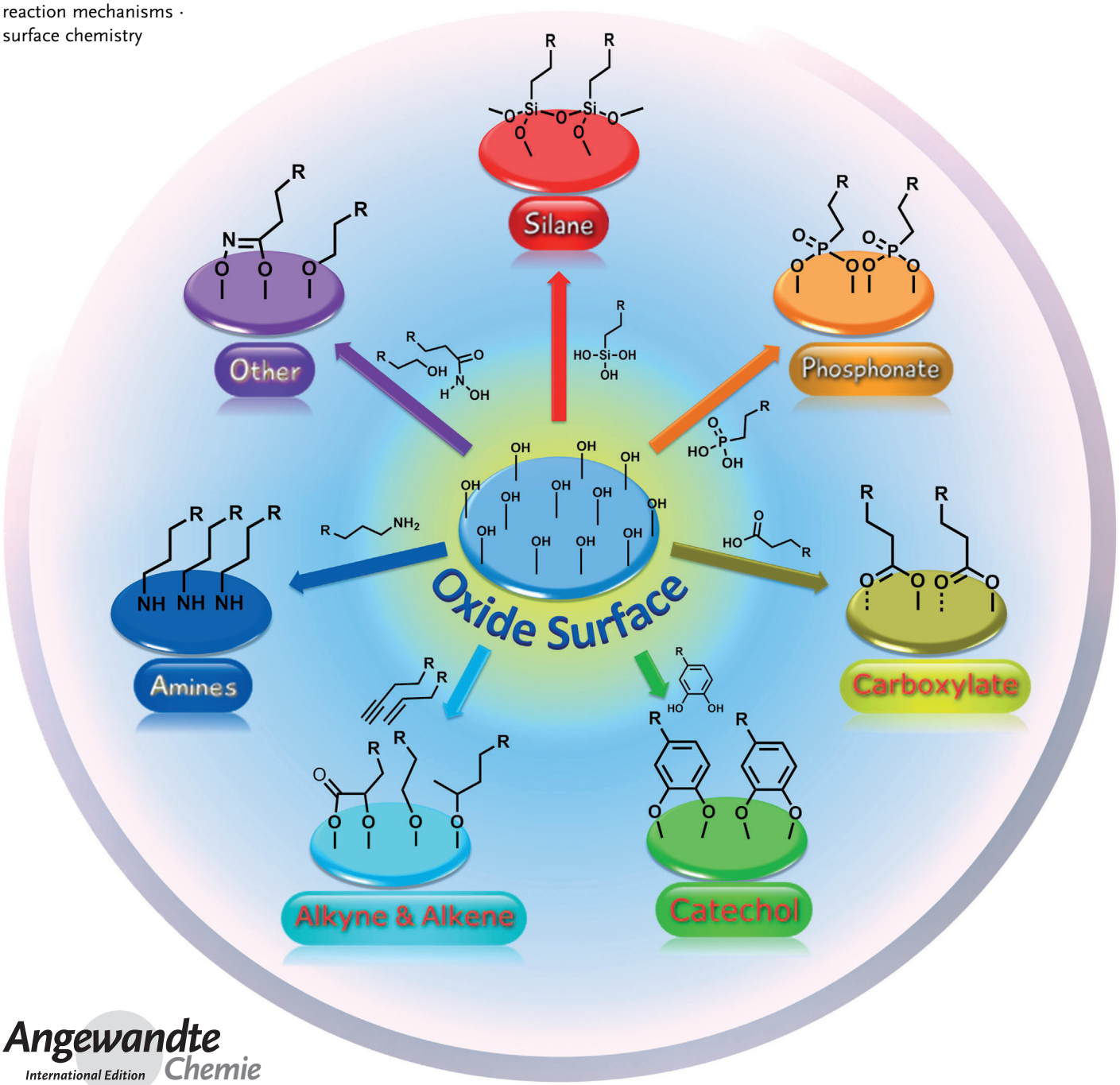

The modification of surfaces by the deposition of a robust overlayer provides an excellent handle with which to tune the properties of a bulk substrate to those of interest. Such control over the surface properties becomes increasingly important with the continuing efforts at downsizing the active components in optoelectronic devices, and the corresponding increase in the surface area/volume ratio. Relevant properties to tune include the degree to which a surface is wetted by water or oil. Analogously, for biosensing applications there is an increasing interest in so-called "romantic surfaces": surfaces that repel all biological entities, apart from one, to which it binds strongly. Such systems require both long lasting and highly specific tuning of the surface properties. This Review presents one approach to obtain robust surface modifications of the surface of oxides, namely the covalent attachment of monolayers.

From the Contents

1. Introduction

Roughly speaking there are two approaches towards surface modification: the attachment of (self-assembled) monolayers (SAMs),[1] and the deposition of polymeric or multi-layers.[2] Both approaches have their own advantages and disadvantages. Monolayers typically provide more molecular control, but display a lower degree of chemical and mechanical robustness. This situation is most evident in the best studied SAMs, namely those of thiols on gold.[3] The Au–S bond formation allows for an easy functionalization, with excellent control over the monolayer structure, which has induced a tremendous amount of applications. However, if monodentate ligands are used, the resulting structure typically does not withstand even simple wiping with cotton wool, a result of the relatively weak Au–S bond. More stable monolayers can therefore be formed if stronger covalent bonds are involved. Recent examples include the formation of C–C bound monolayers on diamond,[4] and of Si–C bound monolayers on oxide-free silicon.[5] While probably the most stable ones,[6] formation of these monolayers typically requires some activation energy, or otherwise specifically synthesized reactive moieties if reactivity at room temperature is desired.[7]

Intermediate stabilities have been observed for a whole range of readily made monolayers on oxides, and these are the focus of this Review. With oxides we will refer to the whole class of materials that can be indicated as MO_x, in which M can be a metal (e.g. Al, Fe, Cr), semiconductor (e.g. Si), or a material that has an oxygen-free bulk but forms surface-bound hydroxy (-OH) groups in air or upon some activation reaction (e.g. on SiC or CrN). Oxides are appealing, as they are typically not only easily accessible and thermodynamically stable, but also can be easily prepared in a wide variety of nanometer-sized structures. Although oxides can differ tremendously in almost any property of interest (such as, mechanical stability, chemical stability, hardness, conductivity, heat transport, cost), many of them share the potential for surface functionalization through the reactivity of surface-bound -OH groups as anchoring points for the formation of densely packed monolayers. In principle, activation can be obtained in a variety of ways. Three of these stand out in terms of the frequency of their use on a lab scale, namely wet etching, dry etching, and plasma activation. Optimum activation methods vary per oxide, but in many cases activation methods have been developed that allow the use of a wide range of attachment chemistries. The structures of various oxides has recently been reviewed in detail, including the possible structures of reactive oxygenates on several oxides.[8]

The Review is divided into the following topics: we give an overview of different attachment chemistries that have been used to covalently attach organic monolayers onto oxides. Six attachment chemistries will be dealt with in detail: silanes (Section 2), phosphonates (Section 3), carboxylates (Section 4), catechols (Section 5), alkenes/alkynes (Section 6) and amines (Section 7). In addition, several other, less-frequently used attachment chemistries will be discussed (Section 8; see Figure 1). We will describe the mode of reaction and resulting structures, and focus on those aspects that make specific attachment chemistries interesting (e.g. a high reaction rate, ease of application, possibility to include photopatterning, high stability of resulting monolayers). Then we outline some characteristic advantages and limitations of each of these approaches. The goal is to summarize the

[*] Dr. S. P. Pujari, Dr. A. T. M. Marcelis, Prof. Dr. H. Zuilhof
Laboratory of Organic Chemistry, Wageningen University
P.O. Box 26, 6703 HB Wageningen (The Netherlands)
E-mail: han.zuilhof@wur.nl
Dr. L. Scheres
Surfix B.V.
Dreijenplein 8, 6703 HB Wageningen (The Netherlands)
Prof. Dr. H. Zuilhof
Department of Chemical and Materials Engineering
King Abdulaziz University
Jeddah (Saudi Arabia)

Dateiname: A306709e
Pfad: L:/daten/Verlage/VCH/ACH/Hefte/1425/
Status Neusatz
Datum: 24 KW., 11. Juni 2014 (Mittwoch)
Pagina: 6323
Seite: 2 te von 35
Umfang (Seiten): 35
Zeit: 9:22:50 Uhr

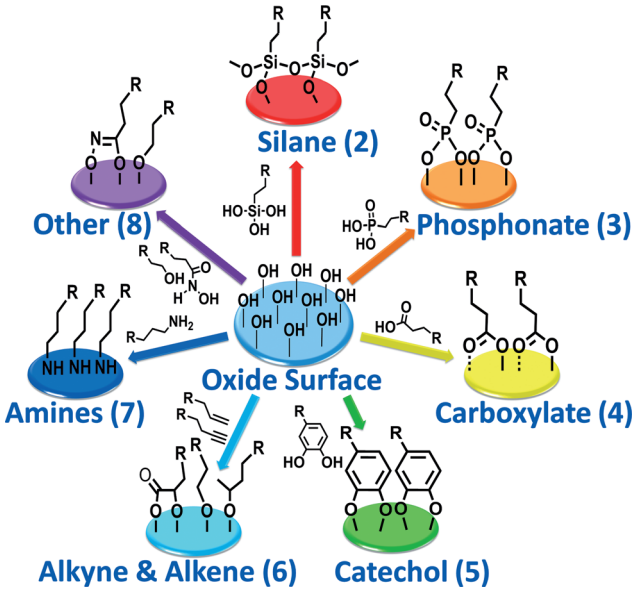

Figure 1. Attachment methods and the resulting modified oxide surfaces (the number in parentheses designates the Section in which a particular chemistry is discussed).

chemistries in such a way that characteristic features are brought out—several of these fields (e.g. silanes on silicon oxides) are so extensive that they have already been the subject of Reviews,[9] so the focus is not on comprehensiveness but on characteristics.

A summarizing Table in the final paragraph shows some characteristic features of each type of attachment chemistry on each oxide under study. Although admittedly oversimplifying, such a Table might help the reader to select an optimal monolayer/surface combination for her/his own purposes. We end the Review with some recent trends, features that we thought were remarkable and opportunities of this field in both mechanistic and application-oriented terms.

2. Silanes

2.1. Reagents and Structure

Surface modification with alkylsilanes is one of the most commonly used methods to prepare monolayers on oxides. Reactions of organosilanes ($RSiX_3$, R_2SiX_2, or R_3SiX, where R is an alkyl group and X is a leaving group, such as chloride, alkoxy, or hydride) with OH-bearing surfaces have found use in widely diverse areas.[9c,10] The main advantage of using silanes for monolayer formation on oxidic surfaces is the rapid formation of a covalent linkage between the substrate and the anchoring group. This covalent bond stabilizes the monolayer, and also allows for easy further chemical modification without compromising the integrity of the monolayer.[11] The properties of these films, that is, chemical composition, thickness, orientation, and lateral order of the alkyl chains have been investigated in detail, and on a wide range of surfaces, such as silica, aluminum oxide, and zinc oxide. (Figure 2).[9c,12,13] Excellent substrates for modification are

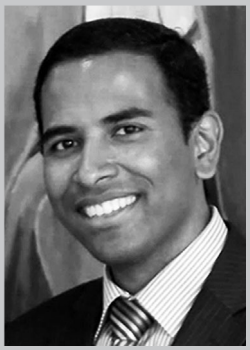

Sidharam P. Pujari received a B.Sc. in Chemistry at the Shivaji University, India and an M.Sc. at the University of Pune, India. He worked at the National Chemical Laboratory in Pune, India, and at the National Taiwan University Science and Technology, Taipei (NTUST) with Prof. Der-Jang Liaw. With Prof. Zuilhof, he recently finished his Ph.D. thesis on covalently bound fluorinated monolayers on silicon and oxide surfaces. He is currently pursuing postdoctoral studies with Prof. Zuilhof in the field of surface/materials chemistry.

Luc Scheres is the CEO of Surfix BV. In 2005 he received his M.Sc. degree in Chemistry and Physics at Utrecht University. Subsequently Luc moved to Wageningen University and obtained his Ph.D. degree with Professor Prof. H. Zuilhof in 2010. After a post-doc at the Technical University of Eindhoven with Professor A. Schenning, he started Surfix BV.

Antonius T. M. Marcelis obtained his Ph.D. in 1982 with J. Reedijk at Leiden University. In the same year he moved to Wageningen University, where he is now an assistant professor in Organic Chemistry. His research interests include organic synthesis, supramolecular chemistry, and physical–organic chemistry.

Han Zuilhof obtained both an M.Sc. in Chemistry and an MA in Philosophy. After a Ph.D. in Chemistry (Leiden University, 1994; with Prof. J. Cornelissen), and postdoctoral work at the University of Rochester with Profs J. P Dinnocenzo and S. Shaik, and Columbia University with Profs N. J. Turro and J. K. Barton he joined the faculty at Wageningen University where has been Professor of Organic Chemistry since 2007. He is the founder of Surfix, serves on the Editorial Advisory Boards of several journals. His interests focus on surface-bound (bio-)organic chemistry and bionanotechnology and loves watching cloudless night skies.

Dateiname: A306709e
Pfad: L:/daten/Verlage/VCH/ACH/Hefte/1425/
Status Neusatz
Datum: 24 KW., 11. Juni 2014 (Mittwoch)

Pagina: 6324
Seite: 3 te von 35
Umfang (Seiten): 35
Zeit: 9:22:50 Uhr

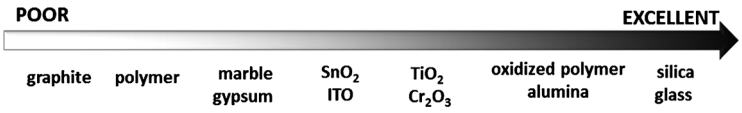

Figure 2. Effectiveness of silane modification of various inorganic substrates. ITO = indium tin oxide.

surfaces containing Si-OH surface groups, but metal oxide surfaces are typically also good substrates.

For surface modification with silanes two approaches can be used: reactions in solution or in the vapor phase. In solution-phase reactions, typically at room temperature, critical factors are the solvent viscosity and polarity, and the amount of water in the liquid medium to hydrolyze the silane molecules. For vapor-phase modification, the surface is usually exposed to a silane for several hours or days at elevated temperatures (50–120 °C). Denser (i.e. more closely packed) monolayers are formed under vapor-phase conditions than under solution-phase conditions.[14] Despite extensive research devoted to this field, uniform silane monolayers are still difficult to obtain.[9b]

For optimal ease of use in combination with short reaction times, chlorosilanes and methoxysilanes are advocated, as highly reactive and moderately reactive monolayer-forming agents, respectively. Better leaving groups (e.g. X = I) give rise to extensive multilayer formation.[15] Worse leaving groups (e.g. R = H) might have several advantages (for R = H the by-product is H_2 gas, which provides a clean reaction environment),[16] but might sometimes, of course, not be sufficiently reactive. Since they only differ in the leaving group, the monolayer structure is, in principle, the same. This structure is affected by the number of reactive leaving groups, for which typically one or three are used, as in $R(CH_3)_2Si$-X and R-SiX_3. Both give rise to characteristic features in the resulting monolayer structure.

The key step in the reaction mechanism (see Section 2.4 for details) is the reaction with water adsorbed on the surface of the metal oxides, first generating silanol groups. Monofunctional organosilanes (R_3SiX, and typically: $R(CH_3)_2SiX$) having only one hydrolysable group (leaving group) in the molecule (usually X = Cl, OR, NMe_2) are attractive in terms of the reproducibility of the resulting surface structures, because only one type of grafting bond ($Si_{surface}$-O-Si_{silane}) is possible for the covalent attachment to the surface. The main limitation of this kind of silane modification is the lower surface coverage, limited by the size of the dimethylsilyl group, as this "sticks out" of the monolayer: the cross-sectional area of alkyldimethylsilyl groups in a densely packed monolayer is 32–38 Å^2, which is up to twice the area of an *n*-alkyl chain. Trifunctional oganosilanes do not suffer from this added steric bulk, but have as a characteristic feature that all three leaving groups can react. This yields the intra-monolayer cross-linking that increases the stability, but typically also oligomerization (homocondensation) in solution prior to or simultaneous with covalent attachment, leading to disordered structures (see also Figure 6 in Section 2.4, for mechanistic details).[17]

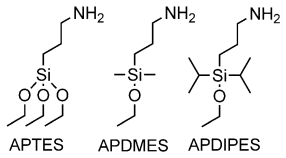

Figure 3. Bulky monofunctional silanes, such as APDIPES, improve the monolayer stability compared to the reference substances APTES and APDMES.[18]

Apart from the number of reactive groups, also the precise molecular structure of the silane influences the stability of the resulting monolayer, as shown by Linford's group with the significantly increased hydrolytic stability of adsorbed aminosilanes when bulky, hydrophobic side groups are attached to the silane.[18] The bulky silane APDIPES has only one reactive group (Figure 3), preventing polymerization even at higher concentrations (whereas this might happen with the frequently used APTES).

2.2. Silane Monolayer Formation from Solution

Since Sagiv's first report on the preparation of silane monolayers from the solution phase,[12c] much research has been devoted to further develop various methods.[9c] Probably the current standard to most reproducibly and rapidly (seconds to minutes) obtain silane SAMs is the immersion of a clean, freshly prepared polar substrate in a fresh millimolar solution of the long-tail trichlorosilane precursor in dry, purified bicyclohexane (C_6H_{11}–C_6H_{11}).[12d,19] The silane concentration is crucial, as confirmed by Zhang et al. with the polar *N*-(2-aminoethyl)(3-aminopropyl)trimethoxysilane (EDA) at various silane concentrations and temperatures as shown in Figure 4.[20]

Anhydrous solvents are typically required for trichlorosilanes, although the presence of some adsorbed water on the

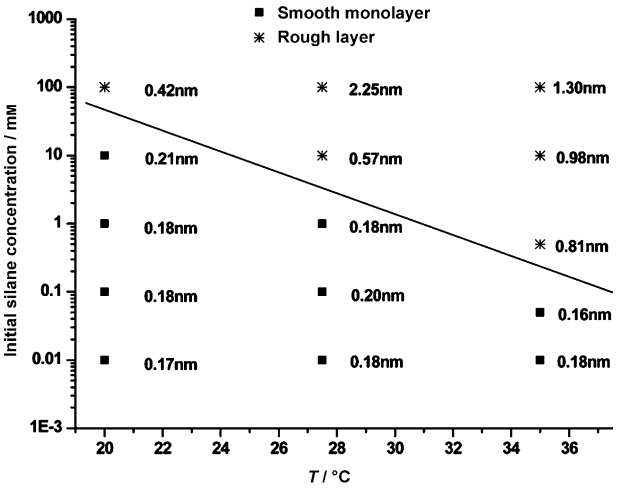

Figure 4. Roughness of EDA layers grown at various temperatures and concentrations. The number next to the measured point is the root mean square (rms) value of the EDA layer grown at that condition. The separation line between smooth and rough layers is a guide for the eye.[20]

Dateiname: A306709e
Pfad: L:/daten/Verlage/VCH/ACH/Hefte/1425/
Status Neusatz
Datum: 24 KW., 11. Juni 2014 (Mittwoch)
Pagina: 6325
Seite: 4 te von 35
Umfang (Seiten): 35
Zeit: 9:22:51 Uhr

surface is essential to obtain a smooth monolayer.[21] It was found that when the water content is very low, incomplete monolayers are formed; however, too much water results in silane polymerization in the bulk solvent phase and roughening of the resulting layer.[12d,14b,19a,b,22] There is extensive, and not fully consistent literature on this topic. Sagiv's group has suggested[12d,19a–c] that bicyclohexane is an ideal solvent, thanks to its high surface tension, low volatility, and low propensity for solubilization of water and polar monolayer-forming species generated at the solid–liquid interface upon the hydrolysis of chlorosilane precursor molecules. In addition, its geometry makes it incompatible with incorporation in the alkyl tail region of a densely packed monolayer.[12d,19a–c] However, many alternatives have been advocated. Heptane,[14c] toluene, cyclohexane, benzene, hexadecane,[23] are among the solvents used.[22a] Typically, the optimal water concentration was found to be 0.15 mg of water in 100 mL of solvent.[22a] Solvents with a high or very low capacity for dissolving water (e.g. 1,4-dioxane, CH_2Cl_2, or $CHCl_3$,[22b,23] or pentane, respectively) are not ideal, as they may overstabilize the alkyltrisilanol species and promote polymerization onto the substrate surface, or cannot supply sufficient water to produce the optimal amount of alkyltrisilanol. Anac et al. observed that the presence of ethyldiisopropylamine facilitates the covalent attachment of chlorosilanes to the surfaces by neutralizing the HCl that is formed during the attachment, without silylation of the amine which occurs when less sterically congested amines are used.[14c]

Other factors also influence the monolayer quality, such as the chain length of the alkyl moiety,[24] and both post-formation annealing[25] and pre-annealing of the silicon oxide (SiO_2) produce significant improvements in the quality of the film and a smaller number of unreacted sites.[26]

Recently, Cao et al. developed a new strategy to fabricate patterned organosilane films onto inorganic substrates using 254 nm irradiation.[27] They observed the formation of a silane monolayer within several minutes at ambient temperature using a silane in the presence of *N*,*N*-dimethylformamide (DMF). They proposed that the carbonyl group of DMF absorbs the UV light and subsequently dissociates, producing the base $HN(CH_3)_2$, which can diffuse to the surface and there promotes the hydrolysis of the silane and subsequent connection to the glass surface.[27]

2.3. Silane Monolayer Formation from the Vapor Phase

In most cases silane films prepared from solution show morphological irregularities that limit the effectiveness of the monolayer for potential technological applications.[28] Vapor-phase deposition is therefore an alternative, as first described by Haller.[29] Monolayer deposition from the vapor phase is attractive because of the decreased formation of siloxane oligomers and contamination of the surface by particles,[30] and turns out to be a highly effective and reproducible method for producing high-quality monolayers.[17a,18,31] In fact, the limited experience of many chemists with gas-phase reactions, rather than problems with features of the chemistry itself, seems a limiting factor here. Chidsey and co-workers investigated a new method of vapor deposition of siloxane monolayers at 110 °C under reduced pressure (1 Torr), using water from the dehydration of $MgSO_4 \cdot 7H_2O$, and the vapor of $CH_3(CH_2)_{13}Si(CD_3O)_3$ (Figure 5). IR spectroscopy revealed the initial presence of unhydrolyzed OCD_3 groups, which disappear with excess silane and water to obtain dense and

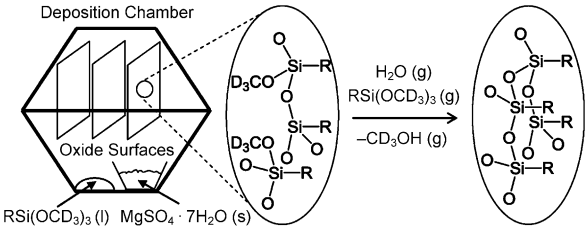

Figure 5. CVD-based synthesis of siloxane monolayers onto oxide surfaces, starting from silanes and $MgSO_4 \cdot 7H_2O$. Middle: An incomplete monolayer with unhydrolyzed methoxy groups. Right: a dense, completely hydrolyzed monolayer on the right.[31b]

optimally bound monolayers.[31b] Supercritical CO_2 has also been used as medium for silane SAM formation.[32]

2.4. Mechanism of Silane SAM Formation

An analysis of the extensive literature data leads to the following three-step mechanism for the formation of monolayers from $RSiX_3$-type silanes (X = Cl, OCH_3; Figure 6). In the first step, organosilanes are hydrolyzed by water molecules that are already adsorbed on the polar oxide surface, to create the corresponding hydroxysilane (typically $RSi(OH)_3$). In the second step, extensive lateral ordering takes place: these hydroxysilanes are hydrogen bonded to the polar oxide surface, but still capable of moving laterally across the surface. This yields aggregation driven by attractive forces such as van der Waals forces between the pendant hydrocarbon chains, hydrogen-bonding, dipole–dipole interactions. Once aggregated, these monomer molecules become significantly less mobile. Finally, condensation occurs between the Si-OH groups to form Si–O–Si bonds, not only with the surface -OH groups, but also with neighboring silanol groups. In this way a cross-linked network between the silanes is formed that also contains many covalent bonds with the underlying substrate.

The initial hydrolysis of Si–Cl or Si–OR bonds thus generates the hydroxysilane that makes self-assembly possible.[33] This step is probably the most critical and controls the final quality and morphology of the SAM. The frequently experienced difficulties in reproducibly making high-quality monolayers relate to this step, as incomplete hydrolysis or excessive hydrolysis result in incomplete monolayers or formation of polysiloxanes on the surface, respectively. This also means that surfaces that do not contain adsorbed water molecules react poorly,[16a] like metal oxides without -OH groups, or silicon, carbon, and organic polymers, which explains their position on the silane reactivity scale indicated in Figure 2. If an insufficient density of surface -OH groups is

Dateiname: A306709e
Pfad: L:/daten/Verlage/VCH/ACH/Hefte/1425/
Status Neusatz
Datum: 24 KW., 11. Juni 2014 (Mittwoch)
Pagina: 6326
Seite: 5 te von 35
Umfang (Seiten): 35
Zeit: 9:22:51 Uhr

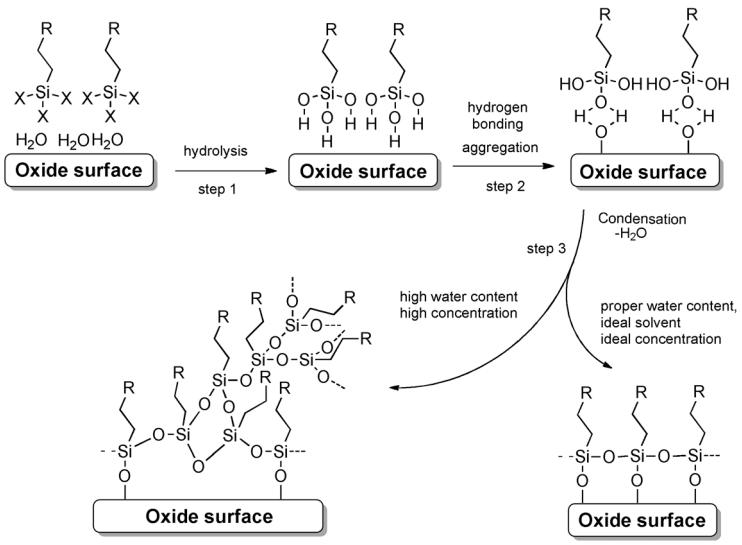

Figure 6. Three-step mechanism for monolayer formation by silanes on OH-terminated surfaces. Note in Step 3, condensation ideally proceeds to form a covalently bound monolayer that is also laterally cross-linked (bottom right), but insufficient control over the water content and other reaction conditions may yield disordered inhomogeneous multilayers (bottom left).

a problem, then plasma activation will form sufficient hydroxy moieties for the formation of highly stable high-quality monolayers, even on plastics such as poly(methylmethacrylate (PMMA) and polystyrene.[34]

2.5. Characterization and Application of Silane SAMs

The different ways in which silanes can be bound to the surface can be distinguished by a variety of techniques. Residual chloride or methoxide moieties would typically be recognizable by for example, IR[31b] or X-ray photoelectron spectroscopy (XPS). For the direct observation of the interfacial Si–O bond formation, IR spectroscopy has been shown to be especially useful. SAM formation on SiO_x can be monitored by the longitudinal optical (LO) absorption band that arises from the vibrations perpendicular to the surface of Si–O bonds at the SAM/SiO_2 interface. In particular, this analysis of the 950 to 1255 cm^{-1} range that includes surface-bound and internally cross-linked Si-O-Si vibrational modes,[26,35] can distinguish between silanes that form a strong chemisorbed bond to the surface and weakly adsorbed polysilanols.[35b,36] In particular, both the precise position and intensity of this LO band around 1200–1255 cm^{-1} can be used to estimate the development of the monolayer.[35b] This technique has for example, been used by Aissaoui et al to study the formation of APTES layers .[37]

Chemical functionalization of oxide surfaces with silane molecules has become an important technique for the fabrication of a variety of devices.[12b,38] Two different strategies have been used to obtain a wide variation in surface groups and properties using silanes. First, silanes can be used that already have the required terminal group at the end of the alkyl chain. Alternatively, the finally required terminal groups can be obtained by a chemical reaction on the end group of an already formed silane surface layer.[9a,39] Both approaches are currently widely used in both industrial and research-oriented applications. For example, APTES[40] is commonly used to obtain amine-terminated surfaces that are applied for promoting protein adhesion and cell growth on biological implants[41] and in lab-on-a-chip applications.[42] Other terminal functional groups, such as alkenes or carboxylic acids, have been used to attach a range of biomolecules.[43] To obtain surfaces with enhanced water- and oil-repellent properties, fluorinated silanes are often used to modify both flat and nano-textured surfaces. There are several examples of highly scalable silane-based modifications to make materials more durable. Walker et al. showed that conformal surface modification of calcite using SAMs of natural fatty acids combined with sub-monolayer fluorinated alkylsilanes generated hydrophobic (HP) and superhydrophobic (SHP) coatings to increase limestone resistance to sulfation, for the protection of historic buildings from acid rain.[44] Analogously, Deng et al. have used silanization of calcinated soot as a simple means to create superamphiphobic surfaces,[45] while a nanocomposite of silanized silica nanoparticles and hexadecyltriethoxysilane was recently used to obtain robust superhydrophobically coated textiles.[46] Making use of the high reaction rate of silanes, inkjet printers were used to obtain a SAM pattern with (115 ± 5) μm features. Contact times in the order of hundred milliseconds are sufficient to form a pattern of (inhomogeneous) self-assembled octadecyltrichlorosilane (OTS) monolayers (Figure 7).[47]

While silane-based monolayers are thus shown to be of great value, two aspects might hamper their use: reproducibility and hydrolytic stability. The frequently noticed poor reproducibility in preparing silane-based monolayers is linked to the sensitivity of the reaction towards reaction conditions. Secondly, the limited hydrolytic stability has been reported to be a critical issue.[22b,37,48] Fadeev et al. showed that OTS monolayers were hydrolyzed almost completely on both TiO_2 and ZrO_2 within 3–24 h, even at neutral pH value and 25 °C. Acidic and basic solutions hydrolyze the monolayers even

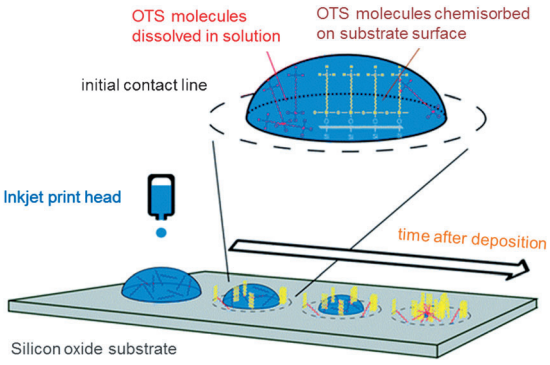

Figure 7. Principle of growing OTS monolayers from inkjet-deposited sessile droplets.[47]

Dateiname: A306709e
Pfad: L:/daten/Verlage/VCH/ACH/Hefte/1425/
Status Neusatz
Datum: 24 KW., 11. Juni 2014 (Mittwoch)
Pagina: 6327
Seite: 6te von 35
Umfang (Seiten): 35
Zeit: 9:22:51 Uhr

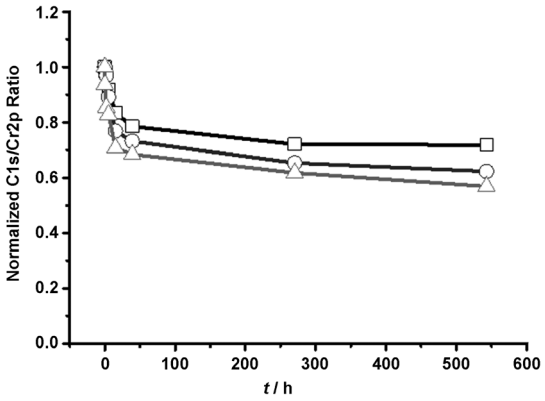

Figure 8. XPS-derived desorption kinetics of monolayers of OTS on CrN surfaces in deionized water (□), at pH 3 (○), and at pH 11 (△).[50]

faster.[49] Analogously, Pujari et al. showed in a comparative study of various attachment chemistries that silane monolayers on hydroxy-terminated CrN surfaces are unstable in aqueous media of various pH values (Figure 8).[50] If monolayers of higher stability are desired, then those derived from alkyl phosphonates (Section 3), catechol (Section 5), and alkenes/alkynes (Section 6) are typically more promising. Aureau et al. have used silane-based monolayers for the deposition of Au nanoparticles, but showed that the performance of Si-C linked monolayers was clearly superior to this.[35c] Chabal and co-workers subsequently showed that simultaneous use of OTS and alkenes to selectively react with a field-effect transistor (FET) device that has both SiO_x- and H-terminated Si areas actually works well, and yields the desired spatial selectivity.[35a]

3. Phosphonates

3.1. Reagents and Methods

Since the seminal work of Ries and Cook,[51] phosphonic acids [R-PO_3H_2] and their phosphonate ester derivatives [R-PO_3R_2] (R = alkyl, sometimes aryl, Figure 9) have become an attractive anchoring group for hydroxylated surfaces. Despite the vast amount of literature on phosphonate-based metal–organic frameworks (MOFs), also called metal phosphonates,[52] the usage of alkyl phosphonates for monolayer assembly is still developing. The most common technique to obtain alkyl phosphonate-based monolayers is immersion or dip coating, that is, liquid-phase reaction conditions, with immersion times lasting from a few minutes to a couple of hours or even days.[53] Because both phosphonic acids and

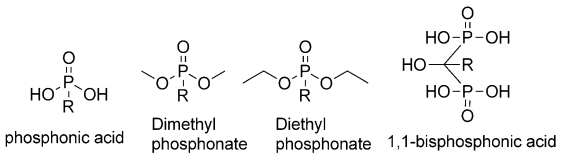

Figure 9. Commonly used phosphonate-derived acids and esters.

phosphonate esters have the ability to self-assemble onto and react with inorganic substrates, a wide variety of solvents can be used, including water.[54] The use of water might be of interest for phosphonic acids which have limited solubility in non-aqueous solvents; however, this is only feasible when the metal oxide is stable and insoluble in the aqueous solution.[52a,55] On the other hand, also when using organic solvents, the choice of solvent is of considerable importance for the quality and stability of the final monolayer. Specifically, a study of solvent effects during alkyl phosphonic acid assembly on ITO concluded that low dielectric solvents and therefore with weak or negligible interactions with the oxide surface promote denser, more stable monolayers in comparison with high dielectric, that is, strongly interacting solvents.[54c]

In general, immersion-based surface modification works well and reproducibly on a wide variety of oxidic substrates, however, some problems might arise when modifying silicon oxide.[56] On SiO_x phosphonic acids only aadsorb by means of weak physical interactions, such as van der Waals interactions and hydrogen bonding, and therefore can easily be washed off. To overcome this problem Hanson et al and Thissen et al.[56] introduced the so called "T-BAG" (tethering by aggregation and growth) method. This approach includes the self-assembly of a weakly physisorbed alkyl phosphonate on a vertical SiO_2 substrate by slow evaporation of solvent, and a subsequent thermal annealing step at 140 °C under low-humidity conditions to induce chemisorption of the phosphonic acids onto the SiO_2 (Figure 10).[56b] An alternative is

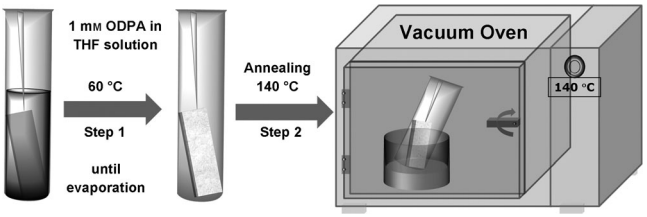

Figure 10. Schematic representation of the T-BAG process.[56b]

spin coating of octadecylphosphonic acid (ODPA) onto mica and aluminum.[57] By using the appropriate nonpolar solvents, the interaction between the phosphonic acid headgroup and the hydrophilic substrate can be enhanced, producing full-coverage monolayer coatings in minutes. Note that, also in this case, the process strongly depends on the dielectric constant of the solvent used, which is preferably around 4 (e.g. trichloroethylene), whereas polar solvents, such as ethanol, hamper monolayer formation and might induce liquid-like multilayers or aggregates.[56a,58] Although several methods produce uniform monolayers, in most cases a final thermal annealing step is required to induce covalent bonding, that is, heterocondensation with the oxidic substrates. To decrease the number of processing steps and time, Graham et al.[59] explored spraying of pentafluorobenzyl phosphonic acid onto heated oxide surfaces. The process relies on the generation of small liquid droplets that impinge on the heated oxide inducing evaporation of the solvent, and deposition of the

Dateiname: A306709e
Pfad: L:/daten/Verlage/VCH/ACH/Hefte/1425/
Status Neusatz
Datum: 24 KW., 11. Juni 2014 (Mittwoch)

Pagina: 6328
Seite: 7 te von 35
Umfang (Seiten): 35
Zeit: 9:22:52 Uhr

phosphonic acid molecules. This simultaneously initiates the formation of covalent linkages with the substrate, making an additional thermal curing step superfluous.

An alternative approach to overcome the weak physical interactions between the phosphonic acid precursor and SiO_x, involves the deposition of an ultrathin layer of aluminum oxide/hydroxide to promote phosphonic acid binding.[60] With differential IR spectroscopy the condensation reaction of octadecylphosphonic acid onto this aluminum oxide/hydroxide substrate was monitored by the loss of the Al-O-H deformation mode (840 cm^{-1}), and the appearance of the Al-O-P stretching vibration (1080–1140 cm^{-1}; see Figure 14 in Section 3.2).

In addition to the abovementioned wet-chemical reaction conditions, also "dry" vapor-phase reactions have been reported, for example, for phenylphosphonic acid on amorphous alumina.[61] At high deposition rates (> 0.05 ML min^{-1}; ML = monolayers) multilayers were formed, whereas at lower rates monolayer coverage was obtained. On the other hand, octylphosphonic acid also has the tendency to form multilayers under vapor-phase conditions,[60b] but those physisorbed molecules could be removed by prolonged thermal desorption, finally leaving solely the covalently bound monolayer, as demonstrated by its thickness and excellent electronic properties.

3.2. Mechanism and Binding Modes

The mechanism of chemisorption of phosphonic acids on metal oxide substrates is greatly affected by reaction conditions, such as temperature, pH value, concentration and solvent, and the type of oxide. On Lewis acidic metal oxide surfaces, binding originates from initial coordination of the phosphoryl oxygen atom (P=O) to a Lewis acidic site on the surface. As a consequence, the P atom becomes more electrophilic and induces the consecutive heterocondensation with the neighboring surface hydroxy groups, resulting in strong covalent P-O-M anchoring (Figure 11, Route 1).[52a,54a,62] On metal oxides lacking Lewis acidity it is generally accepted that the coordination of the phosphoryl oxygen is minimal and initial hydrogen bonding promotes the heterocondensation reaction (Figure 11, Route 2); a reaction that might be accelerated by heat treatment as this could increase the deprotonation rate of the P-OH moiety.[52a,54a,62] That also phosphonate esters undergo these heterocondensation reactions under these mild immersion-based conditions is somewhat remarkable as in solution the hydrolysis of the P–O–C bonds requires relatively harsh conditions, but is probably catalyzed in the same manner.[62a,63] In all cases the surface density of the hydroxy groups is a key parameter, as confirmed by the work of Giza et al.: by applying a water plasma prior to modification, the number of surface hydroxyl groups on oxide-covered aluminum was substantially increased and yielded considerably accelerated adsorption of octadecyl phosphonic acid (ODPA).[64]

Like the assembly mechanism, also the final binding modes of the phosphonates depend on the nature of the oxide substrate, as well as on the applied reaction conditions, for example, thermal annealing. The presence of three oxygen atoms on the phosphonates allows mono-, bi-, and tri-dentate binding modes in combination with possible electrostatic and hydrogen-bonding interactions. In addition, all three oxygen atoms can also bind to the same metal site (chelation) or bind to different metal atoms on the surface.[65] An overview of the resulting complexity in binding modes is depicted in Figure 12.

To better understand the binding modes of phosphonic acids, Mutin et al. made use of high-field ^{17}O magic-angle spinning (MAS, 24 h at 17.6 T) NMR to study the binding of ^{17}O-enriched phosphonic acids deposited on a titania anatase support (Figure 13).[65,66] The clear resonance signal at $\delta =$ 185 ppm provides direct evidence for the formation of the P-O-Ti linkage, while the two neighboring resonance signals at high field correspond to residual P=O and P–OH functionalities, suggesting the existence of multiple binding modes.[65] In addition, Spiess et al. made use of ^1H MAS NMR spectroscopy to investigate the surface H-bonding interactions of carboxylic acid-terminated phosphonates on zirconia and titania, and untangled the H-bonding interactions among the P-OH groups at the monolayer-substrate interface.[67] Such P–O–Ti bonds were also detected by time-of-flight secondary mass spectroscopy (TOF-SIMS) in a study by Menzel and co-workers[68] on titanium modified by the T-BAG method.[56,69] As shown in Figure 13 d,e, the characteristic fragments confirming chemisorption, that is, TiP_2O_6, TiP_2O_7H, and $TiP_3O_6H_2$, were detected in the negative mode.[68]

In addition to the many available advanced surface characterization techniques, density functional theory (DFT) calculations turn out to be an efficient and powerful tool, especially in combination with empirical data, to aid understanding of a chemical process or structure. For instance, in recent work Thissen et al. studied the binding modes of octadecyl phosphonic acid (ODPA) by IR spectroscopy on specifically

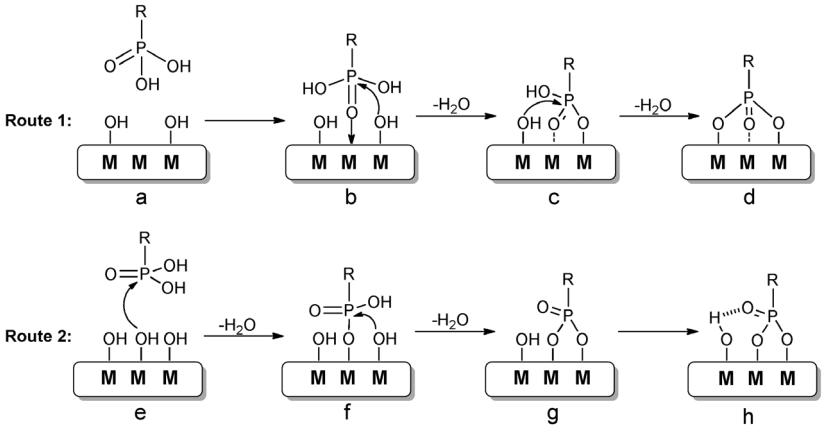

Figure 11. Mechanism of phosphonic acid attachment 1) to Lewis acidic metal oxides and 2) to poorly Lewis acidic metal oxides.[62b]

Dateiname: A306709e
Pfad: L:/daten/Verlage/VCH/ACH/Hefte/1425/
Status Neusatz
Datum: 24 KW., 11. Juni 2014 (Mittwoch)
Pagina: 6329
Seite: 8 te von 35
Umfang (Seiten): 35
Zeit: 9:22:52 Uhr

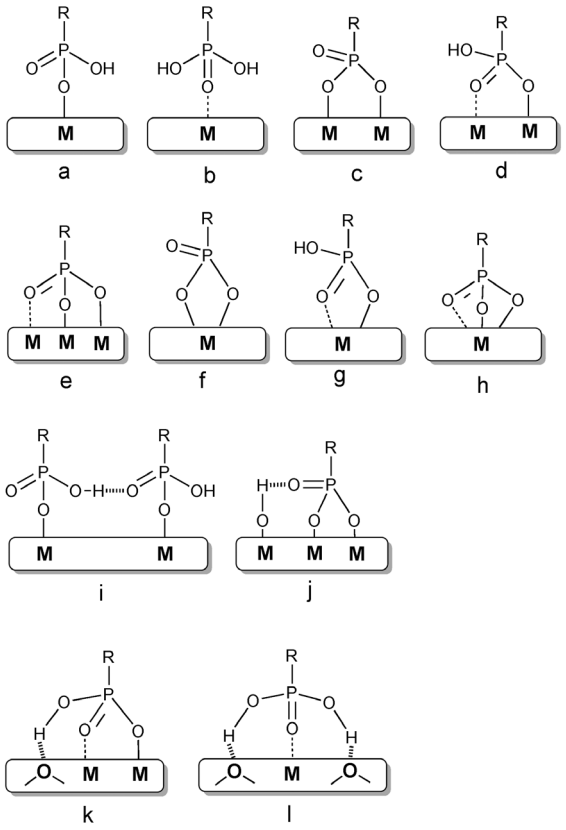

Figure 12. Binding modes of phosphonic acids on a metal oxide surface; M = metal: monodentate (a and b), bridging bidentate (c and d), bridging tridentate (e), chelating bidentate (f and g), chelating tridentate (h), and additional hydrogen-bonding interactions (i–l).[62b,65,66]

tuned oxide-free Si(111) surfaces, that is, 1/3 monolayer hydroxy (1/3 ML OH; ML = monolayer) or 1/3 monolayer aluminum hydroxide (1/3 ML O-Al-$(OH)_3$), both having the remaining 2/3 ML H-terminated Si(111) (Figure 14). For the isolated Si-OH sites on the 1/3 ML OH substrate, monodentate binding was observed, while after $AlCl_3$ treatment, remarkably, a bidentate mode (instead of a tridentate mode) was revealed for the isolated Si-O-Al$(OH)_3$-sites, in good agreement with DFT calculations.[60a] Analogous combined experimental and computational studies have been performed on the orientation and binding modes of phenylphosphonic acid on transparent, conductive indium zinc oxide (IZO), with excellent correlation between experiment (near-edge X-ray absorption fine structure (NEXAF), polarization-modulated infrared reflection–absorption spectroscopy (PM-IRRAS)) and theory.[70] In the same way, Smecca et al. were able to distinguish between carboxylic acid binding and phosphonic acid binding of carboxyalkylphosphonic acid on ZnO nanorods. XPS and IR data supported by DFT provided clear evidence for multidentate binding of solely the phosphonic acid terminus, that is, with negligible carboxylic acid binding.[71]

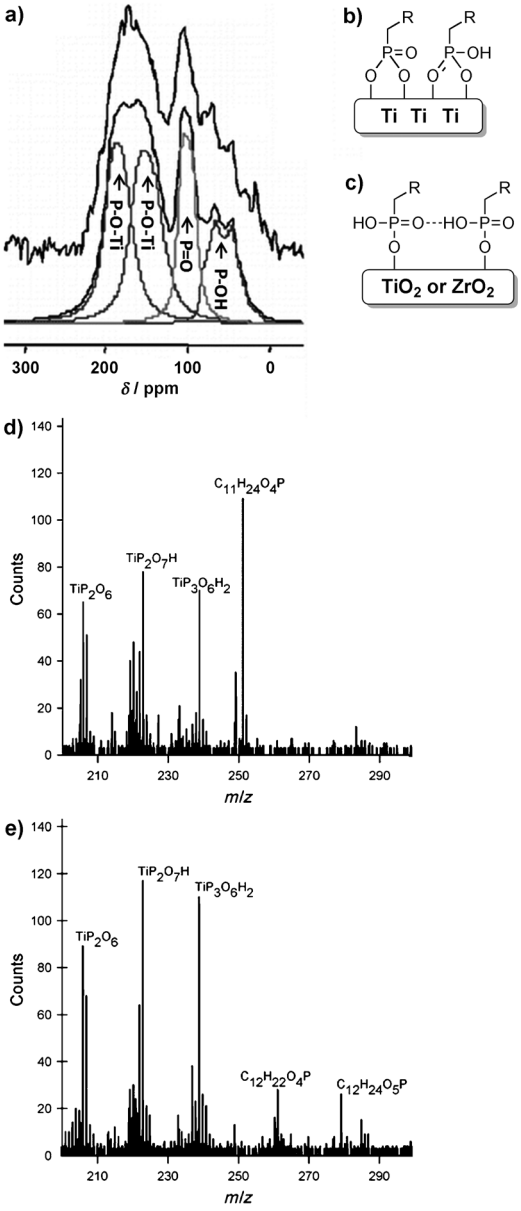

Figure 13. a,b) High-field ^{17}O MAS NMR of ^{17}O-enriched phosphonic acid monolayer deposited on TiO_2 (anatase).[65] c) Hydrogen-bonding interactions among the neighboring phosphonate groups, d,e) ToF-SIMS data of hydroxy- (d) and carboxy-terminated (e) phosphonic acid monolayers on Ti90/Al6V4.[68]

3.3. Applications of Phosphonate-Based Monolayers

Applications of monolayers of phosphonic acids have been reported in various fields, such as separation, organic electronics, catalysis, solar cell, optical devices, biosensors, and medical implants.[52a,62,72] In particular the formation of monolayers from phosphonic acids and phosphonate esters on metals and Lewis acidic metal oxides[49] is of interest for at least three reasons:

1) A relative easy synthesis and purification: phosphonate esters are viscous oils at room temperature and highly soluble in common organic solvents. Their subsequent conversion into phosphonic acids is relative simple and

Dateiname: A306709e
Pfad: L:/daten/Verlage/VCH/ACH/Hefte/1425/
Status Neusatz
Datum: 24 KW., 11. Juni 2014 (Mittwoch)
Pagina: 6330
Seite: 9 te von 35
Umfang (Seiten): 35
Zeit: 9:22:52 Uhr

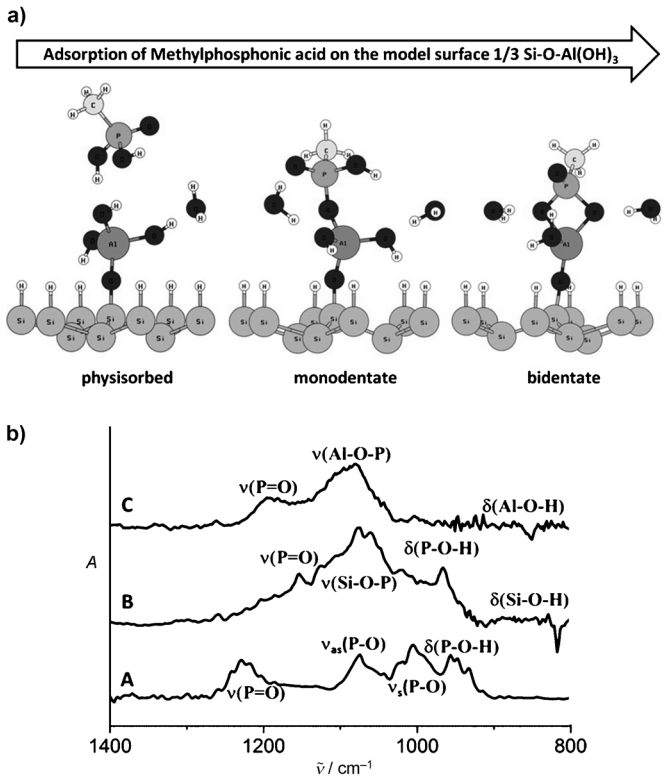

Figure 14. a) Heterocondensation pathway of methylphosphonic acid on the model surface 1/3 ML O-Al$(OH)_3$ resulting in bidentate binding; b) (A) DRIFT spectrum of octadecylphosphonic acid (ODPA) powder; and differential IR spectra of ODPA monolayer B) on 1/3 ML OH surface (monodentate binding), C) on 1/3 ML O-Al$(OH)_3$ surface (bidentate binding), both with the specific non-ODPA modified surface as reference.[60a]

several synthetic procedures have been reported.[52a,54a,62a,73]

2) In comparison with, for example, silane analogues, phosphonate derivatives are considerably less susceptible towards self-condensation reactions, which only occur under high-temperature dehydrating conditions.[62a] This makes them easy to handle and store in ambient conditions. In addition, rigorous exclusion of water during surface modification is not required, in fact, it can even be performed in aqueous solutions.[52a,54a,62]
3) Phosphonic acids and phosphonate esters possess exceptional binding properties, in particular on metals and metals oxides of high oxidation state (+ V tetracoordinate and higher), and owing to the hydrolytic stability of the P-O–metal linkages these monolayers are more resistant to hydrolysis than silane or carboxylic acid-derived monolayers,[49,52a,54a,62,74] and almost comparable to catechol-based or alkene/alkyne-based monolayers (see Sections 5 and 6).

These advantages have led to their use as anticorrosion coatings that prevent oxygen diffusion towards a metal surface by the generation of low-solubility metal complexes (e.g. Ca, Mg, Zn) on phosphonate-treated substrates.[75]

The use of phosphonates also has limitations, for example, the competing dissolution–precipitation process that might occur during phosphonic acid-based surface modification. In this process metal ions from an unstable oxide can be removed from the surface structure by complexation with the phosphonic acid, leading to the formation of insoluble metal phosphonate salts. The extent of this undesired side reaction depends mainly on the stability of the metal oxide and the reaction conditions (pH value, concentration, solvent, and temperature). Using a phosphonate ester instead, or varying the pH value might circumvent this problem.[52a,62a] Another disadvantage, which also emphasizes the complementary character of, for example, silanes and phosphonates, is the limited reactivity of phosphonates towards SiO_2 on which they only weakly physisorb and therefore can easily be washed off.[56] Michel et al.[72a] skillfully made use of this limitation, and actually applied it to selectively biofunctionalize metal oxide substrates consisting of TiO_2 within a matrix of SiO_2. To obtain protein-adhesive properties on TiO_2, the TiO_2 areas were selectively decorated with an aqueous solution of dodecylphosphonic acid (DPA). Subsequently, to obtain protein-repelling properties on the SiO_2, the remaining SiO_2 was modified with poly(L-lysine-*g*-ethylene glycol) (g = graft).[72a] The same principle was used to selectively modify the inner (mainly Si-O-Si) and outer (mainly Al-OH) surface of tubular clay structures of halloysite by silanes and phosphonic acids, respectively, and create an inorganic micelle-like architecture (Figure 15).[76]

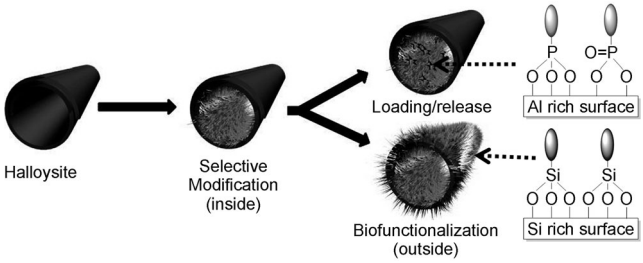

Figure 15. Schematic representation of the selective modification of the inner and outer surface of halloysite clay tubes.[76]

Phosphonate-based surface modifications are also very interesting for biomedical applications. For instance, for the development of new contrast agents based on magnetic inorganic nanoparticles modified with radiolabeled bisphosphonates. Such multimodal nanoparticles allow simultaneous in vivo magnetic resonance imaging (MRI) and optical imaging.[77] In addition, for stainless steel or titanium medical implants, surface modification by (bis)phosphonate anchoring is an attractive route, for example to improve the adhesion of bone tissue and cells, enhance long-term stability, and prevent infections by inhibiting bacterial adhesion.[52a,78] In a further application, Wong and co-workers, created a glycan array by direct immobilization of synthetic glycans with a phosphonic acid terminus onto aluminum oxide-coated glass and employed this new platform for high-throughput analysis of protein-glycan interactions.[79]

Dateiname: A306709e
Pfad: L:/daten/Verlage/VCH/ACH/Hefte/1425/
Status Neusatz
Datum: 24 KW., 11. Juni 2014 (Mittwoch)
Pagina: 6331
Seite: 10te von 35
Umfang (Seiten): 35
Zeit: 9:22:53 Uhr

4. Carboxylates

4.1. Reagents and Methods

Carboxylic acid-based SAMs are among the oldest ones studied systematically,[10b,c,80] with a focus on long-chain aliphatic carboxylic acids, since these were rapidly recognized to form close-packed, highly organized monolayer films.[80c,d,f] The central metal carboxylic acid moiety in such layers has been labeled an "inner-sphere adsorption complex",[81] as it can form carboxylate–metal bonds. These bonds can be detected by mass spectrometry data, for example, from a surface of an Al–Mg alloy coated with lauric acid (CH_3-$(CH_2)_{10}COOH$) the mass spectrum reveals signals for CH_3-$(CH_2)_{10}COOMg^+$, including the ^{25}Mg and ^{26}Mg isotopes of the soap.[82] This metal–oxide bond is usually not very strong,[83] which typically makes monodentate or bidentate monolayers highly unstable in aqueous media.[84] Since release of water is promoted by higher temperatures or vacuum, this explains the formation of more stable SAMs upon annealing/curing. The advantage of these layers is, of course, the extremely wide range of available carboxylates. In addition, the typically environmental friendly nature of carboxylates makes carboxylic acid-based monolayers one of the "greenest" options for monolayer formation.

There are three most frequently used methods to attach aliphatic carboxylic acid monolayers onto metal oxide surfaces:[86] Langmuir–Blodgett (LB) techniques, attachment from dilute solution, and gas-phase techniques, such as vapor-phase growth and aerosol spray deposition. Depending on the process chosen to form these monolayers (see Section 4.1.1–4.1.3), both carboxylic acid and carboxylate ions (typically used as their Li, Na, or NBu_4 salts) can be used, and in both cases the largest component of the driving force is the bonding between the carboxylate anion and a surface metal cation.[85]

4.1.1. Langmuir–Blodgett (LB) Techniques

The traditional means of forming aliphatic carboxylic acid monolayers is to transfer a mechanically compressed, densely packed, oriented monolayer on water to a solid substrate by the Langmuir–Blodgett (LB) technique.[87] An advantage of LB monolayers is the high ordering these films may have. Disadvantages are, however, the relatively weak interaction with the substrate owing to the presence of water, so the transferred monolayer may not even be resistant to simple rinsing with solvent. Secondly, the high ordering on the water surface may only be metastable, and as such can relax on the solid substrate to different structural forms with different physical properties.

4.1.2. Solution Processes

In most reports, the SAM preparation is based on solution processes using 0.1 to 100 mM concentrations of carboxylic acids in non-polar solvents (e.g. THF).[88] Although very cheap, solution growth has major technological drawbacks: its slowness and the use of organic solvents. Post-treatment by heating at 120 °C was found to increase monolayer stability, as a result of bidentate attachment of the carboxylate.[88] Recently Kim et al. pretreated TiO_2 nanoparticles with aqueous nitric acid solution (pH 1) to effectively increase the collision frequency of carboxylates to the now positively charged surface, and obtained an 18-times faster adsorption of ruthenium dye carboxylates.[89] Adsorption of carboxylic acids on TiO_2 nanoparticles from solution normally leads to a weak and unstable binding of the carboxylic acid molecules. Qu et al. used a solvothermal strategy for the modification of TiO_2 nanoparticles with carboxylic acids in ethanol/water 1:4 in an autoclave at 100 °C, to provide carboxylic acid-modified TiO_2 nanoparticles with a much higher modification efficiency than the conventional room-temperature immersion method (Figure 16).[90] This seems to be a good and general method for obtaining better quality carboxylic acid SAM on oxide surfaces.

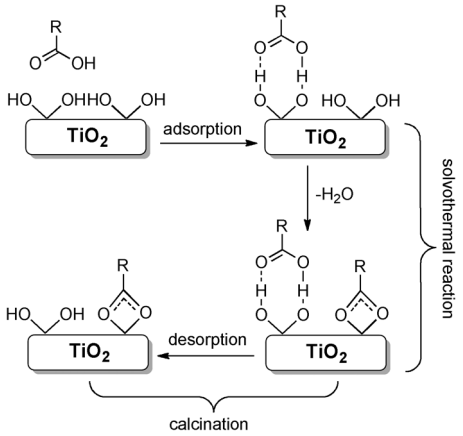

Figure 16. Schematic illustration of the modification of TiO_2 nanoparticles with carboxylic acids by the solvothermal strategy.[90]

4.1.3. Gas-Phase Processes

Martz et al. developed a vapor growth method of suitable carboxylated derivatives on ITO and Al and plasma-treated GaAs substrates.[91] The principle is based on exposing activated surfaces to a vapor of the grafting molecules under high vacuum. There are basically three advantages to this method: no solvent is needed, the resulting monolayers are more homogeneous than those grown from solution (in which intercalated solvent molecules might co-adsorb on the surface and screen the surfaces dipoles, or might react with the substrate), and gas-phase methods are typically faster and better scalable.[91b,92] Bernasek and co-workers developed a new method for the preparation of SAMs of carboxylic acids on native oxides of metals.[93] First, tetra-*tert*-butoxyzirconium ($(tBuO)_4Zr$) is allowed to react with a hydroxylated metal oxide surface, and the Zr binds strongly upon loss of two equivalents of *t*BuOH. Next, the surface is exposed to carboxylic acids that replace the remaining two alcohol moieties (Figure 17). This yields a significantly improved monolayer stability. In another gas-phase method to obtain SAMs, carboxylic acid solutions in dry THF were sprayed

Dateiname: A306709e
Pfad: L:/daten/Verlage/VCH/ACH/Hefte/1425/
Status Neusatz
Datum: 24 KW., 11. Juni 2014 (Mittwoch)
Pagina: 6332
Seite: 11 te von 35
Umfang (Seiten): 35
Zeit: 9:22:53 Uhr

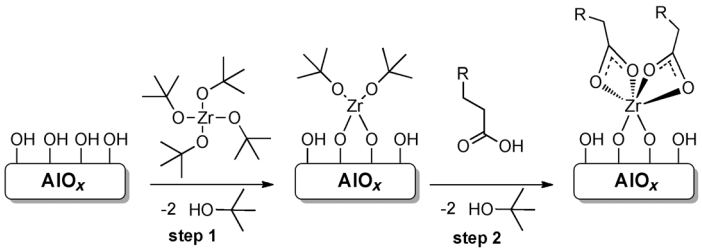

Figure 17. Highly improved binding of *n*-octanoic acid to zirconium alkoxide-treated hydroxylated Al surfaces by formation of a zirconium η^2-carboxylate.[93]

with an aerosol sprayer onto ice-cold metal oxide surfaces, after which the surfaces were immediately transferred to a 100–150 °C oven for 30–45 min.[80b,86a] It proved necessary to optimize the reaction conditions (temperature, acid concentration, number of spray coatings, drying conditions) in each case for optimal SAM formation.[80b]

4.2. Binding Modes and Mechanism

Several binding modes of carboxylic acids on oxide surfaces have been described.[82,83,85a,b,94] Carboxylic acid groups are capable of binding to the oxide surface through "outer-sphere adsorption complexes" and "inner-sphere adsorption complexes". In outer-sphere complexes H-bond interactions are important (**CA-II** or **CA-III**; Figure 18), whereas in inner-sphere complexes coordinative bonds between the carboxylate oxygen and the metal ions are present. This may be a monodentate metal–ester coordination (**CA-IV**) or a bidentate coordination, either bridging between two metal centers (**CA-V**) or chelating, that is, with one metal center (**CA-VI**). Furthermore, adsorption may occur through an acid–base reaction leaving the conjugate base COO^- bonded to a Lewis acid at the surface (**CA-I**).

The binding mode observed is dependent on the substrate, the carboxylic acid, and the preparation conditions. The adsorption mode of carboxylic acids on surfaces has been investigated both theoretically and experimentally, the latter typically by IR spectroscopy.[95] In such studies it was shown that in a LB transferred monolayer only H-bonded carboxylic acids were present, whereas monolayers that were transferred under vacuum conditions or heat treated give inner-sphere surface complexes. Dobson and McQuillan reported an in situ IR spectroscopic analysis of the adsorption of aromatic carboxylic acids on TiO_2, ZrO_2, Al_2O_3, and Ta_2O_5 from aqueous solutions.[95a] Benzoic acid absorbed very strongly on ZrO_2 in a bridging bidentate fashion, but showed only weak adsorption to TiO_2 and Ta_2O_5. Salicylic and phthalic acids adsorbed on the metal oxides through bidentate interactions, involving coordination through both carboxylate and the *ortho* hydroxy or carboxylate groups. Thiosalicylic acid adsorbed to the metal oxides as a chelating bidentate carboxylate with no coordination through the thiol substituent group (Figure 19).[95a] This is not surprising, as the soft sulfur-containing substituent group is not expected to participate in coordination to the hard high-oxidation state metal ions.

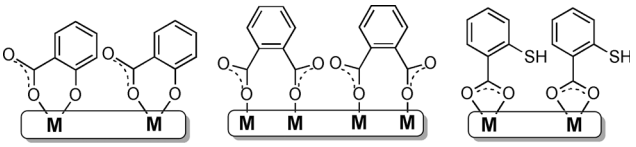

Figure 19. Binding modes of salicylic acid (2-hydroxybenzoic acid), phthalic acid (1,2-dicarboxybenzene), and thiosalicylic acid to metal oxide surfaces.[95a]

An interesting dependence on the substrate was found for the adsorption of succinic acid (HOOC-CH_2-CH_2-COOH) onto oxidized Zn and Fe surfaces.[96] Rinsing both of the succinic acid-modified surfaces with THF showed that much adsorbed material was lost. However, in the case of the Zn substrate no O–H stretching vibration was found, and also the C=O stretching vibration indicated that both carboxylate groups were coordinated to the metal ions. In contrast, on the Fe substrate an O–H stretch vibration was clearly visible, and the position of the C=O vibration indicated H-bonded material.[96] Another substrate dependence was found for the adsorption of acetic acid onto silica and aluminoborosilicate glass fiber surfaces. Stapleton et al. studied the acetic acid adsorption on sodium aluminoborosilicate glass fiber surfaces and pure silica with FTIR and ^{13}C NMR spectroscopy under vacuum conditions at 125 °C.[97] On silica, silyl ester linkages can be detected, whereas on the aluminoborosilicate, sodium (and perhaps other) carboxylates form in preference to ester linkages (Figure 20). This difference was attributed to the absence of isolated silanols on the aluminoborosilicate surface.[97]

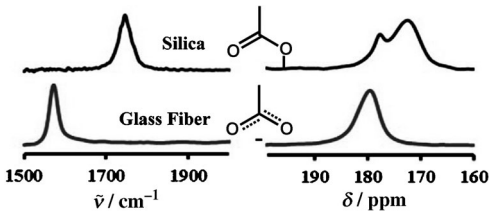

Figure 20. FTIR (left) and ^{13}C NMR (right) spectra of the carbonyl region after acetic acid adsorption on silica and aluminoborosilicate.[97]

Cho and Tao[98] investigated the film thickness and tilt angle of fluorinated carboxylic acids adsorbed from an organic solution and found that the binding modes of the carboxylic acid SAMs on Al and Ag are different. On an Al surface the head group binds monodentately, resulting in an almost untilted linear

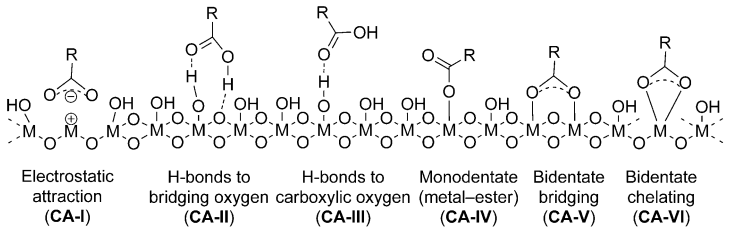

Figure 18. Possible binding modes of COOH or COO- groups to metal oxide surfaces.

Dateiname: A306709e
Pfad: L:/daten/Verlage/VCH/ACH/Hefte/1425/
Status Neusatz
Datum: 24 KW., 11. Juni 2014 (Mittwoch)
Pagina: 6333
Seite: 12 te von 35
Umfang (Seiten): 35
Zeit: 9:22:54 Uhr

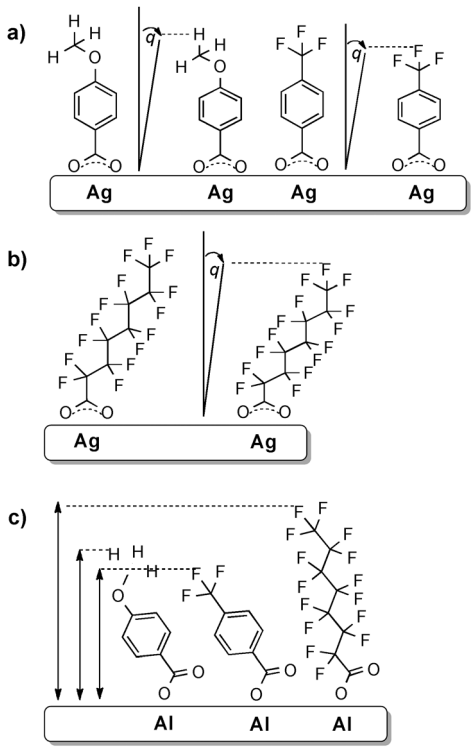

Figure 21. Adsorption modes and tilt angles (q) of aromatic and fluoroalkyl carboxylic acids on oxidic Ag and Al surfaces.[98]

chain acid, while on Ag the head group binds bidentately, resulting in a more tilted chain conformation (Figure 21). Monodentate binding, for example, as observed by Ting et al. for SAMs of stearic acid (SA) on sol–gel HfO_2, is revealed by the presence of a carbonyl C=O stretch at approximately 1740 cm^{-1}.[94b]

Recently, Chernyshova et al. performed a comprehensive spectroscopic and theoretical study on the adsorption of sodium laurate, $CH_3(CH_2)_{10}COONa$, from an aqueous solution onto hematite (Fe_2O_3) nanoparticles.[85a,b] The FTIR spectrum of the material (Figure 22) is characterized by the antisymmetric $\nu_{as}CO_2$ and symmetric ν_sCO_2 stretching bands of the carboxylate group at 1540 and 1410 cm^{-1}, respectively. These bands were assigned to an inner-sphere monodentate mononuclear (ISMM) complex with a H-bonded second carboxylate oxygen atom (R-C(=O···H)-O-M). The asymmetry of these bands suggests the presence of at least one more pair of bands at 1530 and 1425 cm^{-1}, assigned to an outer-sphere (OS) complex in which the alkanoate is protonated by a water molecule that is coordinated to the Fe^{III} cation.[85a] So it was concluded that under these conditions a mixture of inner-sphere and outer-sphere complexes is present.

4.3. Applications of Carboxylate-Based Monolayers

Carboxylate-based monolayers have been the option of first choice for coating TiO_2 nanoparticles in dye-sensitized solar-cell research.[99] The synthetic accessibility and ease of application has likely led to this use, despite their well-documented long-term instability as a result of hydrolysis.[100] The binding of carboxylates to an oxidic surface is typically weaker and less hydrolytically stable than almost any of the other adsorbents described in this Review. Their use as monodentate surface-binding agents is therefore likely be replaced by other agents, unless these limitations can be overcome or are compensated by other properties of the resulting monolayers. One approach towards improved carboxylate-based monolayers involves the use of multidentate carboxylic acid materials, which has recently been demonstrated in several interesting applications. Bishop et al.[101] studied the binding of trifunctional carboxylic acid **2** to ZnO nanoparticles (NPs; Figure 23). Upon treatment of the NP with a solution of **2** in MeCN, a new strong broad signal appeared in the IR spectrum at 1603 cm^{-1} and a weaker broad band centered at 1425 cm^{-1}, consistent with the antisymmetric and symmetric stretches of a zinc carboxylate species. In addition, surface-bound **2** exhibits a free acid C=O stretch in the region 1736 to 1714 cm^{-1} which is weak relative to the zinc carboxylate stretches. These results indicate that some of the carboxylic acid groups of **2** are not bound to Zn. Similar spectra were found upon surface modification of Fe_2O_3 and TiO_2 nanoparticles. In contrast, WO_3 NP do not show the typical carboxylate vibrations: the extremely low isoelectric point of WO_3 relative to those of the other metal oxides studied apparently inhibits carboxylate formation, and only outer-sphere adsorption is observed.

Multidentate carboxylates have also been used to modify the conductivity of cuprate superconductors. Carmeli et al. attached both electron-accepting and

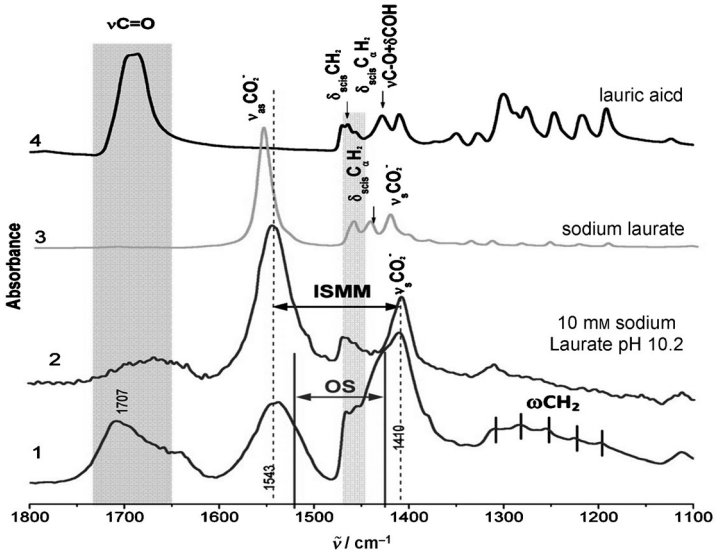

Figure 22. In situ FTIR-HATR (HATR = horizontal attenuated total reflectance) spectra of 1) hematite treated for 25 min with a 10^{-3} M solution of sodium laurate at pH 7.15 ± 0.05 with no added electrolyte. For comparison, spectra of 2) an aqueous 10^{-2} M sodium laurate at pH 10.2, 3) solid sodium laurate, and 4) solid lauric acid are also shown.[85a]

Dateiname: A306709e
Pfad: L:/daten/Verlage/VCH/ACH/Hefte/1425/
Status Neusatz
Datum: 24 KW., 11. Juni 2014 (Mittwoch)
Pagina: 6334
Seite: 13 te von 35
Umfang (Seiten): 35
Zeit: 9:22:54 Uhr

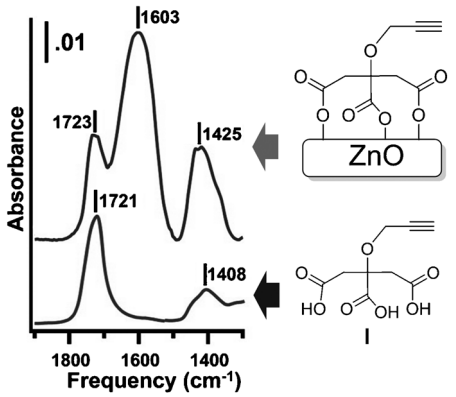

Figure 23. Tricarboxylate **2** forms multiple bonds to the surface as indicated by the IR spectra of **2** on the surface of ZnO nanoparticles (top); for reference: IR spectrum of neat **2** (bottom).[101]

electron-donating moieties by carboxylate binding onto high-temperature cuprate superconductors (Figure 24).[102] For the electron-accepting moieties, carboxyfullerene is used, which can interact with the surface through multiple carboxylate moieties, resulting in a dense and multidentate-induced high-stability monolayer on oxide surfaces.[103] Analogously, the binding of an electron-donating copper porphyrin moiety to the cuprate was achieved with two alkylcarboxylate linking groups. Each of these structures (electron-donating and electron-accepting) was also in contact with nanoparticles or nanowires, with the overall aim to increase the critical temperature (T_c) of such superconductors. Such a novel way to change the T_c through strongly bound functionalized carboxylate monolayers may pave the way to new dissipationless memory storage and switches based on high-T_c superconductors.[102] Finally, carboxylic acids are also used on an industrial scale for surface coatings, typically as lubricants, corrosion-resistant materials, and (linkers to) catalysts. They are also investigated as promising materials for the protection of metal oxide surfaces.[84,104]

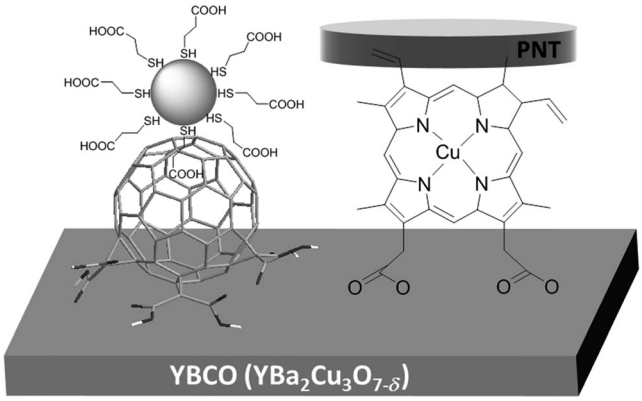

Figure 24. Deposition of various carboxylate-linked monolayers on high-temperature cuprate superconductors yields SAM-induced electron doping or hole doping, which results in an increase in T_c value.[102]

5. Catechols

5.1. Reagents and Methods

In a relatively recent surface-modification technique, use is made of *ortho*-dihydroxyaryl compounds, such a catechol and dopamine. Their mode of attachment is a biomimetic one, as it hinges on chemistry that is also found in the adhesive-pad proteins secreted by marine mussels to give extremely strong binding.[105] It was observed that mussel adhesive proteins (MAPs) derive their binding strength, to a considerable degree, from the presence of the non-standard, but still widely occurring, amino acid 3,4-dihydroxyphenylalanine (DOPA).[106] In fact, for some MAPs, DOPA constituted up to 30% of the amino acid composition.[107] That mussels and other underwater organisms depend for their surface adhesion on DOPA-based materials emphasizes three of the biggest advantages of catechol-based surface modifications:

1) the reaction works on a truly wide variety of surfaces, including on wet surfaces and on highly apolar ones, such as Teflon,[108]
2) with the use of specific catechol derivatives, that is, dopamine and analogues, an extremely strong binding can be achieved,[109]
3) this can be achieved without further heating of the medium and/or substrate.

Although the surface attachment is thus not specific to oxidic surfaces, we only focus on binding to oxidic surfaces.

The binding of catechol-derived films has been studied intensely over the last few years (for Reviews see Refs. [77b,106,107,110]), which has indicated a highly complex structure for the attached film. This complexity is due to the fact that the binding mode has two components: the surface anchoring by the catechol moiety, and the follow-up oxidation of surface-bound catechol moieties in the presence of more catechol in solution, to form multifunctional, highly cross-linked polymeric films.[111] As indicated in an recent Review on materials that have come into reach through this chemistry,[110a] this implies that for optimal binding strength, the degree of oxidation from catechols to *ortho*-quinones is highly important, since *ortho*-quinones do not bind strongly to many of the surfaces that catechols stick to efficiently,[112] however, this oxidation is required to induce the strength-inducing cross-linking.

This combination of surface attachment and oxidative cross-linking can turn polydopamine and derivatives thereof into an extremely versatile primers for further surface functionalizations, as shown by the seminal work of Messersmith and co-workers.[109a] This group describes an easy-to-use procedure for the oxidation of dopamine by air in (slightly basic) water, to yield the spontaneous deposition of a polydopamine polymeric film on a wide range of surfaces. Since this film has many functional groups available for further reactions, this has developed into a highly stable priming platform.[107] The structure of the resulting film is still a topic of intense debate as reviewed by Ball and co-workers,[113] but seems to be highly related to the formation of eumelanin

Dateiname: A306709e
Pfad: L:/daten/Verlage/VCH/ACH/Hefte/1425/
Status Neusatz
Datum: 24 KW., 11. Juni 2014 (Mittwoch)

Pagina: 6335
Seite: 14te von 35
Umfang (Seiten): 35
Zeit: 9:22:54 Uhr

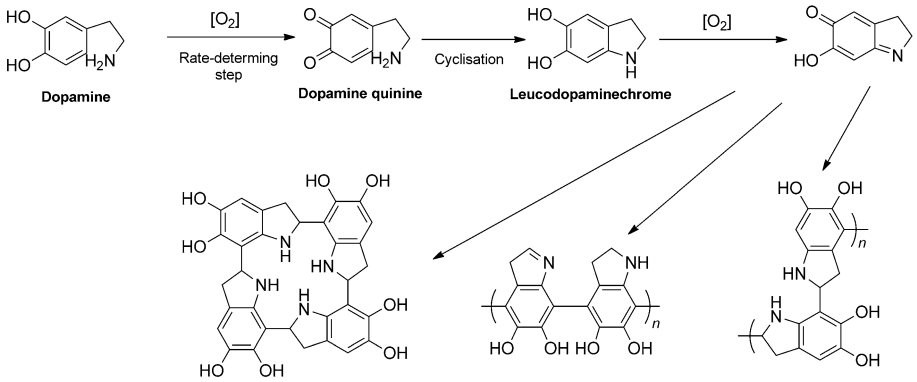

Figure 25. Mechanism of the oxidative steps from catechol to the most stable tetramer of 5,6-dihydroxyindole (left) and polydopamines (middle and right).

films, and thus likely involves a whole series of steps (Figure 25).

The ongoing reactions within such polymeric films also affect the binding strength as demonstrated by surface-force experiments by Israelachvili and co-workers.[114] They obtained the force–distance profiles and adhesion and cohesion energies of the films, and found that the adhesion energies of the films to mica and TiO_2 surfaces increase with the catechol concentration, but also nearly doubled over time (1 h versus 41 h), which was attributed to rearrangements of the DOPA residues within the film.

5.2. Structure of Catechol-Based Monolayers

To keep the attached film monomeric and structured, this oxidation of the catechol needs to be prevented to avoid the formation of unorganized thick polymer layers. An approach for this has been developed by Zürcher and co-workers, by the introduction of electron-withdrawing groups in catechol.[115] This development hinged on a detailed evaluation of a range of electron-poor derivatives, as indicated in Figure 26. Compound **1**, and especially the synthetically more practical nitro compound **5**, display the desired effective monolayer formation. This is caused by the increased acidity of the

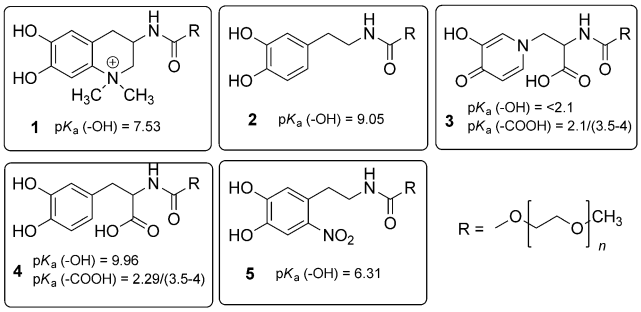

Figure 26. Electron-poor catechol derivatives (in this case with a poly(ethylene glycol) (PEG) chain attached) stimulate monolayer formation: anacat (**1**), dopamine (**2**), mimosine (**3**), dopa (**4**), nitrodopamine (**5**).[115a]

catechol hydroxy groups, which improves the binding strength of the individual catechol moieties.[115a]

ortho-Dihydroxyaryl compounds can attach to a hydroxy-terminated surface in a variety of binding modes.[106] Analysis of the literature indicates the following mechanism (Figure 27): First, catechol approaches an OH-terminated surface (in this case: titanium oxide) and forms a physisorbed species, which is surface-bound by two H-bonds.[116] Subsequently, a monodentate mononuclear complex is formed, meaning that one

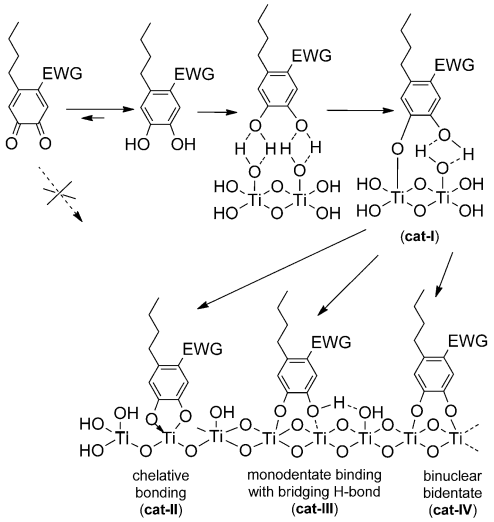

Figure 27. Four possible configurations of catechol on TiO_2 surface.

catechol OH is involved and one Ti atom (**cat-I**). From this intermediate, three alternatives become feasible:

1) a bidentate mononuclear complex (**cat-II**), in which a single Ti atom binds coordinatively with the two O atoms of the catechol,
2) a monodentate binuclear complex (**cat-III**), in which an adjacent Ti atom has lost an -OH moiety, and can now bind to a catechol -OH moiety, or
3) a bidentate binuclear complex (**cat-IV**), in which the two -OH moieties of the catechol form bonds with two different Ti atoms.

Different research groups have speculated on the relative stability of these structures, with sometimes conflicting conclusions. Recently, detailed IR and computational studies by Jing et al. provided indications for the stability of the binuclear bidentate complex.[117] They also suggest that the mononuclear monodentate complex is formed first in the pH range 5 to 9, and can over time be modified to the binuclear bidentate structure.[118]

Dateiname: A306709e
Pfad: L:/daten/Verlage/VCH/ACH/Hefte/1425/
Status Neusatz
Datum: 24 KW., 11. Juni 2014 (Mittwoch)
Pagina: 6336
Seite: 15 te von 35
Umfang (Seiten): 35
Zeit: 9:22:55 Uhr

The formation of the highly stable coordinative chelate structure involves the replacement of a surface -OH group by a deprotonated ligand.[119] This mode of attachment has been shown to be operative for Ti oxides, but also for Fe_2O_3 nanoparticles.[120] This binding mode also allows the use of such catechol–metal ion structures as metal-sequestering structures in a variety of organisms.[106]

The binuclear bidentate structure (sometimes called: bridged bidentate structure; **cat-IV**) is reported for the catechol assembly of PEG–DOPA structures on TiO_2 (Figure 26),[121] as inferred from slight changes in the surface -OH groups upon changes in the PEG surface density or PEG adlayer thickness.[121a] In line with this observation, it has been indicated that the chelating, mononuclear bidentate structures (**cat-II**) would, for TiO_2, imply the formation of the uncommon hepta-coordination.[122] In contrast, surface Ti ions retain their normal hexacoordination environment in the bridged species **cat-IV**. Solid-state ^{13}C NMR and comparative simulated ^{13}C NMR spectra of catechols on titania nanotubes showed that these NMR data were also more in line with a binuclear bidentate structure than with a mononuclear chelate structure, but only these two possibilities were included in the comparison.[123] Finally, Lee et al. investigated the single-molecule binding strength by AFM force–distance measurements, and observed a very strong yet reversible binding of DOPA to the titanium surface (Figure 28).[124] Bidentate bonding was inferred, given the much higher

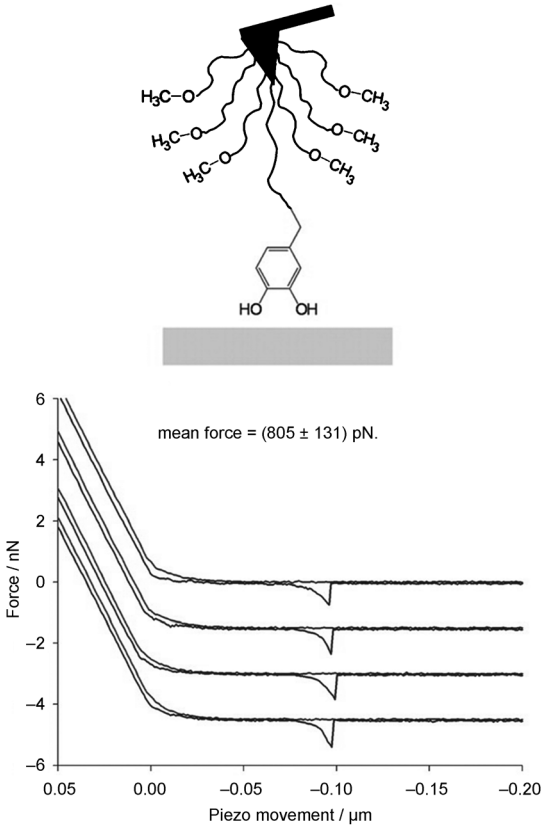

Figure 28. Schematic representation of a DOPA-functionalized AFM tip and typical single-molecule force–distance curves of DOPA interacting reversibly with a Ti surface.[124]

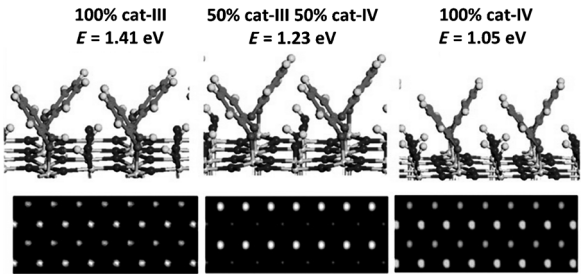

Figure 29. Calculated adsorption geometries (top) and simulated STM images (bottom) of 0.5 ML of catechol on TiO_2 (110) with adsorption energies per molecule listed for each model. In these STM images the spots are in registry with the geometric structure shown above, for example, the brighter spots in the image for the surface with 50% **cat-III** and 50% **cat-IV** (middle) correspond to the **cat-III** molecule.[125]

dissociation force (805 ± 131 pN) than observed for *N*-Boc-Tyrosine (97 pN; Boc = *tert*-butoxycarbonyl), which interacts through one hydroxy moiety with the substrate. They also noted that upon oxidation of the catechol moiety, the bonding to the surface is weakened.[124]

Such clear preference for one binding mode is not substantiated by theory. For example, Selloni, Diebald, and co-workers did calculations on dopamine-coated TiO_2 surfaces for various binding modes: H-bond stabilized mononuclear monodentate (**cat-III**), binuclear bidentate (**cat-IV**), and a 1:1 mixture of **cat-III** and **cat-IV**, by plane-wave pseudo potential DFT calculations (Figure 29). Interestingly, the lowest binding energy was calculated for the bidentate structure, the mixed structure (i.e. the one suggested by Rodenstein et al. for their complexes),[115b] was intermediate, while the most stable surface situation was provided by a homogeneous coverage of the TiO2 surface by H-bond stabilized, monodentate mononuclear structures, although different orientations of the catechol on the surface, or the mixing in of some binuclear bidentate structures does not raise the energy tremendously.[125]

For the third binding mode, Rodenstein et al.[115b] reported that binding of nitrodopamine (ND) derivatives to the TiO_2 surface results in two possible configurations: H-bond stabilized mononuclear monodentate (**cat-III**) and binuclear bidentate configurations (**cat-IV**) of ND molecules grafting on TiO_2 (Figure 30). These different binding states of the catechol's hydroxy groups lead to differences in the electron distribution within the benzene ring and thus also in the attached nitro group, and this can be detected in the N1s XPS data (Figure 30). Compounds ND and perfluoroalkyl nitrodopamine (PFAND) show two peaks at 405.1 and 406.6 eV associated with the nitro group. For ND, there are two additional peaks at 400.1 and 401.9 eV, attributed to partial protonation of the amine group. This splitting was not observed in the case of the amide nitrogen atom of PFAND at 400.4 eV, since its protonation is not possible. The ratio of the amine or amide peaks versus that of the nitro peak in the N1s XPS spectrum is greater than 1 for both molecules, which implies a possible reduction of NO_2 to NO_x or indicates some loss of NO_2 induced by the X-ray radiation or emitted photoelectrons. Such an effect could also be the reason for the

Dateiname: A306709e
Pfad: L:/daten/Verlage/VCH/ACH/Hefte/1425/
Status Neusatz
Datum: 24 KW., 11. Juni 2014 (Mittwoch)

Pagina: 6337
Seite: 16te von 35
Umfang (Seiten): 35
Zeit: 9:22:55 Uhr

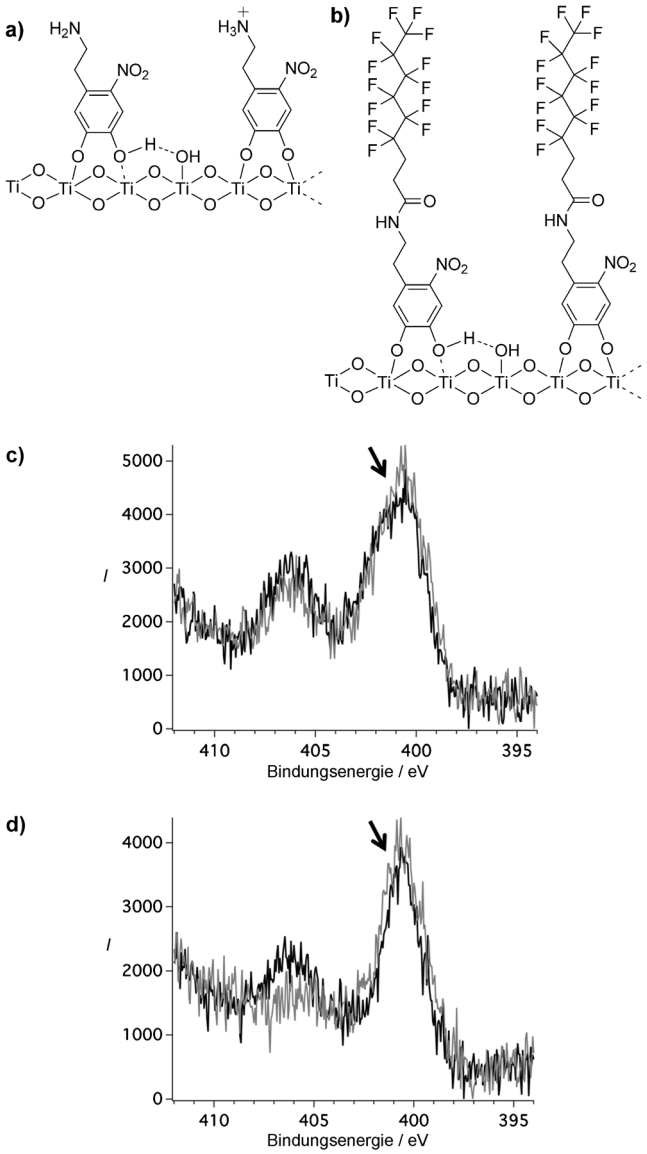

Figure 30. Hydrogen-bond stabilized mononuclear monodentate and binuclear bidentate binding modes as proposed for a) ND and b) PFAND. N1s XPS data at the beginning (black line) and after 4.5 h (gray line) of XPS measurement of c) ND and d) PFAND.[115b]

diminishing PFAND nitro peak during the X-ray exposure (Figure 30 c,d).[115b]

These three modes of attachment (Figure 27, **cat-II**, **cat-III**, and **cat-IV**) are thus typically referred to as the most stable ones. The interconversion between several of these surface-bound catechol structures on TiO_2 was studied by Diebold et al., who combined DFT calculations with STM and photoemission studies.[125,126] This yields a detailed molecular picture of the various binding modes and their relative energies.[126] In addition to the structures from Figure 27, on a modified surface, some catechol derivatives, specifically DOPA, can at low pH values, also interact with the oxidic surface through the other end of the molecule as indicated by a clear shift in the surface-enhanced Raman spectroscopy (SERS) data. Upon decreasing the pH to 2, a broad signal at

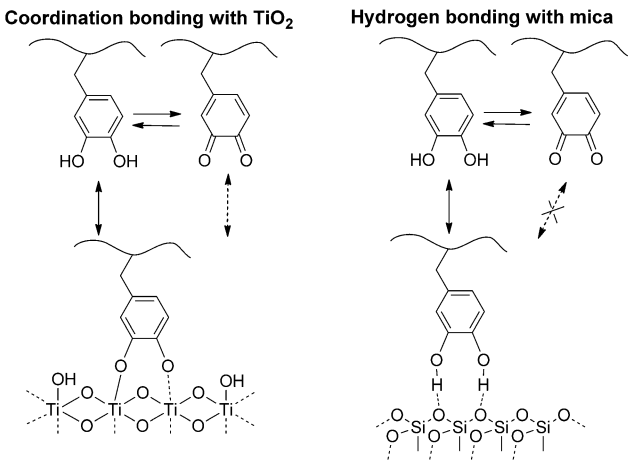

Figure 31. Proposed binding mechanisms of DOPA to TiO_2 and mica surfaces.[114a]

approximately 1680 cm^{-1} increases significantly, while a new signal appears at about 1301 cm^{-1}.[118]

A final characteristic of catechol chemistry is that it does not function equally well on all surfaces. For example, TiO_2 seems to be a nearly ideal substrate, whereas binding to SiO_2 or mica is typically weak, through H-bonding (Figure 31).[110d,114a,115a] In addition, even the quinones have some H-bonding interactions with TiO_2, but on mica such interactions are nearly absent, making catechols not very suited for attachment onto mica.

5.3. Applications of Catechol-Based Monolayers

Catechol-based surface modifications give rise to a large field of applications. These are largely based on the oxidative formation of strong-binding polymer films as indicated in a recent Review.[110a] However, increasingly use is being found for well-defined catechol-based monolayers with specific functionalities, such as for the stabilization of nanoparticles, light absorption, reversible redox chemistry, and band-gap engineering which is essential for solar-cell applications,[127] and for biomedical applications. We will discuss a few representative examples.

The presence of additional, electron-withdrawing substituents on the catechol ring to prevent oxidation also allows tuning of the binding strength.[110a,d,127,128] Catechol derivatives are often used as anchors to various metal oxide nanoparticles, including TiO_2 and iron oxides. While catechol itself binds weakly and reversibly to Fe_3O_4 nanoparticles, the binding affinity of mimosine is high enough to remove Fe^{3+} ions through complexation, which gradually dissolves such nanoparticles (Figure 32).[119,128c] Nitrocatechols have an intermediate affinity: they strongly adsorb, without dissolving the Fe_3O_4 nanoparticles. Fine tuning of the catechol structure can thus be used to either stabilize or destabilize such materials. In principle, this may also be used to selectively remove an iron oxide coating from a nanoparticle with another core, but this has not been reported to date.

Dateiname: A306709e
Pfad: L:/daten/Verlage/VCH/ACH/Hefte/1425/
Status Neusatz
Datum: 24 KW., 11. Juni 2014 (Mittwoch)
Pagina: 6338
Seite: 17 te von 35
Umfang (Seiten): 35
Zeit: 9:22:55 Uhr

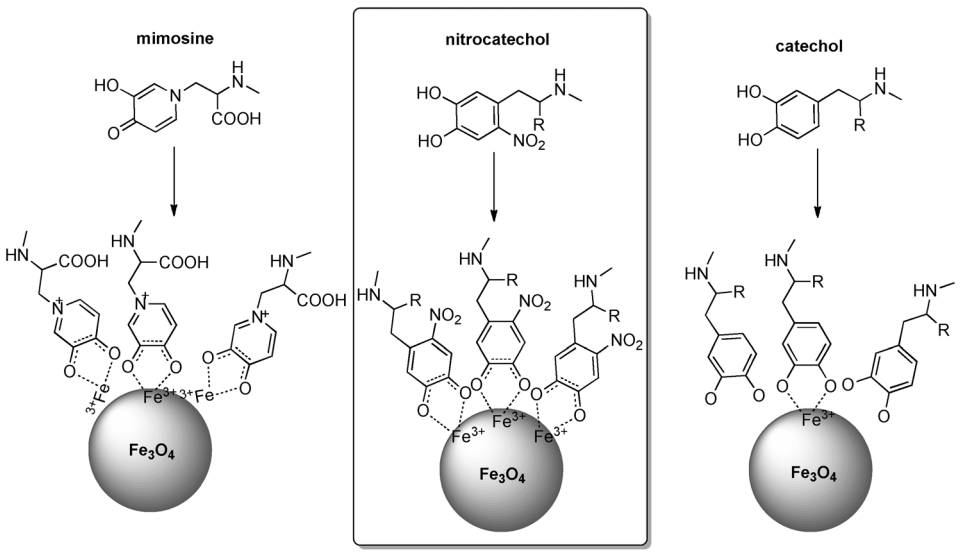

Figure 32. Catechols and especially nitrocatechol bind effectively to iron oxide nanoparticles, and thus provide a stable coating. However, mimosine binds Fe^{3+} so strongly, that this actually dissolves the nanoparticles.[119]

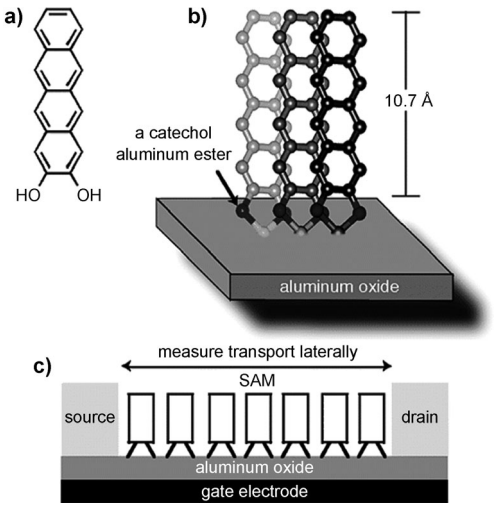

Figure 33. a) *ortho*-Dihydroxy-functionalized tetracene. b) Schematic representation of the bonding and orientation of this molecule on Al_2O_3 (not intended to indicate in-plane ordering). c) Schematic representation of the SAM transistor.[121b]

For the construction of hybrid inorganic–organic structures, for example, for optoelectronics, the aryl ring does not necessarily need to be a benzene ring, but may also be part of a larger aromatic structure, as shown for SAMs of 1,2-dihydroxytetracene on Al_2O_3. These spontaneously form dense π–π stacks, perpendicularly oriented to the surface and anchored through the catechol (Figure 33). The tetracene monolayer was subsequently shown to be an active channel for hole transport in a nanoscale FET.[121b]

In addition to using larger aromatic-ring or benzene moieties with electron-withdrawing groups—that increase the binding strength to many substrates, but also affect other electronic properties—an alternative, multi-binding strategy can be followed by making use of multiple catechol–substrate interactions. This approach was chosen to attach, for example, dendritic PEG compounds.[129] PEG dendrimers were covalently attached to anchors with one, two, or three covalently bound catechol groups. When three catechol groups were present, the dendrons attached rapidly and irreversibly to TiO_2 as monolayers with persistent antifouling properties.[129b]

Recently Hoecker et al. deposited acyl homoserine lactone and a nitrodopamine onto biocompatible TiO_2 beads by an operationally simple dip-and-rinse procedure, and showed that these beads are capable of inducing quorum sensing (QS).[128a] This hybrid system expands the catechol surface-modification platform and provides a straightforward method for the preparation of coated surfaces in medical devices able to interrupt the QS signaling pathway in a wide range of different bacterial strains.[130] Finally, nitrocatechol-based systems have been elegantly used to deliver a nanoparticle-bound cargo in a light-induced manner, by specific photochemical bond cleavage that makes use of the photoreactivity of this nitrobenzene system (Figure 34).[134b]

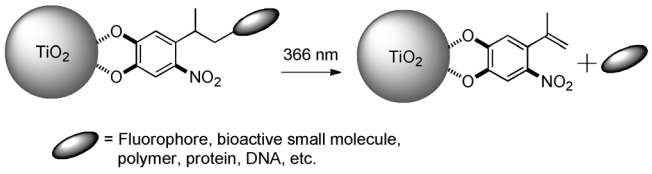

Figure 34. Irradiation of the photolabile 2-(2-nitrophenyl)propyl (NPP) protecting group as TiO_2 anchor allows for the fast, light-induced loss of such surface-linked loading.[128b]

6. Alkenes and Alkynes

6.1. Photochemical Approaches

The previously mentioned attachment chemistries focus on thermal attachment, rather than photo-induced reactions. Photopatterning therefore typically requires the photoresist approach well-known in lithography, or a destructive mode of patterning (laser ablation of monolayers).[131] This stimulated the search for photochemical reactions that actually would produce a well-defined monolayer, and thus allow constructive photopatterning.

The first example thereof was provided by the Zuilhof group for the surface modification of silicon carbide upon irradiation of an alkene-covered substrate with UV light (254 nm).[132] The surface of this material is actually termi-

Dateiname: A306709e
Pfad: L:/daten/Verlage/VCH/ACH/Hefte/1425/
Status Neusatz
Datum: 24 KW., 11. Juni 2014 (Mittwoch)
Pagina: 6339
Seite: 18te von 35
Umfang (Seiten): 35
Zeit: 9:22:56 Uhr

nated with hydroxy groups (Si-OH and C-OH) upon wet etching with dilute (2.5% in water) HF.[133] Irradiation of such an alkene-covered surface then yields covalent attachment of these alkenes, as for example, indicated by the development of the water contact angle up to 107° (Figure 35).[132a]

This reaction displayed a clear wavelength-dependence, as irradiation with 275 or 330 nm never gave water contact angles over 95°, which is indicative of incomplete monolayers. The reaction seems to proceed by a Markovnikov addition, as irradiation of a 1-alkene that contains no methyl group, for example, the CH_2F-terminated 11-fluoroundec-1-ene, yields a clear CH_3 signal in the IR spectra (Figure 36). This situation suggests that some form of acid catalysis is involved, for example, by the increased acidity of surface-bound OH moieties upon irradiation. In addition, the CH_2 stretching vibrations appear at 2856 and 2926 cm^{-1}. These frequencies are typical for monolayers that do not display a high degree of short-range ordering. This result would be in line with attachment at the 2-position and the formation of a methyl group close to the surface that does not allow the hydrocarbon chains to closely pack together.

Subsequently this work was extended to a wide variety of other oxides. UV irradiation of SiO_x surfaces, such as glass or synthetic fused silica, in the presence of terminal alkenes smoothly yields the covalent attachment of a dense monolayer, with the static water contact angle reaching a maximum value of 109°.[134] IR spectroscopy again confirms formation of the expected dense but disordered monolayer, but in this case also displays an increasing intensity of the C–H stretching vibrations beyond saturation of the contact angle. This result implies that the absorbed layer is steadily growing in thickness, even though no further change in the contact angle is observed. The mode of reaction again turned out to be a Markovnikov addition, as shown by IR spectroscopy after a surface modification with 11-fluoroundecene, which introduces a clear CH_3 stretching signal. The resulting monolayers were shown to be stable up to 400 °C, and their high quality was indicated by the effectiveness to function as a resist against platinum atomic-layer deposition (ALD). This approach thus provides a mild, room-temperature method to locally modify oxide surfaces, including glass, with non-corrosive chemicals, that is, alkenes.[134]

The mechanism was further delineated by studying the wavelength dependence of this photochemical reaction. It had been reported before by Wayner and co-workers that 300 nm irradiation of SiO_x in the presence of 1-decene yielded a static water contact angle of 59°.[135] Irradiation with wavelengths greater than 275 nm of fused silica in the presence of 1-hexadecene also yielded only 60°. This implies that the additional modification is caused by the 254 nm radiation,[134] although the precise nature of the activation process was not clarified.

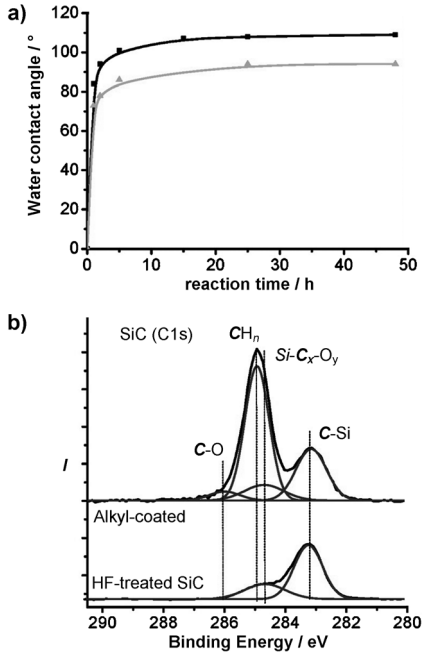

Figure 35. a) Static water contact angles measured on SiC substrates modified with 1-hexadecene using irradiation at 254 (■) and 330 nm (▲) for different reaction times. b) Normalized narrow-scan XPS data (C1s region) measured on SiC substrates: etched (HF-treated) and coated with 1-hexadecene for 24 h under irradiation with 254 nm wavelength.[132a]

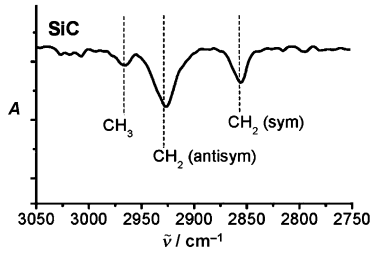

Figure 36. IRRA spectrum measured on 11-fluoroundec-1-ene monolayers on a SiC substrate.[132a]

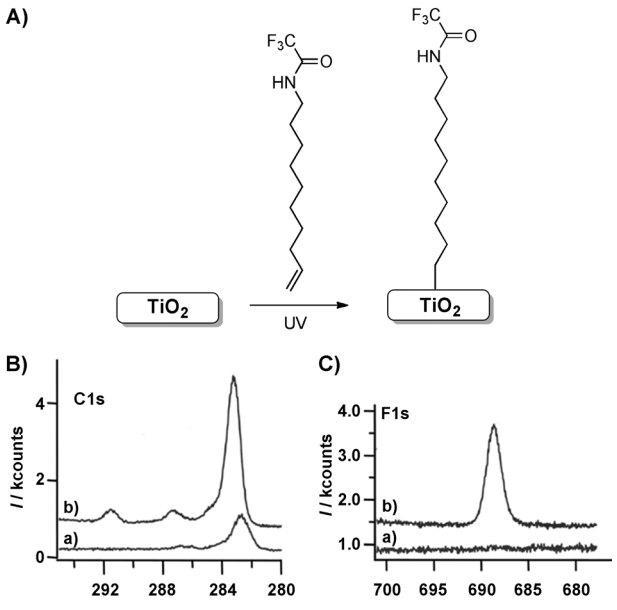

Figure 37. A) Photochemical attachment of 1-alkenes onto TiO_2, as inferred from the growth of characteristic XPS signals C1s (B) and F1s (C) before (a) and after attachment (b).[136]

The Hamers group demonstrated that an analogous surface reaction worked on TiO_2.[136] Irradiation of thin films of TiO_2 covered with trifluoroacetamide-protected 10-aminodec-1-ene (TFAAD) using 254 nm light (10 mW cm^{-2}) yields covalent attachment (Figure 37). Both the C1s and F1s XPS spectra display clear and characteristic signals that indicate the efficiency of this reaction (15 h irradiation time). Analogous to the irradiation of 1-alkenes on glass, disordered monolayers are formed. The IR spectrum, however, did not display any CH_3 signals, suggesting that in this case bonding occurs through the terminal C atom of the olefin group.

Hamers et al. label the effectiveness of this reaction as actually quite surprising, because TiO_2 is a widely established photocatalyst for degrading organic molecules. Mechanistically, the light is indicated to yield positively charged surface-bound hydroxyl radicals that may form a weak complex with the organic alkene, induce nucleophilic attack, and facilitate the transfer of an H atom needed to saturate the carbon atoms.[137] This reaction mechanism has been further explored using alkenes of varying reduction potentials.[138] This research has led to the conclusion that grafting of organic alkenes onto TiO_2 requires short-wavelength light able to photoexcite electrons from mid-gap surface states or possibly from electrons in the conduction band into acceptor levels of the adjacent alkene reactant molecules. The irreversible electron emission leaves the sample positively charged and enhances the subsequent reaction with the electron-rich vinyl group of the organic alkenes, to yield covalent surface attachment.

Both for the photochemical attachment onto glass and onto TiO_2, prolonged irradiation leads to multilayer formation for some alkenes (up to 10 nm has been reported). For the attachment onto TiO_2 this phenomenon has been related to the structure of the alkene.[139] Internal alkenes are shown to be hardly reactive, and geminal substitution slows down multilayer formation, but does not stop it (Figure 38 A). These results suggest a mechanism for multilayer formation as indicated in Figure 38 B.

Analogous photochemical attachments have since been developed on a variety of -OH terminated surfaces. Indium tin oxide (ITO) can be photochemically grafted at room temperature using 1-alkenes, allowing the direct patterning of an organic monolayer (Figure 39).[140] The attachment of 1-alkenes occurs via the formation of an C-O-In(Sn) linkage, and yields a highly stable monolayer even at elevated temperatures. For the tetradec-1-ene used in this case only monolayer formation was observed. Since ITO is transparent, ellipsometry does not work to estimate the layer thickness, but XPS is actually easily applicable, as the extent of the decrease in the substrate In 3d signal can be used to estimate the thickness of the organic layer. This method yielded a thickness of 1.4 nm after 16 h of irradiation, that is, slightly less than the length of a C_{14}-alkene, indicating that the layer formation is largely self-limited to a monolayer. This is consistent with the observation of photografting 1-hexene on TiO_2 surface,[139] but contrasts with the observation of eventual multilayer formation under these conditions on

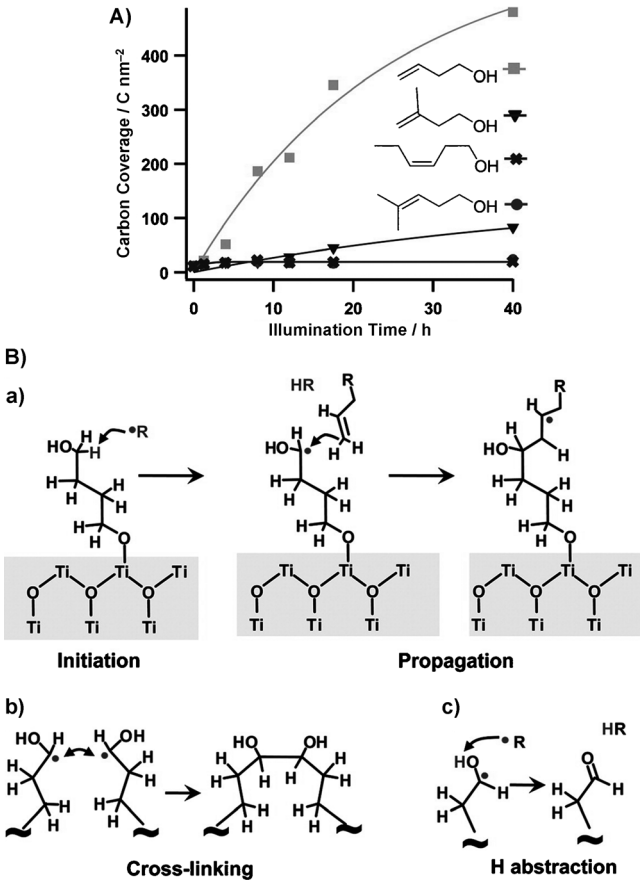

Figure 38. A) C1s XPS coverage kinetics for rutile (110) grafted with various alkenes; B) Proposed mechanism for multilayer formation.[139]

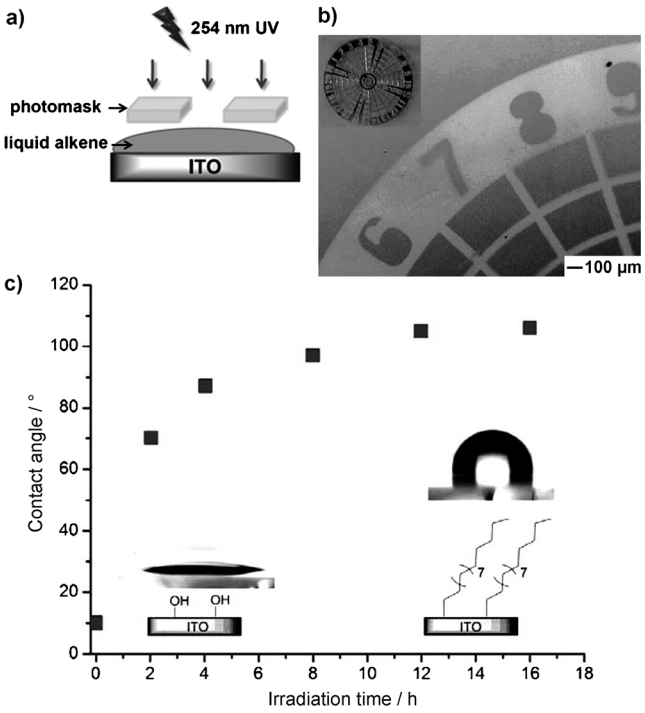

Figure 39. a,b) Constructive photopatterning onto ITO by irradiation through a mask of an ITO surface covered with an alkene. c) Contact angle of a developing C_{14}-alkene-derived organic layer on ITO as function of UV irradiation time.[140a]

Dateiname: A306709e
Pfad: L:/daten/Verlage/VCH/ACH/Hefte/1425/
Status Neusatz
Datum: 24 KW., 11. Juni 2014 (Mittwoch)
Pagina: 6341
Seite: 20 te von 35
Umfang (Seiten): 35
Zeit: 9:22:57 Uhr

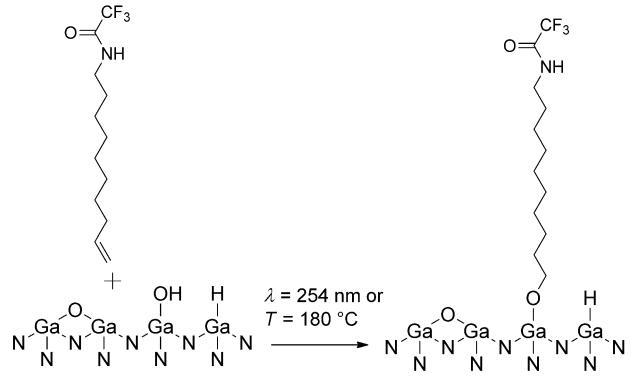

Figure 40. Proposed reaction scheme of the functionalization of GaN surfaces with alkenes.[144]

SiC and SiO_2 substrates,[132a,134] and/or OH-terminated alkenes on TiO_2.[139]

Analogous photochemical reactions have been reported on ZnO(1010) single crystals and ZnO nanorods,[141] zirconium oxide,[142] SnO_2 nanoparticle thin films,[143] and GaN.[144] In the GaN case the molecules are attached to the GaN surface by a Ga-O-C bridge, as indicated in Figure 40. This image also indicates nicely that on many hydroxy-containing surfaces the actual surface composition can be quite heterogeneous, as GaN is no exception in this respect.

6.2. Thermal Attachment of Alkenes/Alkynes

As already indicated briefly in Section 6.1, such photochemical reactions also have a thermal analogue on some of these surfaces. Typically, this reaction works on a wider scale of substrates than the photochemical analogue. The initial paper of Mischki et al. reported a static water contact angle of 91° on glass after heating with 1-decene at 150 °C for 16 h, and an acid-catalyzed Markovnikov addition was proposed as the operative mechanism.[135] For the modification of hydroxy-terminated SiC surfaces, a water contact angle of 107° was obtained upon heating with 1-octadecene at 130 °C for 6 h.[132b] Using alkenes to modify a platinum electrode that is already covered with a thin layer of platinum oxide yields analogous monolayers, and provides an alternative entry point to the modification of metals.[145]

An only recently explored hydroxy-terminated surface is plasma-activated chromium nitride (CrN). CrN is of increasing interest owing to a combination of five rather remarkable properties:

1) outstanding wear and high-temperature corrosion resistance (even surpassing TiN),
2) low friction coefficient,
3) very high hardness (25 GPa or HK 2800), and not shattering as easily as other ultra-hard, but non-metallic carbides or diamonds,
4) low electrical resistivity (640 $\mu\Omega\,cm^{-1}$) and high melting point (ca. 1770 °C for 1:1 CrN),
5) high biocompatibility and low toxicity, in contrast to, for example, hexavalent chromium.

The use of this material would thus likely become even more promising if the surface properties of CrN could be tuned to be optimal, for example, for high-wear conditions, or be fine-tuned to minimize the response by the immune system

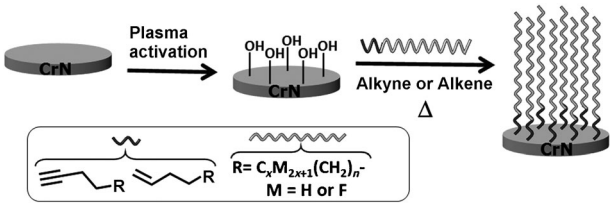

Figure 41. Schematic representation of the formation of alkyne and alkene-derived organic monolayers on a plasma-activated, hydroxy-terminated CrN surface.[146]

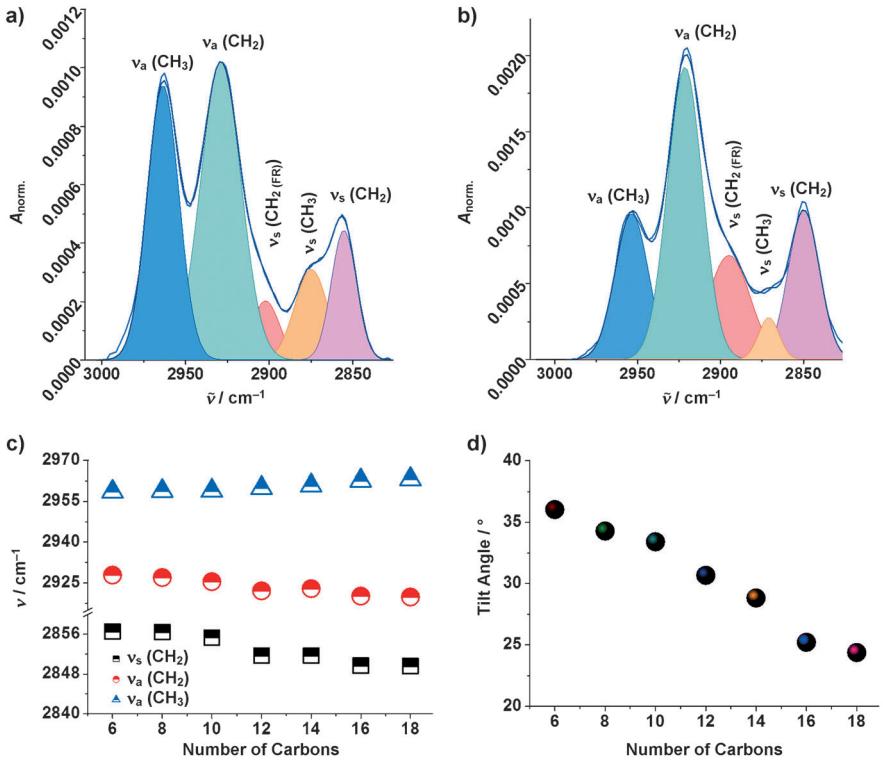

Figure 42. Deconvoluted IRRAS spectrum of a) 1-hexyne and b) 1-octadecyne monolayers on CrN surfaces. c) Overview: peak positions for 1-hexyne to 1-octadecyne monolayers: symmetric methylene stretch (ν_a CH_2, half-filled squares), anti-symmetric methylene stretch (ν_a CH_2, half-filled circles), and asymmetric methyl stretch (ν_a CH_3, half-filled triangles). d) Tilt angle with respect to the surface normal for varying molecular lengths.[146]

Dateiname: A306709e
Pfad: L:/daten/Verlage/VCH/ACH/Hefte/1425/
Status Neusatz
Datum: 24 KW., 11. Juni 2014 (Mittwoch)

Pagina: 6342
Seite: 21 te von 35
Umfang (Seiten): 35
Zeit: 9:22:57 Uhr

upon placement of a medical implant in the body. Such applications would require a precisely tuned modification of the surface, as for example, obtainable using covalently attached organic monolayers. Also for this material the attachment of unsaturated hydrocarbons offers a versatile approach using non-corrosive chemicals, as indicated in Figure 41.[50,146]

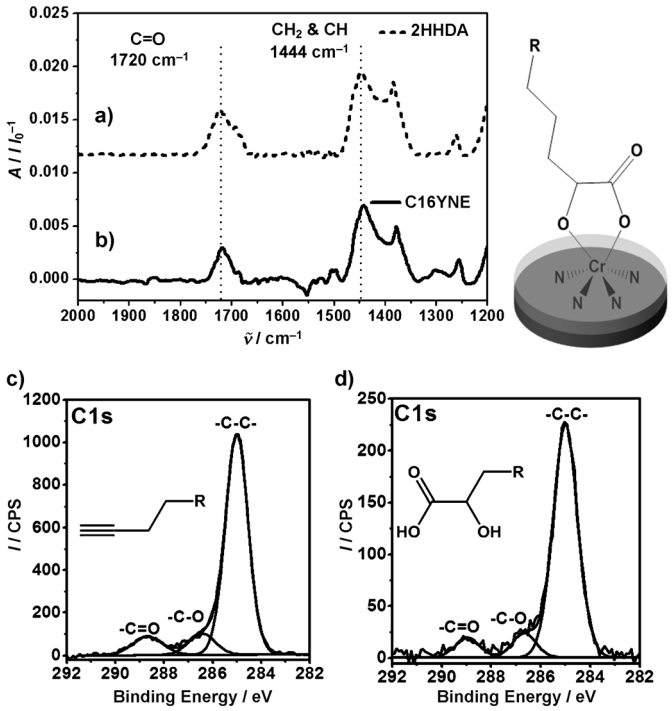

Figure 43. a) IRRAS spectra of a 2-hydroxyhexadecanoic acid (2HHDA)-derived monolayer and b) 1-hexadecyne-derived (C16YNE) monolayer on plasma-activated CrN surfaces. Binding mode of 2HHDA onto the oxidized CrN surface, resulting from the oxidative adsorption of the terminal alkyne functionality. c,d) XPS C1s narrow scan of 1-hexadecyne and 2-hydroxyhexadecanoic acid monolayers on plasma-activated CrN surfaces.[146]

This study displayed a series of novel mechanistic insights. First, whereas the attachment of 1-alkenes required 160 °C for 12 h to reach a limiting water contact angle of 110°, for 1-alkynes only 100 °C was required to obtain similar results in 8 h. Such much faster surface modification by alkynes than by alkenes has been shown before on, for example, H-terminated silicon,[5,147] but clearly also applies on oxides although the mechanism is likely very different. Second, the mode of attachment is completely different from that reported above in at least three respects: a combination of IR, XPS, and computational studies (DFT calculations) shows that these materials form only monolayers, that they display a high degree of short-range order and that an oxidative mode of attachment is followed. The observed monolayer thicknesses range from 0.6 to 2.2 nm for C_6-alkyne to C_{18}-alkyne monolayers, respectively, in line with the formation of dense monolayers with all-*trans* alkyl chains. This confirms the lack of multilayer formation for any of the materials. With increasing alkyl chain lengths, these films become increasingly well-ordered and less tilted, as clear from a detailed IR analysis (Figure 42).[146]

Finally, the mode of attachment of 1-alkynes was confirmed to yield a 2-hydroxy-1-carboxylate structure, as was shown by a one to one comparison of independently made monolayers (Figure 43). Accurately benchmarked DFT simulations (based on B3LYP/6-311G(d,p) level calculation) of C1s XPS spectra,[148] showed that a C=O signal is to be expected at 289.5 eV, while -*C*-C=O carbon atom should give rise to a signal at 287.6 eV, in close to agreement with the experiment. The mechanism for such an oxidation reaction is not fully clear yet, also in view of the heterogeneity of the surface, but such reactions have also been observed for the analogous attachment of 1-alkynes onto porous aluminum oxide.[149] For 1-alkenes oxidative attachment to yield 1-carboxylic acids has been observed both on CrN and Al_2O_3. In contrast, we recently found that 1-alkyne groups likely react with the hydroxy-terminated SiC surface through a double Markovnikov addition, forming a doubly bound, acetal-containing heteroatomic six-membered ring,[150] suggesting yet another pathway for the reaction of unsaturated hydrocarbons with OH-terminated surfaces.

6.3. Applications of Alkene/Alkyne-Based Monolayers

The strong points of this alkene or alkyne attachment onto -OH terminated surfaces can be indicated by a few examples that critically hinge on characteristic features of this reaction. The first example relates to the stability of the resulting layer.[6,132b,151] Thermally prepared monolayers of 1-hexadecene on SiC were heated for 4 h in 2 M HCl at 90 °C and did not display an observable change in the static water contact angle (107°).[132b] Similarly, photochemical grafting of an ester-functionalized alkene onto nanocrystalline TiO_2 (anatase) yielded a structure that, after an initial loss of 30–40 % of ester monolayers within in the first hour of immersion, remained

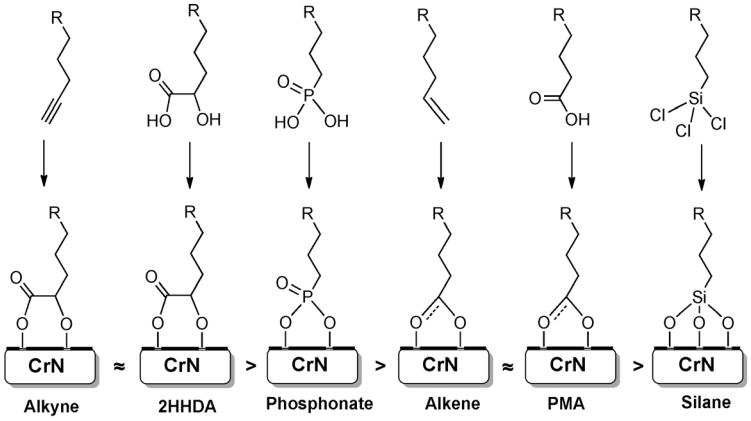

Figure 44. C1s XPS-derived stability order of organic monolayers with different anchoring groups on hydroxy-terminated CrN. PMA = palmitic acid.[50]

Dateiname: A306709e
Pfad: L:/daten/Verlage/VCH/ACH/Hefte/1425/
Status Neusatz
Datum: 24 KW., 11. Juni 2014 (Mittwoch)
Pagina: 6343
Seite: 22 te von 35
Umfang (Seiten): 35
Zeit: 9:22:59 Uhr

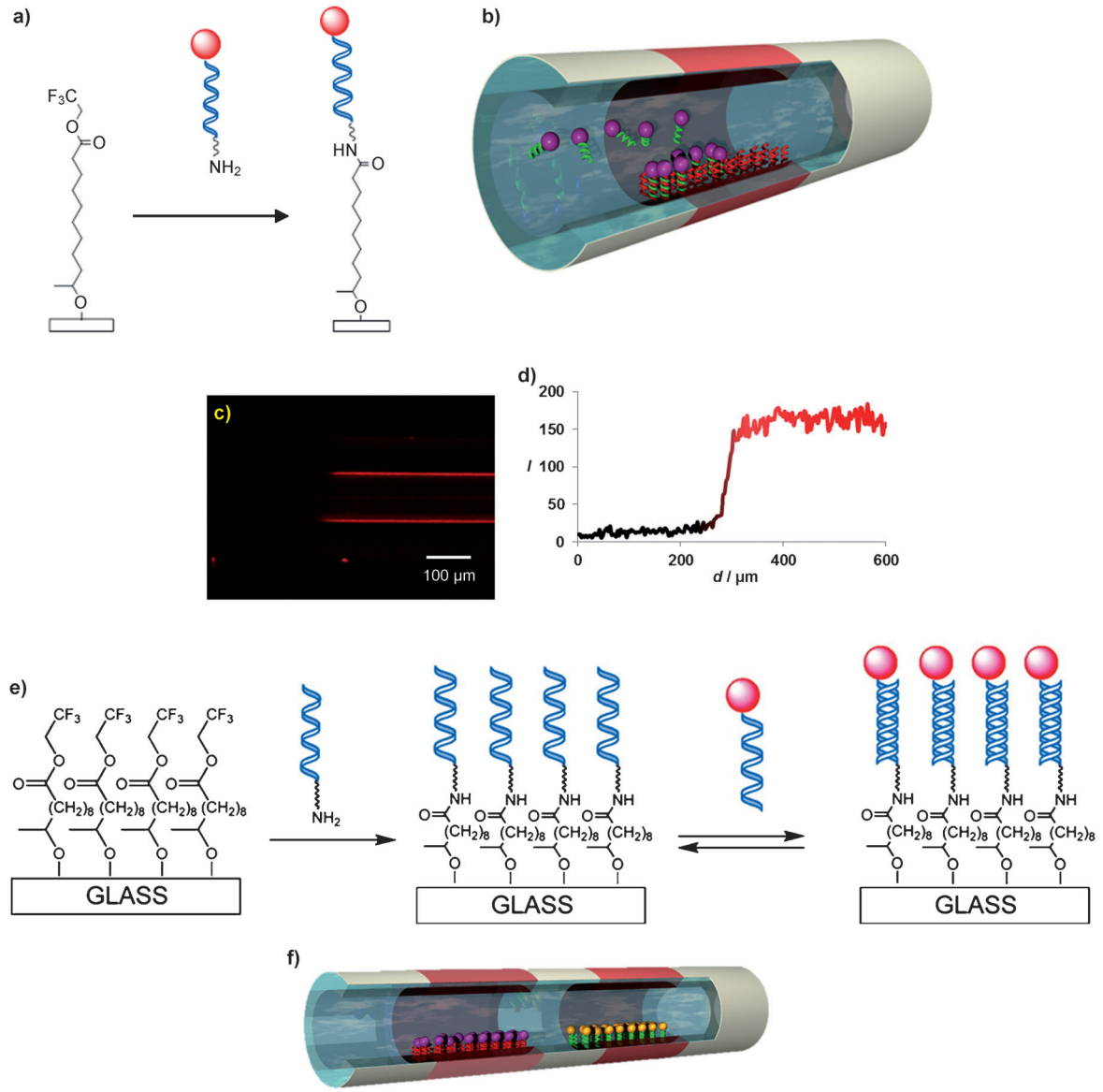

Figure 45. a,b) Local irradiation of a glass microchannel, b) the microchannel provides local attachment of an activated ester. c,d) Subsequent reaction with fluorescently labeled DNA displays the local functionalization of DNA. The confocal image of a modified capillary with an inner diameter of 100 µm indicates the transition distance. e) Covalent functionalization with a non-fluorescent oligo-DNA, which is then used to hybridize with fluorescently labeled DNA, to show the possibility of local hybridization.[152a] f) Spatially selective immobilization of two different DNA fragments has been used to position two enzymatic DNA–protein hybrids that are part of an enzymatic cascade reaction.[152b]

stable to the limit of the experiment, which was 50 days at elevated temperatures and a range of pH values.[137] On some oxides this may have to do with the formation of cross-linked multilayers. The potential of this is similar to that observed above for multilayers of, for example, dopamine (Section 5), namely that of highly stable, highly functionalized thin films. Even though the above examples are among the best ones obtained for this class of attachment chemistry, on many surfaces alkene-based and alkyne-based monolayers display a significantly higher stability than for example, silane-based or carboxylate-derived ones,[140a] and systematic evaluations thereof are in progress.[6] This stability aspect was studied in great detail for plasma-activated CrN surfaces coated by silane, phosphonate, alkene, and alkyne attachment chemistries (Figure 44).[50] Overall, all monolayers provided a good long-term stability in warm media, with the overall stability order 1-alkynes ≈ 2-hydroxy-1-carboxylic acids > phosphonate > 1-alkenes ≈ carboxylates > silanes.

The second example relates to the option to use photochemistry for constructive photopatterning and is rather unique in monolayer formation on oxide surfaces. This feature did, for example, allow the local attachment of DNA at the inside of a microchannel and follow-up hybridization experiments (Figure 45).[152] After the attachment of an activated ester using UV irradiation, a NH_2-functionalized oligoDNA is covalently bound. If this DNA is fluorescently labeled, the local attachment of DNA can be detected (Figure 45 c,d). Building on this approach, hybridization

Dateiname: A306709e
Pfad: L:/daten/Verlage/VCH/ACH/Hefte/1425/
Status Neusatz
Datum: 24 KW., 11. Juni 2014 (Mittwoch)
Pagina: 6344
Seite: 23 te von 35
Umfang (Seiten): 35
Zeit: 9:23:00 Uhr

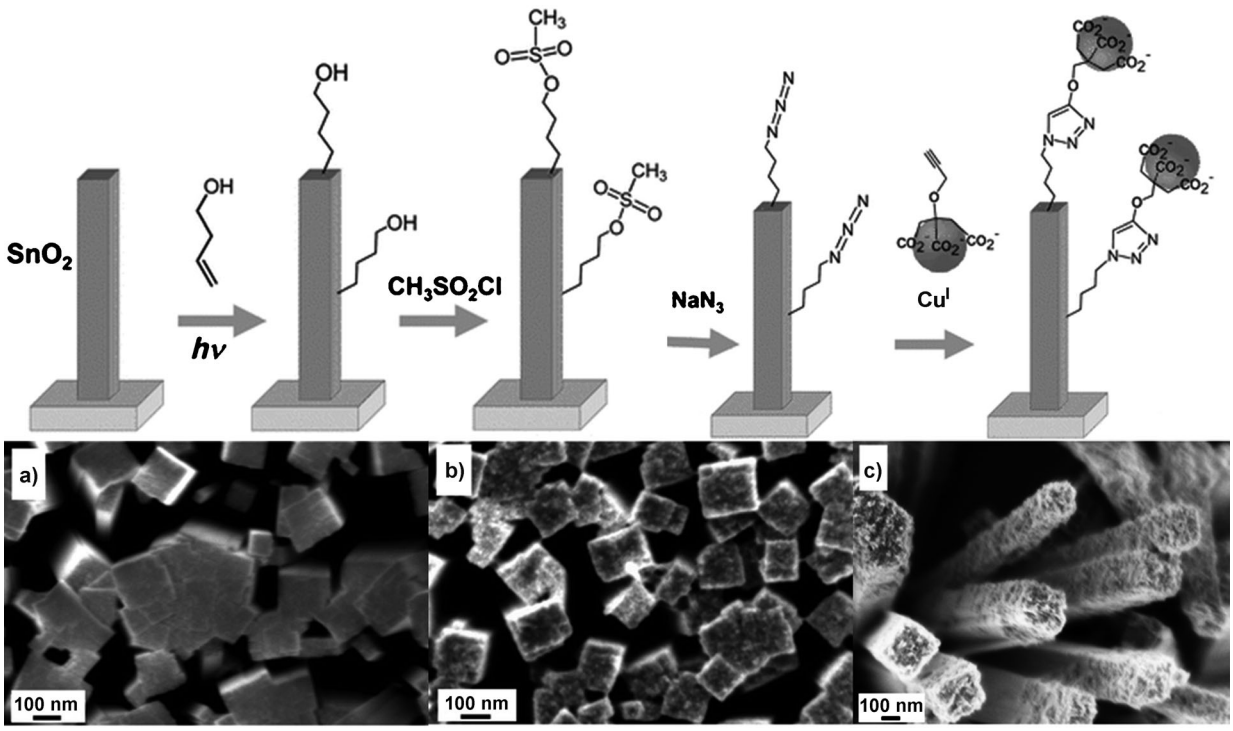

Figure 46. Top: Stepwise formation of an azide-terminated SnO_2 surface and subsequent CuAAC reaction with alkyne to allow the attachment of TiO_2 nanoparticles. Bottom: SEM images of SnO_2 nanorods. a) Uncoated SnO_2 nanorods; b) SnO_2 nanorods coated with TiO_2 nanoparticles, and c) higher-resolution SEM image of an SnO_2–TiO_2 adduct.[143b]

experiments on locally attached DNA can be performed with complementary oligo-DNA strands, which can again be visualized easily if the DNA strands are fluorescently labelled (Figure 45 e). This also allowed the spatially selective attachment of several DNA-enzyme hybrids for the construction of enzymatic cascade reactions (Figure 45 f).[152b] Clearly, this patterning is only feasible because of the photochemical nature of the initial surface modification reaction.

The photochemical reaction of -OH-terminated alkenes is a very attractive mode of surface functionalization, as it provides a stable, high density of surface alcohol groups that allow a two-step approach towards surface functionalization.[39] Recently Shah et al. elegantly used functionalization with 3-buten-1-ol to bind TiO_2 nanoparticles to SnO_2 nanorods through a 1-alkyne that was terminally functionalized with three carboxylic acid moieties, eventually yielding an enhancement of the interfacial charge transfer compared to the unmodified SnO_2 nanorods (Figure 46).[143b] A similar approach has also shown to be effective for the biofunctionalization of titanium substrates.[153]

The photochemical attachment of 5-hexen-1-ol onto ITO has to be used for the construction of "romantic surfaces": surfaces that repel every biological entity apart from the desired one.[140b] To this aim, a monolayer with many alcohol moieties served as a platform for further surface functionalization by the smooth attachment of initiators for an atom-transfer radical polymerization (ATRP) by an acid bromide-to-alcohol coupling reaction. Next, a surface-initiated ATRP (SI-ATRP) reaction was used to attach zwitterionic polymer brushes to the ITO surface (Figure 47). Such zwitterionic polymers generated by SI-ATRP reactions generally exhibit very good antifouling properties.[154] Since the SI-ATRP approach continuously leaves a Br atom at the top of the growing polymer chain, this allows conversion of that bromine into an azide moiety after the polymerization reaction. Finally then a copper-free click reaction was performed using the strain-promoted alkyne-azide click (SPAAC) reaction,[155] so as to allow an optimal substrate for follow-up biological experiments (Figure 47). Coupling with a biotin-labeled cyclooctyne-derivative thus yielded the local attachment of biotin onto a generically protein-repellent surface. The potential of this was displayed by the location-specific binding of streptavidin, whereas the generally 'sticky' protein BSA is deposited everywhere apart from on the biotin-labeled area.[140b]

7. Amines

Alkyl amines have been used to coat OH-terminated surfaces (aromatic amines bind weakly and have not been widely used).[156] Molecularly thin films of octadecylamine self-assembled on mica can be prepared by immersion of the sample in chloroform solutions. The resulting films are always in the form of islands. Bonding between mica and octadecylamine is much weaker than those of, for example, alkylsilanes, and rinsing with the solvent easily removes the molecules. The molecular films are mechanically weak, and repetitive scanning with an AFM tip, even using a very low pressure on the tip causes damage.[157]

Dateiname: A306709e
Pfad: L:/daten/Verlage/VCH/ACH/Hefte/1425/
Status Neusatz
Datum: 24 KW., 11. Juni 2014 (Mittwoch)
Pagina: 6345
Seite: 24 te von 35
Umfang (Seiten): 35
Zeit: 9:23:02 Uhr

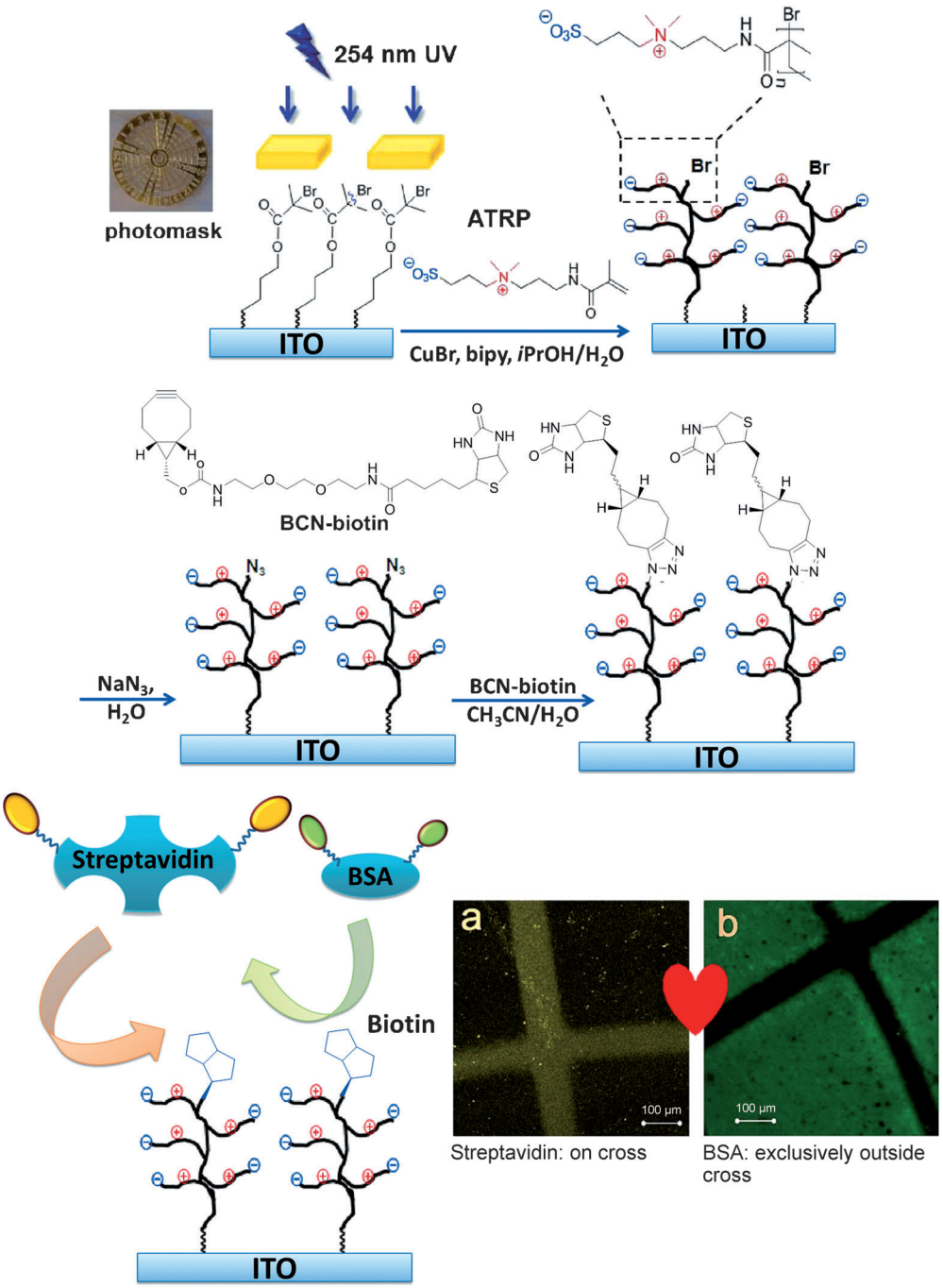

Figure 47. Construction of "romantic surfaces": Homogeneous deposition of an ATRP initiator and subsequent local patterning (254 nm light) burns away this initiator only at the irradiated places. Follow-up Si-ATRP then yields zwitterionic polymer brushes only at the places which were not irradiated in this second step.[140b] Next the polymer brush is top-functionalized with biotin in a SPAAC reaction, and displays very specific, locally tunable protein-adsorption behavior.[140b] Scale bars: 100 µm.

The binding of the molecules to the mica surface is strongly dependent on the presence of water, and water also facilitates the diffusivity of the molecules on the surface and accelerates the ripening process leading to aggregation into large islands and the elimination of defects. The nature of the bonding interactions can be surprisingly diverse, as illustrated by the different structures formed upon assembly of octadecylamine onto mica surface from either chloroform or ethanol. Octadecylamine adsorbs onto mica, either forming partial monolayers (islands) of nearly upright molecules when prepared from a relatively concentrated chloroform solution, or—when prepared from ethanol solutions—covering the surface completely with multilayers having alternating methyl and amino terminations. The partial coverage found with chloroform was shown to be the result of the incomplete displacement of the residual water film on mica by the hydrophobic solvent and octadecylamine desorption on water patches. This problem disappears with the hydrophilic ethanol

Dateiname: A306709e
Pfad: L:/daten/Verlage/VCH/ACH/Hefte/1425/
Status Neusatz
Datum: 24 KW., 11. Juni 2014 (Mittwoch)
Pagina: 6346
Seite: 25 te von 35
Umfang (Seiten): 35
Zeit: 9:23:03 Uhr

solvent, and full coverage is achieved, but then the stronger interaction with the solvent is apparently enough to disrupt the formation of a homogeneous monolayer. Micellar formation in ethanol was proposed as the mechanism leading to the formation of stacks of layers with alternating end-group termination.[158]

The following interactions are therefore expected to be important in SAM formation with amines. First, the amine moiety will form a H-bond with the surface -OH moieties, for example, surface silanols on quartz or glass. Second, the amine moiety is also expected to be protonated to some extent from its interaction with water. Such protonation decreases the cohesive energy owing to electrostatic repulsion between charged head groups (see also Ref. [159]) and keeps counterions near the surface. Third, specifically for amine monolayers in air, approximately 35–40% of the NH_2 moieties form carbamates because of atmospheric CO_2 dissolved in the adsorbed water layer.[160] This leads to a fast reaction of CO_2 with the amine, under the formation of alkyl ammonium alkylcarbamates, for which a considerable driving force is present.[161] These carbamates are typically deprotonated by adjacent amines, yielding monolayer-stabilizing alternating charges near the surface (Figure 48). This hypothesis is supported by three signals in the N 1s XPS data at 399.2, 400.4, and 401.7 eV, arising to free amino (NH_2), carbamates, and protonated NH_3^+ groups, respectively.[158] Finally, ATR-IR data of ODA/mica SAM islands further support this through the appearance of a new broad band around 1569 cm^{-1}, which is assigned to the deformation and vibration of the whole $-NH-COO^-$ group in carbamates. In addition, carbamate signals are always accompanied by bands at 1486 and 1645 cm^{-1}, arising from the NH_3^+ groups.

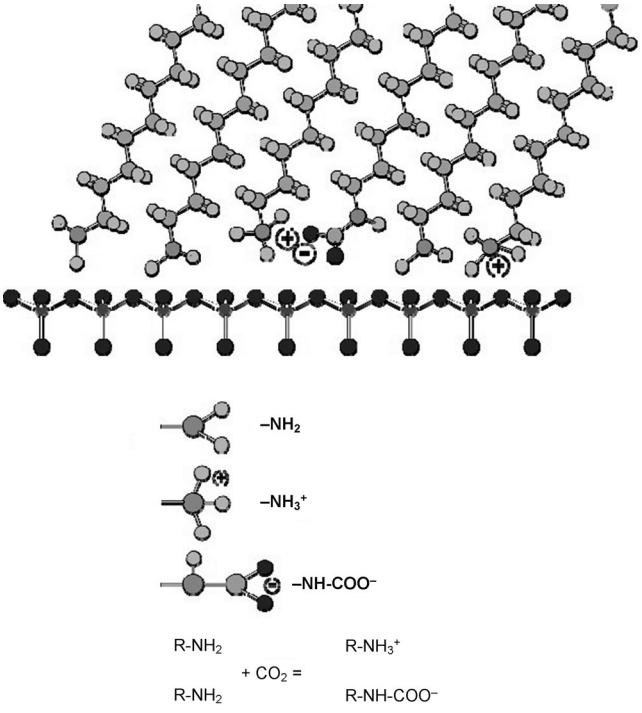

Figure 48. Structure of alkylamine monolayers on quartz as formed under ambient conditions in air.[160]

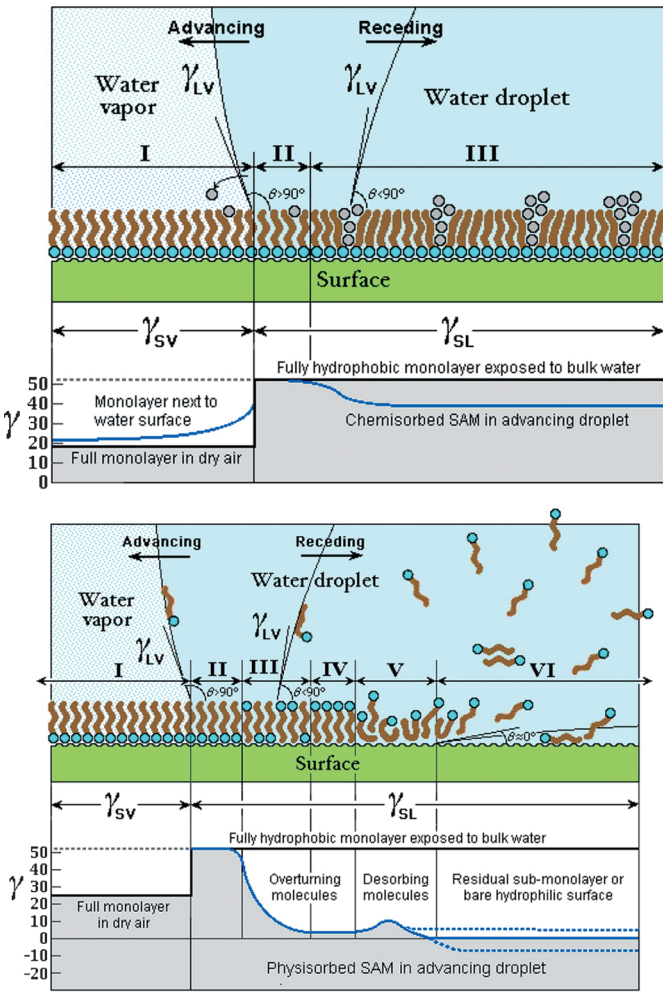

Figure 49. Wetting behavior of strongly bound (left) and weakly bound (right) monolayers.[164]

Detailed binding studies have been performed for the adsorption of amines onto Fe surfaces.[162] By a combination of SEM, IR, electrochemical impedance spectroscopy (EIS), and molecular modeling studies it was inferred that the N atom was most likely bound to iron in the pseudo-4-fold hollow sites of the Fe(110) surface.[162] Such Fe–N bonds on iron or stainless steel allow the use of alkylamines as inhibitors for iron and steel corrosion.[163]

The relatively weak surface attachment of amines may also induce dynamics in the monolayer, with a significant effect on, for example, the wetting behavior.[164] Whereas in a strongly bound (chemisorbed) layer, hysteresis in water contact angle measurements occurs owing to the presence of small pockets/defects in which water can reside, for more weakly bound monolayers, such as those of amines, the monolayer is a metastable state that can undergo a water-induced flipflop. Such a flipflop makes the monolayer more hydrophilic, however it is also bound even more weakly (Figure 49).

Amines have been widely used to form monolayers (ca. 5×10^{15} chains cm^{-2}) on cuprate high-temperature superconductors, such as $Bi_2Sr_2CaCu_2O_8$ and $YBa_2Cu_3O_7$, and are of interest since they do not adversely affect the bulk proper-

Dateiname: A306709e
Pfad: L:/daten/Verlage/VCH/ACH/Hefte/1425/
Status Neusatz
Datum: 24 KW., 11. Juni 2014 (Mittwoch)
Pagina: 6347
Seite: 26 te von 35
Umfang (Seiten): 35
Zeit: 9:23:07 Uhr

ties.[165] The adsorption involves the coordination of N atoms to Lewis acidic Cu sites on the surface, as was inferred from SIMS data that show an $[M+Cu]^+$ peak at m/z 363 with the expected Cu isotope distribution.[166] No peaks were observed for $[M+Ba]^+$ and $[M+Y]^+$ fragments. Hydrogen bonding between the amino groups of the adsorbates and O atom sites on the surface is not required for adsorption, because tertiary amines also form stable monolayer films.

8. Other types of monolayers

Several classes of compounds have over the years been used to a somewhat smaller degree, or have only very recently come up as alternative, surface-binding agents. In this Section we discuss the attachment chemistry of thiols (Section 8.1), alkyl iodides and alcohols as ether-forming moieties (Section 8.2), hydroxamic acids (Section 8.3), and boron compounds (Section 8.4).

8.1. Thiols

In contrast with the extremely well-studied case of thiols on gold,[3a] thiols on oxides have not been studied as much, although they do form SAMs on this surface as well. For the study of thiols on the readily oxidized copper surface Love et al. mention "*The chemistry is, however, not as forgiving in our experience as it is for silver, and considerable care is needed to prepare high-quality SAMs on copper. As a result of these experimental difficulties, the structures formed on this metal remain incompletely understood.*" The mechanism of the initial metal oxidation steps on alkanethiol-covered copper continues to be studied, for example, making use of surface-sensitive vibrational sum frequency spectroscopies.[167] Overall it can be stated that copper continues to oxidize underneath thiol-bound monolayers, but SAMs diminish corrosion considerably.[168]

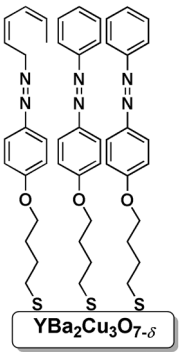

Figure 50. Reversibly switchable AZ monolayer on $YBa_2Cu_3O_{7-\delta}$.

On well-defined oxides, such as ZnO-$(10\bar{1}0)$ single-crystal surfaces, thiol-linked monolayers are found to be quite stable, as indicated, for example, by the mechanical force required to dislodge $C_{16}H_{33}PO_3H_2$ and $C_{18}H_{37}SH$ monolayers: whereas a small scratching force and an approximately 0.02 V cantilever deflection (force ca. 40 nN) in contact mode are enough to remove the $C_{16}H_{33}PO_3H_2$ layer, a loading of over 0.5 V (ca. 1 μN) is required to scratch the grafted $C_{18}H_{37}SH$ monolayer.[169] Continued etching of the oxide underneath the monolayer takes place, as observed from etching pits. The stability of thiol-bound monolayers can be increased by the use of bipodal thiols, as demonstrated for the adsorption of H_2N-$(CH_2)_{11}$-$CH(CH_2SH)_2$. Such bipodal layers unfortunately, of course also suffer from a reduced diffusion along the surface which is required for optimal monolayer formation.[170] Yet, despite the lack of clarity in the mechanism and ill-defined surfaces, thiol-based monolayers can be used, for example, to link other, more weakly binding materials, such as amines, to a surface, as shown for the attachment of hexane-1,6-diamine onto copper through surface-bound 2-mercaptoethanol.[171]

A very nice example of the use of thiol-linked monolayers is found for binding to cuprate superconducting films.[102] An optically switchable, azobenzene derivative (1-butanethiol,4[4-(phenylazo)phenoxy] (AZ); Figure 50), was used along with light to reversibly modulate the value of the critical temperature of high-T_c superconductors, such as $YBa_2Cu_3O_{7-\delta}$. As a result of a light-induced change in conformation and thus in dipole, AZ monolayers had previously been shown to change the transport and superconducting properties of thin niobium films.[172] Their application to a much wider range of oxides thus turns out to be possible.

8.2. Ether-Forming Moieties: Alkyl Iodides and Alcohols

Alkyl iodides can smoothly form a monolayer on hydroxy-terminated surfaces through a surface analogue of the Williamson ether synthesis.[173] This process has been studied in detail on TiO_2 surfaces, and the kinetics revealed an activation barrier of approximately 59 kJ mol^{-1} for the formation of the Ti-O-C linkage. The resulting monolayer displays a mixed stability (some sites being removed easily, some are very stable), which reflects the different binding sites of the monolayer caused by the heterogeneity of the TiO_2 surface. TiO_2 anatase surfaces are terminated with Ti and O atoms with lower coordination numbers (4 and 5 for Ti; 2 for O) than those of the bulk phase (6 for Ti and 3 for O). The relative amounts of these undercoordinated species vary between different crystal planes. Figure 51 a shows a model of a section of the anatase(101) surface, which shows that there are at least two distinct types of OH groups on the surface (labeled as $Ti_5^{4+}OH$ and $(Ti_5^{4+})_2OH$, which display very different properties (e.g. pK_a difference of more than 10).[173] These different sites can both react with alkyl iodides, but yield Ti-O–C bonds of rather different stabilities.

Such ether-linked monolayers can also be formed from alcohols. Whereas the room-temperature adsorption of monodentate alcohol-linked monolayers onto OH-terminated

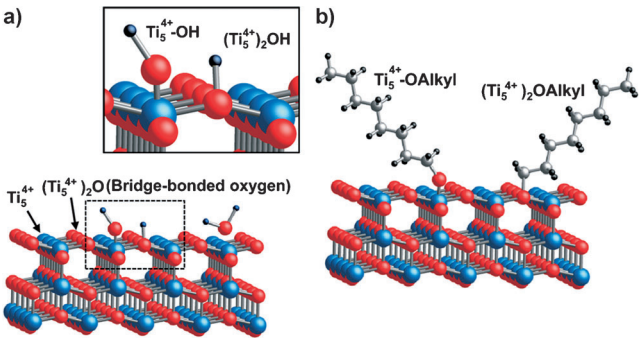

Figure 51. The two different binding sites for the hydroxy groups (a) and the alkoxy groups (b) on the anatase TiO_2 (101) surface.[173]

Dateiname: A306709e
Pfad: L:/daten/Verlage/VCH/ACH/Hefte/1425/
Status Neusatz
Datum: 24 KW., 11. Juni 2014 (Mittwoch)

Pagina: 6348
Seite: 27 te von 35
Umfang (Seiten): 35
Zeit: 9:23:09 Uhr

surfaces yields monolayers that are bound too weakly to be of practical value, heat-induced monolayer formation can actually yield stable layers. Especially multipodal alcohols are able to form stable layers, on, for example, SiO_2 and TiO_2 through a thermally induced removal of water (Figure 52).[174] Such thermally prepared, ether-linked layers were more stable than, for example, carboxylate-bound monolayers, when a monopodal molecule was present. But especially with a bipodal material superior stability (>1 month in deionized water or acetonitrile at room temperature) was displayed in comparison with the more commonly used carboxylate linkage.

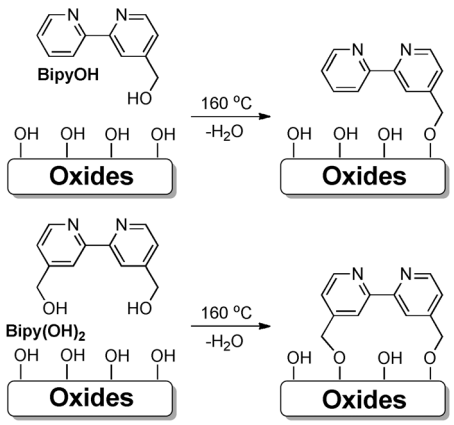

Figure 52. Preparation of grafted bipyridine layers from hydroxy-functionalized bipyridines.[174]

8.3. Hydroxamic Acids

Hydroxamic acids (R-(C=O)NHOH) are well-known excellent chelating ligands for many transition-metal cations,[175] and have already been used in applications such as corrosion protection. Hydroxamic acid exists in two tautomeric forms, with the keto form dominating in acid media and the enol form in alkaline environments (Figure 53). The keto tautomer behaves as a mono-acid, while the enol can provide two sites for chelation. On many oxides, hydroxamic acids can undergo facile double deprotonation, thus providing dianionic anchoring groups, which allows the formation of oxidation- and water-stable five-membered chelate rings of arylhydroxamates on suitable oxides, for example, TiO_2.[99,100]

Alkyl hydroxamic acids bind relatively weakly on TiO_2, but still form SAMs that are more stable than those from carboxylic acids (although not as stable as those from alkyl phosphonic acids, catechols, or alkenes).[80e] The higher monolayer stability with hydroxamates relative to carboxylates is caused by the larger bite angle (ca. 75°) of the hydroxamate, which forms five-membered chelate rings with metal ions, whereas carboxylates either form strained, four-membered chelate rings (bite angle ca. 60°) or monodentate species (see Section 4).

Hydroxamates have been shown, especially by Crabtree and co-workers, to be very useful for studies of light-induced electron transfer of dyes attached onto TiO_2, as relevant for

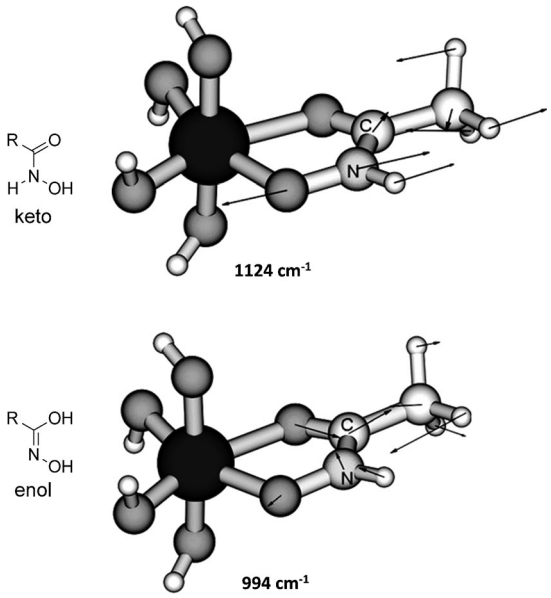

Figure 53. Left: Tautomeric forms of hydroxamic acids. Right: Characteristic vibrations of TiO_2-bound hydroxamic acids.[176]

the development of dye-sensitized solar cells (DSSCs). In this case the higher stability with respect to carboxylates makes such hydroxamate-based DSSCs more resistant to humidity, and allows the detailed study of the ultrafast interfacial electron transfer.[177] This was also borne out when hydroxamates were compared with carboxylate, phosphonate, and acetylacetonate as monolayer-forming groups: the hydroxamates turned out to be clearly superior linker groups to TiO_2 in terms of stability or electron injection efficiency.[100] Specifically, phosphonate anchors may be more stable, but the hydroxamates more than overcome that by increased electron injection efficiencies for the hydroxamate-anchored Grätzel-type N719 ruthenium dye.[99]

8.4. Boron Compounds

Given the intrinsically high affinity of boron for oxygen, boronic acids and derivatives thereof can form stable layers onto OH-terminated surfaces, as has recently been shown by Yerushalmi and co-workers.[178] Such layers are easily investigated by IR spectroscopy owing to the highly polar B–O bond. This reactivity is analogous to that used to obtain silica-supported boron compounds, such as $SiO\text{-}B(C_6F_5)_3\text{-}[HNEt_2Ph]$, from the reaction of $B(C_6F_5)_3$ with silanol groups.[179] Such a supported, single-site Lewis acid, $\equiv SiOB(C_6F_5)_2$, is effective as a co-catalyst in the polymerization of ethene.[180]

9. Summary and Outlook

The examples presented in this Review provide an overview of this exciting and still rapidly growing field. Surface modifications have in many cases reached sufficient

Dateiname: A306709e
Pfad: L:/daten/Verlage/VCH/ACH/Hefte/1425/
Status Neusatz
Datum: 24 KW., 11. Juni 2014 (Mittwoch)
Pagina: 6349
Seite: 28 te von 35
Umfang (Seiten): 35
Zeit: 9:23:10 Uhr

robustness for a routine and large-scale application, yet there is still both room and need for improvements in several areas that require further research. In this final Section we therefore focus on some trends and new, as of yet underexposed issues.

Historically silanes and carboxylates have been studied most. Whenever the hydrolytic stability is an issue, it is to be expected that these anchoring groups are going to be replaced by phosphonates, catechols, or alkenes/alkynes, as these generally provide a more stable monolayer coverage under mild, non-corrosive reaction conditions. Yet, the environmental friendliness of carboxylic acids, or the high reaction rates of silanes may be reasons to stick to this chemistry. In addition, multidentate approaches to for example, carboxylic acid or phosphonate attachments may also overcome these limitations. Regarding method development, it becomes increasingly clear that gas-phase methods provide significant opportunities for quality improvement of several types of monolayers, and for the scaling-up of the formation of nearly all types of organic monolayers on oxides. This is not least because the solvent typically plays a negative role in many of the discussed approaches.

The demand for increased stability may increasingly gain from minute but very specific inorganic modifications of the inorganic surface, prior to monolayer attachment. Examples of one-atom-thick additional gluing layers include Bernasek's use of a Zr layer on AlOH to bind carboxylates,[93] or Chabal's approach to deposit AlOH onto SiOH to bind phosphonates.[60a] In this way the limited stability of an oxide to a specific organic anchor may be overcome. Yet, such poor binding can also be used in a positive manner, to obtain spatially selective binding on a heterogeneous surface, such as obtained for silanes and alkenes on hydrogen-terminated versus oxidized Si substrates,[35a] or of silanes and phosphonates on halloysite clay tubes.[76] A recent alternative for spatial selectivity is the use of photochemical attachments, which has been shown to work on substrates as varied as glass,[134,152b] ITO,[140] and SnO_2.[143b] In this field, also more mechanistic information is clearly needed for further development of stable monolayers. A problem that needs to be addressed is, for example, determining the mechansim of formation of multilayers in catechol or alkene attachments. Such mechanistic studies would also be of interest in the field of curing effects on, for example, phosphonate-derived monolayers, again in view of the stability that can be obtained. Finally, more mechanistic studies would hopefully lead to the development of even milder monolayer-forming agents. In the field of, for example, oxide-free, H-terminated Si, the development of agents such as ynenes[7] typically reduced the reaction temperatures from over 100 °C to room temperature with concomitant improvement of monolayer quality or stability. The field of oxide modifications is also still in need of such agents, of which, for example, nitrocatechol as developed from the initial DOPA or catechol-based monolayers is a nice initial example.[130a]

Finally, Table 1 undertakes a somewhat daunting summary of the entire field. Although admittedly oversimplifying,

Table 1: Overview of reported substrate–monolayer combinations with a rough indication of the quality of the monolayer obtained.

Oxide Surface and Activation method[182]	Silane[9b,c]	Phosphonate	Carboxylate	Catechol	Alkene/Alkyne	Amine	Other(b)
glass[a,b]	++ [9b,12d,183]		+/− [97]	+ [184]	++ [134]	++ [159,160]	R-B-Cl[178] Arsonic acid[181a]
SiO_x[9a][a–c]	++ [9c,12d]	+/− [56a]	+ [97]	+/− [185]	++ [134]		
SiC[186][d]	++ [187]	+ [188]			++ [132b,186,189]		
Al_2O_3[190][e,a,f]	++ [190,191]	++ [181f]	+/− [192]	++ [193]	++ [149,151]		
TiO_2[194][g,h]	+/− [195]	++ [56a,73]	+/− [80b]	++ [115b]	++ [137]		R-OH[174] HA[80e] R-I[173]
ITO[b,i,h]	+/− [196]	++ [62b,197]	+/− [198]	+/− [199]	++ [140]	+ [196b]	R-SH[198]
V/Cr/Steel[h,j]	++ [50,200]	++ [50,201]	+/− [50]	+ [153]	+/− [50,146]	+ [202]	R-SH [203]
SnO_2	++ [204]		++ [143b]				
Ta_2O_3[b,h]	++ [205]						
ZnO	+/− [206]	++ [169]	++			+ [169]	R-SH R-OH[169]
WO_3		++ [207]	++ [101]				
Cuprates			++ [102]		+ [165,166]		R-SH [102]
Nb_2O_5[h]	++ [172]					+ [208]	

[a] HCl/MeOH (1:1). [b] $NH_4OH/H_2O_2/H_2O$ (1:1:5, 65 °C), 5 min. [c] (1:1 30% H_2O_2/38% HCl) at 80 °C for 15 min. [d] HF 2.5%, 2 min. [e] 99% H_2SO_4, diluted to 10% *v*/*v* in DI water for 2 min at 0 °C. [f] Refluxing H_2O_2 (30%). [g] UV irradiation ($\lambda = 254$ nm, 10 mW cm^{-2}) in air overnight. [h] UV/ozone cleaning. [i] 0.5 M K_2CO_3 in a 3:1 methanol/H_2O mixture for 30 min. [j] air plasma.

Dateiname: A306709e
Pfad: L:/daten/Verlage/VCH/ACH/Hefte/1425/
Status Neusatz
Datum: 24 KW., 11. Juni 2014 (Mittwoch)
Pagina: 6350
Seite: 29 te von 35
Umfang (Seiten): 35
Zeit: 9:23:10 Uhr

it aims to summarize the monolayer quality obtained per substrate for each of the attachment chemistries reviewed herein. In the first column, the type of surface is indicated together with "best-practice" methods to properly activate that surface towards a hydroxy-oriented surface modification. In the remaining columns a rough quality indicator (++, +, etc.) is given of the substrate–monolayer combination. Of course, "quality" is dependent on the perspective and goals, and includes features such as structural organization, ease of use, and long-term stability. Hopefully this summarizing Table might help the reader to select an optimal monolayer–surface combination for their own purposes. In addition, this Table points to remaining challenges in terms of improved monolayer quality or the unknown territory of many as of yet unexplored combinations. Such novel combinations or entirely new attachment chemistries—which are currently being developed rapidly by many groups worldwide.[7,50,130b,181]—might also bring about the goal of extremely strong surface coatings that on cue might also be fully removed, in extension to, for example, the strong but mechanically removable coating of catechol on Ti.[125]

Received: July 31, 2013
Published online: May 21, 2014

[1] T. Kondo, R. Yamada, K. Uosaki, *Organized Organic Ultrathin Films, Fundamentals and Applications*, Wiley-VCH, Weinheim, **2013**, pp. 7–42.

[2] F. Renate, S. Holger, A. J. A. Tobias, *Surface Design: Applications in Bioscience and Nanotechnology*, Wiley-VCH, Weinheim, **2009**.

[3] a) J. C. Love, L. A. Estroff, J. K. Kriebel, R. G. Nuzzo, G. M. Whitesides, *Chem. Rev.* **2005**, *105*, 1103–1169; b) C. Vericat, M. E. Vela, G. Benitez, P. Carro, R. C. Salvarezza, *Chem. Soc. Rev.* **2010**, *39*, 1805–1834; c) E. Pensa, E. Cortés, G. Corthey, P. Carro, C. Vericat, M. H. Fonticelli, G. Benítez, A. A. Rubert, R. C. Salvarezza, *Acc. Chem. Res.* **2012**, *45*, 1183–1192; d) O. Zenasni, A. C. Jamison, T. R. Lee, *Soft Matter* **2013**, *9*, 6356–6370; e) H. Häkkinen, *Nat. Chem.* **2012**, *4*, 443–455.

[4] a) C. Stavis, T. L. Clare, J. E. Butler, A. D. Radadia, R. Carr, H. Zeng, W. P. King, J. A. Carlisle, A. Aksimentiev, R. Bashir, R. J. Hamers, *Proc. Natl. Acad. Sci. USA* **2011**, *108*, 983–988; b) W. Yang, O. Auciello, J. E. Butler, W. Cai, J. A. Carlisle, J. E. Gerbi, D. M. Gruen, T. Knickerbocker, T. L. Lasseter, J. N. Russell, L. M. Smith, R. J. Hamers, *Nat. Mater.* **2002**, *1*, 253–257; c) R. E. Ruther, M. L. Rigsby, J. B. Gerken, S. R. Hogendoorn, E. C. Landis, S. S. Stahl, R. J. Hamers, *J. Am. Chem. Soc.* **2011**, *133*, 5692–5694; d) R. E. Ruther, Q. Cui, R. J. Hamers, *J. Am. Chem. Soc.* **2013**, *135*, 5751–5761.

[5] Y. Li, S. Calder, O. Yaffe, D. Cahen, H. Haick, L. Kronik, H. Zuilhof, *Langmuir* **2012**, *28*, 9920–9929.

[6] N. S. Bhairamadgi, S. P. Pujari, F. G. Trovela, A. Debrassi, A. A. Khamis, J. M. Alonso, A. A. Al-Zahrani, T. Wennekes, H. A. Al-Turaif, C. van Rijn, Y. A. Alhamed, H. Zuilhof, *Langmuir*, **2014**, revision Manuscript ID: la-2014-00533f.

[7] B. Rijksen, S. P. Pujari, L. Scheres, C. J. M. van Rijn, J. E. Baio, T. Weidner, H. Zuilhof, *Langmuir* **2012**, *28*, 6577–6588.

[8] *Chem. Rev.* **2013**, *113*, (Issue no. 6 of Chemical Reviews 2013 deals entirely with the surface chemistry of oxides. These provide excellent entry points to various aspects of the surface side of this topic. Of specific interest to the general topic of this Review can be mentioned: J. M. Vohs, *Chem. Rev.* **2013**, *113*, 4136–4163.).

[9] a) S. Onclin, B. J. Ravoo, D. N. Reinhoudt, *Angew. Chem.* **2005**, *117*, 6438–6462; *Angew. Chem. Int. Ed.* **2005**, *44*, 6282–6304; b) C. Haensch, S. Hoeppener, U. S. Schubert, *Chem. Soc. Rev.* **2010**, *39*, 2323–2334; c) N. Herzer, S. Hoeppener, U. S. Schubert, *Chem. Commun.* **2010**, *46*, 5634–5652.

[10] a) E. P. Plueddemann, *Silane coupling agents*, Plenum, New York/London, **1982**; b) A. Ulman, *Chem. Rev.* **1996**, *96*, 1533–1554; c) A. Ulman, *An introduction to ultrathin organic films: from Langmuir–Blodgett to self-assembly*, Academic Press, Boston, **1991**.

[11] M. Grandbois, M. Beyer, M. Rief, H. Clausen-Schaumann, H. E. Gaub, *Science* **1999**, *283*, 1727–1730.

[12] a) R. Tian, O. Seitz, M. Li, W. Hu, Y. J. Chabal, J. Gao, *Langmuir* **2010**, *26*, 4563–4566; b) S. R. Walter, J. Youn, J. D. Emery, S. Kewalramani, J. W. Hennek, M. J. Bedzyk, A. Facchetti, T. J. Marks, F. M. Geiger, *J. Am. Chem. Soc.* **2012**, *134*, 11726–11733; c) J. Sagiv, *J. Am. Chem. Soc.* **1980**, *102*, 92–98; d) K. Wen, R. Maoz, H. Cohen, J. Sagiv, A. Gibaud, A. Desert, B. M. Ocko, *ACS Nano* **2008**, *2*, 579–599.

[13] A. Y. Fadeev, T. J. McCarthy, *J. Am. Chem. Soc.* **1999**, *121*, 12184–12185.

[14] a) Y. Lin, L. Wang, J. W. Krumpfer, J. J. Watkins, T. J. McCarthy, *Langmuir* **2013**, *29*, 1329–1332; b) A. Y. Fadeev, T. J. McCarthy, *Langmuir* **1999**, *15*, 3759–3766; c) I. Anac, T. J. McCarthy, *J. Colloid Interface Sci.* **2009**, *331*, 138–142.

[15] a) R. Chen, H. Kim, P. C. McIntyre, S. F. Bent, *Chem. Mater.* **2005**, *17*, 536–544; b) X. Jiang, S. F. Bent, *J. Phys. Chem. C* **2009**, *113*, 17613–17625.

[16] a) R. Helmy, R. W. Wenslow, A. Y. Fadeev, *J. Am. Chem. Soc.* **2004**, *126*, 7595–7600; b) see Ref. [13].

[17] a) D. Hausmann, J. Becker, S. Wang, R. G. Gordon, *Science* **2002**, *298*, 402–406; b) L. Netzer, R. Iscovici, J. Sagiv, *Thin Solid Films* **1983**, *99*, 235–241; c) A. Wang, H. Tang, T. Cao, S. O. Salley, K. Y. S. Ng, *J. Colloid Interface Sci.* **2005**, *291*, 438–447.

[18] F. Zhang, K. Sautter, A. M. Larsen, D. A. Findley, R. C. Davis, H. Samha, M. R. Linford, *Langmuir* **2010**, *26*, 14648–14654.

[19] a) J. Gun, J. Sagiv, *J. Colloid Interface Sci.* **1986**, *112*, 457–472; b) R. Maoz, H. Cohen, J. Sagiv, *Langmuir* **1998**, *14*, 5988–5993; c) S. Liu, R. Maoz, J. Sagiv, *Nano Lett.* **2004**, *4*, 845–851; d) A. Zeira, D. Chowdhury, R. Maoz, J. Sagiv, *ACS Nano* **2008**, *2*, 2554–2568.

[20] J. Zhang, J. Hoogboom, P. H. J. Kouwer, A. E. Rowan, T. Rasing, *J. Phys. Chem. C* **2008**, *112*, 20105–20108.

[21] N. Rozlosnik, M. C. Gerstenberg, N. B. Larsen, *Langmuir* **2003**, *19*, 1182–1188.

[22] a) M. E. McGovern, K. M. R. Kallury, M. Thompson, *Langmuir* **1994**, *10*, 3607–3614; b) T. Manifar, A. Rezaee, M. Sheikhzadeh, S. Mittler, *Appl. Surf. Sci.* **2008**, *254*, 4611–4619.

[23] Y.-a. Cheng, B. Zheng, P.-h. Chuang, S. Hsieh, *Langmuir* **2010**, *26*, 8256–8261.

[24] S. Desbief, L. Patrone, D. Goguenheim, D. Guerin, D. Vuillaume, *Phys. Chem. Chem. Phys.* **2011**, *13*, 2870–2879.

[25] C. P. Tripp, M. L. Hair, *Langmuir* **1995**, *11*, 149–155.

[26] R. M. Pasternack, S. R. Amy, Y. J. Chabal, *Langmuir* **2008**, *24*, 12963–12971.

[27] X. Cao, T. Zhang, J. Deng, L. Jiang, W. Yang, *ACS Appl. Mater. Interfaces* **2013**, *5*, 494–499.

[28] S. Xiang, G. Xing, W. Xue, C. Lu, J.-M. Lin, *Analyst* **2012**, *137*, 1669–1673.

[29] I. Haller, *J. Am. Chem. Soc.* **1978**, *100*, 8050–8055.

[30] J.-R. Li, J. C. Garno, *Nano Lett.* **2008**, *8*, 1916–1922.

[31] a) A. Hozumi, K. Ushiyama, H. Sugimura, O. Takai, *Langmuir* **1999**, *15*, 7600–7604; b) R. D. Lowe, M. A. Pellow, T. D. P. Stack, C. E. D. Chidsey, *Langmuir* **2011**, *27*, 9928–9935.

[32] a) W. Gu, C. P. Tripp, *Langmuir* **2006**, *22*, 5748–5752; b) X. Jia, T. J. McCarthy, *Langmuir* **2002**, *18*, 683–687.

Dateiname: A306709e
Pfad: L:/daten/Verlage/VCH/ACH/Hefte/1425/
Status Neusatz
Datum: 24 KW., 11. Juni 2014 (Mittwoch)

Pagina: 6351
Seite: 30 te von 35
Umfang (Seiten): 35
Zeit: 9:23:11 Uhr

[33] G. E. Fryxell, S. V. Mattigod, Y. Lin, H. Wu, S. Fiskum, K. Parker, F. Zheng, W. Yantasee, T. S. Zemanian, R. S. Addleman, J. Liu, K. Kemner, S. Kelly, X. Feng, *J. Mater. Chem.* **2007**, *17*, 2863 – 2874.

[34] S. P. Pujari, K. Ellinas, A. Tserepi, E. Gogolides, H. Zuilhof, *ACS Appl. Mater. Interfaces* **2014**, revision Manuscript ID: am-2014-000432.R1

[35] a) O. Seitz, P. G. Fernandes, G. A. Mahmud, H. C. Wen, H. J. Stiegler, R. A. Chapman, E. M. Vogel, Y. J. Chabal, *Langmuir* **2011**, *27*, 7337 – 7340; b) See Ref. [12a]; c) D. Aureau, Y. Varin, K. Roodenko, O. Seitz, O. Pluchery, Y. J. Chabal, *J. Phys. Chem. C* **2010**, *114*, 14180 – 14186; d) N. A. Lapin, Y. J. Chabal, *J. Phys. Chem. B* **2009**, *113*, 8776 – 8783.

[36] C. P. Tripp, M. L. Hair, *Langmuir* **1992**, *8*, 1961 – 1967.

[37] N. Aissaoui, L. Bergaoui, J. Landoulsi, J.-F. Lambert, S. Boujday, *Langmuir* **2012**, *28*, 656 – 665.

[38] a) M. Halik, H. Klauk, U. Zschieschang, G. Schmid, C. Dehm, M. Schutz, S. Maisch, F. Effenberger, M. Brunnbauer, F. Stellacci, *Nature* **2004**, *431*, 963 – 966; b) S. Kobayashi, T. Nishikawa, T. Takenobu, S. Mori, T. Shimoda, T. Mitani, H. Shimotani, N. Yoshimoto, S. Ogawa, Y. Iwasa, *Nat. Mater.* **2004**, *3*, 317 – 322; c) Y. Ahn, Y. Jang, N. Selvapalam, G. Yun, K. Kim, *Angew. Chem.* **2013**, *125*, 3222 – 3226; *Angew. Chem. Int. Ed.* **2013**, *52*, 3140 – 3144.

[39] J. J. Gooding, S. Ciampi, *Chem. Soc. Rev.* **2011**, *40*, 2704 – 2718.

[40] Y. Liu, V. N. Khabashesku, N. J. Halas, *J. Am. Chem. Soc.* **2005**, *127*, 3712 – 3713.

[41] G. Balasundaram, M. Sato, T. J. Webster, *Biomaterials* **2006**, *27*, 2798 – 2805.

[42] J. A. Howarter, J. P. Youngblood, *Langmuir* **2006**, *22*, 11142 – 11147.

[43] a) A. Zeira, D. Chowdhury, S. Hoeppener, S. Liu, J. Berson, S. R. Cohen, R. Maoz, J. Sagiv, *Langmuir* **2009**, *25*, 13984 – 14001; b) R. A. Shircliff, P. Stradins, H. Moutinho, J. Fennell, M. L. Ghirardi, S. W. Cowley, H. M. Branz, I. T. Martin, *Langmuir* **2013**, *29*, 4057 – 4067.

[44] R. A. Walker, K. Wilson, A. F. Lee, J. Woodford, V. H. Grassian, J. Baltrusaitis, G. Rubasinghege, G. Cibin, A. Dent, *Sci. Rep.* **2012**, *2*, 880 – 885.

[45] X. Deng, L. Mammen, H.-J. Butt, D. Vollmer, *Science* **2012**, *335*, 67 – 70.

[46] J. Zhang, B. Li, L. Wu, A. Wang, *Chem. Commun.* **2013**, DOI: 10.1039/C1033CC43238F.

[47] C. Belgardt, E. Sowade, T. Blaudeck, T. Baumgartel, H. Graaf, C. von Borczyskowski, R. R. Baumann, *Phys. Chem. Chem. Phys.* **2013**, *15*, 7494 – 7504.

[48] B. M. Silverman, K. A. Wieghaus, J. Schwartz, *Langmuir* **2005**, *21*, 225 – 228.

[49] S. Marcinko, A. Y. Fadeev, *Langmuir* **2004**, *20*, 2270 – 2273.

[50] S. P. Pujari, Y. Li, R. Regeling, H. Zuilhof, *Langmuir* **2013**, *29*, 10405 – 10415.

[51] H. E. Ries, Jr., H. D. Cook, *J. Colloid Sci.* **1954**, *9*, 535 – 546.

[52] a) C. Queffélec, M. Petit, P. Janvier, D. A. Knight, B. Bujoli, *Chem. Rev.* **2012**, *112*, 3777 – 3807; b) A. Clearfield, K. Demadis, *Metal Phosphonate Chemistry*: *From Synthesis to Applications*, RSC, London, **2012**; c) K. J. Gagnon, H. P. Perry, A. Clearfield, *Chem. Rev.* **2012**, *112*, 1034 – 1054.

[53] P. Thissen, M. Valtiner, G. Grundmeier, *Langmuir* **2010**, *26*, 156 – 164.

[54] a) G. Guerrero, P. H. Mutin, A. Vioux, *J. Mater. Chem.* **2001**, *11*, 3161 – 3165; b) T. Hauffman, O. Blajiev, J. Snauwaert, C. van Haesendonck, A. Hubin, H. Terryn, *Langmuir* **2008**, *24*, 13450 – 13456; c) X. Chen, E. Luais, N. Darwish, S. Ciampi, P. Thordarson, J. J. Gooding, *Langmuir* **2012**, *28*, 9487 – 9495; d) R. Hofer, M. Textor, N. D. Spencer, *Langmuir* **2001**, *17*, 4014 – 4020.

[55] a) G. Cao, H. G. Hong, T. E. Mallouk, *Acc. Chem. Res.* **1992**, *25*, 420 – 427; b) P. G. Mingalyov, G. V. Lisichkin, *Russ. Chem. Rev.* **2006**, *75*, 541 – 557.

[56] a) E. L. Hanson, J. Schwartz, B. Nickel, N. Koch, M. F. Danisman, *J. Am. Chem. Soc.* **2003**, *125*, 16074 – 16080; b) A. Vega, P. Thissen, Y. J. Chabal, *Langmuir* **2012**, *28*, 8046 – 8051.

[57] H.-Y. Nie, M. J. Walzak, N. S. McIntyre, *J. Phys. Chem. B* **2006**, *110*, 21101 – 21108.

[58] H. Y. Nie, M. J. Walzak, N. S. McIntyre, *Langmuir* **2002**, *18*, 2955 – 2958.

[59] A. Bulusu, S. A. Paniagua, B. A. MacLeod, A. K. Sigdel, J. J. Berry, D. C. Olson, S. R. Marder, S. Graham, *Langmuir* **2013**, *29*, 3935 – 3942.

[60] a) P. Thissen, A. Vega, T. Peixoto, Y. J. Chabal, *Langmuir* **2012**, *28*, 17494 – 17505; b) S. Gupta, H. Gleskova, *Org. Electron.* **2013**, *14*, 354 – 361.

[61] N. Tsud, M. Yoshitake, *Surf. Sci.* **2007**, *601*, 3060 – 3066.

[62] a) P. H. Mutin, G. Guerrero, A. Vioux, *J. Mater. Chem.* **2005**, *15*, 3761 – 3768; b) P. J. Hotchkiss, S. C. Jones, S. A. Paniagua, A. Sharma, B. Kippelen, N. R. Armstrong, S. R. Marder, *Acc. Chem. Res.* **2012**, *45*, 337 – 346.

[63] G. Guerrero, P. H. Mutin, A. Vioux, *Chem. Mater.* **2001**, *13*, 4367 – 4373.

[64] M. Giza, P. Thissen, G. Grundmeier, *Langmuir* **2008**, *24*, 8688 – 8694.

[65] F. Brodard-Severac, G. Guerrero, J. Maquet, P. Florian, C. Gervais, P. H. Mutin, *Chem. Mater.* **2008**, *20*, 5191 – 5196.

[66] V. Lafond, C. Gervais, J. Maquet, D. Prochnow, F. Babonneau, P. H. Mutin, *Chem. Mater.* **2003**, *15*, 4098 – 4103.

[67] S. Pawsey, M. McCormick, S. De Paul, R. Graf, Y. S. Lee, L. Reven, H. W. Spiess, *J. Am. Chem. Soc.* **2003**, *125*, 4174 – 4184.

[68] N. Adden, L. J. Gamble, D. G. Castner, A. Hoffmann, G. Gross, H. Menzel, *Langmuir* **2006**, *22*, 8197 – 8204.

[69] S. A. Paniagua, P. J. Hotchkiss, S. C. Jones, S. R. Marder, A. Mudalige, F. S. Marrikar, J. E. Pemberton, N. R. Armstrong, *J. Phys. Chem. C* **2008**, *112*, 7809 – 7817.

[70] M. Gliboff, L. Sang, K. M. Knesting, M. C. Schalnat, A. Mudalige, E. L. Ratcliff, H. Li, A. K. Sigdel, A. J. Giordano, J. J. Berry, D. Nordlund, G. T. Seidler, J.-L. Brédas, S. R. Marder, J. E. Pemberton, D. S. Ginger, *Langmuir* **2013**, *29*, 2166 – 2174.

[71] E. Smecca, A. Motta, M. E. Fragalà, Y. Aleeva, G. G. Condorelli, *J. Phys. Chem. C* **2013**, *117*, 5364 – 5372.

[72] a) R. Michel, J. W. Lussi, G. Csucs, I. Reviakine, G. Danuser, B. Ketterer, J. A. Hubbell, M. Textor, N. D. Spencer, *Langmuir* **2002**, *18*, 3281 – 3287; b) H. Ma, O. Acton, D. O. Hutchins, N. Cernetic, A. K. Y. Jen, *Phys. Chem. Chem. Phys.* **2012**, *14*, 14110 – 14126; c) D. Liu, X. Xu, Y. Su, Z. He, J. Xu, Q. Miao, *Angew. Chem.* **2013**, *125*, 6342 – 6347; *Angew. Chem. Int. Ed.* **2013**, *52*, 6222 – 6227.

[73] N. Griep-Raming, M. Karger, H. Menzel, *Langmuir* **2004**, *20*, 11811 – 11814.

[74] M. de Los Reyes, P. J. Majewski, N. Scales, V. Luca, *ACS Appl. Mater. Interfaces* **2013**, *5*, 4120 – 4128.

[75] K. D. Demadis, M. Papadaki, R. G. Raptis, H. Zhao, *Chem. Mater.* **2008**, *20*, 4835 – 4846.

[76] W. O. Yah, A. Takahara, Y. M. Lvov, *J. Am. Chem. Soc.* **2012**, *134*, 1853 – 1859.

[77] a) R. Torres Martin de Rosales, R. Tavaré, R. L. Paul, M. Jauregui-Osoro, A. Protti, A. Glaria, G. Varma, I. Szanda, P. J. Blower, *Angew. Chem.* **2011**, *123*, 5623 – 5627; *Angew. Chem. Int. Ed.* **2011**, *50*, 5509 – 5513; b) K. E. Sapsford, W. R. Algar, L. Berti, K. B. Gemmill, B. J. Casey, E. Oh, M. H. Stewart, I. L. Medintz, *Chem. Rev.* **2013**, *113*, 1904 – 2074; c) R. Torres Martin de Rosales, R. Tavaré, A. Glaria, G. Varma, A. Protti, P. J. Blower, *Bioconjugate Chem.* **2011**, *22*, 455 – 465; d) I. Řehoř, V. Vilímová, P. Jendelová, V. c. Kubíček, D. Jirák,

Dateiname: A306709e
Pfad: L:/daten/Verlage/VCH/ACH/Hefte/1425/
Status Neusatz
Datum: 24 KW., 11. Juni 2014 (Mittwoch)

Pagina: 6352
Seite: 31 te von 35
Umfang (Seiten): 35
Zeit: 9:23:11 Uhr

V. t. Herynek, M. Kapcalová, J. Kotek, J. Černý, P. Hermann, I. Lukeš, *J. Med. Chem.* **2011**, *54*, 5185 – 5194.

[78] a) S. Mukherjee, C. Huang, F. Guerra, K. Wang, E. Oldfield, *J. Am. Chem. Soc.* **2009**, *131*, 8374 – 8375; b) S. Mukherjee, Y. Song, E. Oldfield, *J. Am. Chem. Soc.* **2008**, *130*, 1264 – 1273; c) D. Campoccia, L. Montanaro, C. R. Arciola, *Biomaterials* **2006**, *27*, 2331 – 2339.

[79] S.-H. Chang, J.-L. Han, S. Y. Tseng, H.-Y. Lee, C.-W. Lin, Y.-C. Lin, W.-Y. Jeng, A. H. J. Wang, C.-Y. Wu, C.-H. Wong, *J. Am. Chem. Soc.* **2010**, *132*, 13371 – 13380.

[80] a) Y. T. Tao, *J. Am. Chem. Soc.* **1993**, *115*, 4350 – 4358; b) G. A. Buckholtz, E. S. Gawalt, *Materials* **2012**, *5*, 1206 – 1218; c) D. L. Allara, R. G. Nuzzo, *Langmuir* **1985**, *1*, 52 – 66; d) D. L. Allara, R. G. Nuzzo, *Langmuir* **1985**, *1*, 45 – 52; e) J. P. Folkers, C. B. Gorman, P. E. Laibinis, S. Buchholz, G. M. Whitesides, R. G. Nuzzo, *Langmuir* **1995**, *11*, 813 – 824; f) N. E. Schlotter, M. D. Porter, T. B. Bright, D. L. Allara, *Chem. Phys. Lett.* **1986**, *132*, 93 – 98.

[81] G. E. Brown, V. E. Henrich, W. H. Casey, D. L. Clark, C. Eggleston, A. Felmy, D. W. Goodman, M. Grätzel, G. Maciel, M. I. McCarthy, K. H. Nealson, D. A. Sverjensky, M. F. Toney, J. M. Zachara, *Chem. Rev.* **1999**, *99*, 77 – 174.

[82] D. J. Miller, L. Sun, M. J. Walzak, N. S. McLntyre, D. Chvedov, A. Rosenfeld, *Surf. Interface Anal.* **2003**, *35*, 463 – 476.

[83] T. Bauer, T. Schmaltz, T. Lenz, M. Halik, B. Meyer, T. Clark, *ACS Appl. Mater. Interfaces* **2013**, *5*, 6073 – 6080.

[84] M. S. Lim, K. Feng, X. Chen, N. Wu, A. Raman, J. Nightingale, E. S. Gawalt, D. Korakakis, L. A. Hornak, A. T. Timperman, *Langmuir* **2007**, *23*, 2444 – 2452.

[85] a) I. V. Chernyshova, S. Ponnurangam, P. Somasundaran, *Langmuir* **2011**, *27*, 10007 – 10018; b) S. Ponnurangam, I. V. Chernyshova, P. Somasundaran, *Langmuir* **2012**, *28*, 10661 – 10671; c) K. Norén, P. Persson, *Geochim. Cosmochim. Acta* **2007**, *71*, 5717 – 5730.

[86] a) A. Raman, R. Quiñones, L. Barriger, R. Eastman, A. Parsi, E. S. Gawalt, *Langmuir* **2010**, *26*, 1747 – 1754; b) E. R. Garland, E. P. Rosen, L. I. Clarke, T. Baer, *Phys. Chem. Chem. Phys.* **2008**, *10*, 3156 – 3161.

[87] L. H. Dubois, B. R. Zegarski, R. G. Nuzzo, *Langmuir* **1986**, *2*, 412 – 417.

[88] A. Raman, E. S. Gawalt, *Langmuir* **2007**, *23*, 2284 – 2288.

[89] B. Kim, S. W. Park, J.-Y. Kim, K. Yoo, J. A. Lee, M.-W. Lee, D.-K. Lee, J. Y. Kim, B. Kim, H. Kim, S. Han, H. J. Son, M. J. Ko, *ACS Appl. Mater. Interfaces* **2013**, *5*, 5201 – 5207.

[90] Q. Qu, H. Geng, R. Peng, Q. Cui, X. Gu, F. Li, M. Wang, *Langmuir* **2010**, *26*, 9539 – 9546.

[91] a) J. Martz, L. Zuppiroli, F. Nüesch, *Langmuir* **2004**, *20*, 11428 – 11432; b) F. Nüesch, M. Carrara, L. Zuppiroli, *Langmuir* **2003**, *19*, 4871 – 4875.

[92] a) F. D. Fleischli, S. Suárez, M. Schaer, L. Zuppiroli, *Langmuir* **2010**, *26*, 15044 – 15049; b) A. von Mühlenen, N. Errien, M. Schaer, M.-N. Bussac, L. Zuppiroli, *Phys. Rev. B* **2007**, *75*, 115338.

[93] Y. G. Aronoff, B. Chen, G. Lu, C. Seto, J. Schwartz, S. L. Bernasek, *J. Am. Chem. Soc.* **1997**, *119*, 259 – 262.

[94] a) S. Pawsey, K. Yach, J. Halla, L. Reven, *Langmuir* **2000**, *16*, 3294 – 3303; b) G. G. Ting, O. Acton, H. Ma, J. W. Ka, A. K. Y. Jen, *Langmuir* **2009**, *25*, 2140 – 2147.

[95] a) K. D. Dobson, A. J. McQuillan, *Spectrochim. Acta Part A* **2000**, *56*, 557 – 565; b) P.-F. Guo, H.-B. Liu, X. Liu, H.-F. Li, W.-Y. Huang, S.-J. Xiao, *J. Phys. Chem. C* **2010**, *114*, 333 – 341; c) V. Zeleňák, Z. Vargová, K. Györyová, *Spectrochim. Acta Part A* **2007**, *66*, 262 – 272.

[96] P. Taheri, J. Wielant, T. Hauffman, J. R. Flores, F. Hannour, J. H. W. de Wit, J. M. C. Mol, H. Terryn, *Electrochim. Acta* **2011**, *56*, 1904 – 1911.

[97] J. J. Stapleton, D. L. Suchy, J. Banerjee, K. T. Mueller, C. G. Pantano, *ACS Appl. Mater. Interfaces* **2010**, *2*, 3303 – 3309.

[98] C.-P. Cho, Y.-T. Tao, *Langmuir* **2007**, *23*, 7090 – 7095.

[99] T. P. Brewster, S. J. Konezny, S. W. Sheehan, L. A. Martini, C. A. Schmuttenmaer, V. S. Batista, R. H. Crabtree, *Inorg. Chem.* **2013**, *52*, 6752 – 6764.

[100] L. A. Martini, G. F. Moore, R. L. Milot, L. Z. Cai, S. W. Sheehan, C. A. Schmuttenmaer, G. W. Brudvig, R. H. Crabtree, *J. Phys. Chem. C* **2013**, *117*, 14526 – 14533.

[101] L. M. Bishop, J. C. Yeager, X. Chen, J. N. Wheeler, M. D. Torelli, M. C. Benson, S. D. Burke, J. A. Pedersen, R. J. Hamers, *Langmuir* **2012**, *28*, 1322 – 1329.

[102] I. Carmeli, A. Lewin, E. Flekser, I. Diamant, Q. Zhang, J. Shen, M. Gozin, S. Richter, Y. Dagan, *Angew. Chem.* **2012**, *124*, 7274 – 7277; *Angew. Chem. Int. Ed.* **2012**, *51*, 7162 – 7165.

[103] E. D. Mentovich, B. Belgorodsky, I. Kalifa, S. Richter, *Adv. Mater.* **2010**, *22*, 2182 – 2186.

[104] a) S. Szillies, G. Grundmeier, D. Tabatabai, F. Feil, W. Fürbeth, N. Fink, P. Thissen, *Appl. Surf. Sci.* **2013**, *283*, 339 – 347; b) J. Zhang, J. Zhang, *Tribol. Lett.* **2013**, *49*, 77 – 83; c) C. Arisio, C. A. Cassou, M. Lieberman, *Langmuir* **2013**, *29*, 5145 – 5149; d) M. M. Islam, B. Diawara, P. Marcus, D. Costa, *Catal. Today* **2011**, *177*, 39 – 49.

[105] X. Fan, L. Lin, J. L. Dalsin, P. B. Messersmith, *J. Am. Chem. Soc.* **2005**, *127*, 15843 – 15847.

[106] Q. Ye, F. Zhou, W. Liu, *Chem. Soc. Rev.* **2011**, *40*, 4244 – 4258.

[107] C. E. Brubaker, P. B. Messersmith, *Langmuir* **2012**, *28*, 2200 – 2205.

[108] B. H. Kim, D. H. Lee, J. Y. Kim, D. O. Shin, H. Y. Jeong, S. Hong, J. M. Yun, C. M. Koo, H. Lee, S. O. Kim, *Adv. Mater.* **2011**, *23*, 5618 – 5622.

[109] a) H. Lee, S. M. Dellatore, W. M. Miller, P. B. Messersmith, *Science* **2007**, *318*, 426 – 430; b) H. Lee, *Nature* **2010**, *465*, 298 – 299; c) I. You, S. M. Kang, S. Lee, Y. O. Cho, J. B. Kim, S. B. Lee, Y. S. Nam, H. Lee, *Angew. Chem.* **2012**, *124*, 6230 – 6234; *Angew. Chem. Int. Ed.* **2012**, *51*, 6126 – 6130; d) S. M. Kang, I. You, W. K. Cho, H. K. Shon, T. G. Lee, I. S. Choi, J. M. Karp, H. Lee, *Angew. Chem.* **2010**, *122*, 9591 – 9594; *Angew. Chem. Int. Ed.* **2010**, *49*, 9401 – 9404.

[110] a) J. Sedó, J. Saiz-Poseu, F. Busqué, D. Ruiz-Molina, *Adv. Mater.* **2013**, *25*, 653 – 701; b) V. Ball, D. Del Frari, M. Michel, M. J. Buehler, V. Toniazzo, M. K. Singh, J. Gracio, D. Ruch, *Bionanoscience* **2012**, *2*, 16 – 34; c) E. Faure, C. Falentin-Daudré, C. Jérôme, J. Lyskawa, D. Fournier, P. Woisel, C. Detrembleur, *Prog. Polym. Sci.* **2013**, *38*, 236 – 270; d) B. P. Lee, P. B. Messersmith, J. N. Israelachvili, J. H. Waite, *Annu. Rev. Mater. Res.* **2011**, *41*, 99 – 132.

[111] a) M. J. Sever, J. T. Weisser, J. Monahan, S. Srinivasan, J. J. Wilker, *Angew. Chem.* **2004**, *116*, 454 – 456; *Angew. Chem. Int. Ed.* **2004**, *43*, 448 – 450; b) M. J. Harrington, A. Masic, N. Holten-Andersen, J. H. Waite, P. Fratzl, *Science* **2010**, *328*, 216 – 220.

[112] M. Guvendiren, D. A. Brass, P. B. Messersmith, K. R. Shull, *J. Adhes.* **2009**, *85*, 631 – 645.

[113] See Ref. [110b].

[114] a) T. H. Anderson, J. Yu, A. Estrada, M. U. Hammer, J. H. Waite, J. N. Israelachvili, *Adv. Funct. Mater.* **2010**, *20*, 4196 – 4205; b) J. Yu, W. Wei, M. S. Menyo, A. Masic, J. H. Waite, J. N. Israelachvili, *Biomacromolecules* **2013**, *14*, 1072 – 1077.

[115] a) B. Malisova, S. Tosatti, M. Textor, K. Gademann, S. Zürcher, *Langmuir* **2010**, *26*, 4018 – 4026; b) M. Rodenstein, S. Zürcher, S. G. P. Tosatti, N. D. Spencer, *Langmuir* **2010**, *26*, 16211 – 16220.

[116] Y. Wang, I. Zhitomirsky, *J. Colloid Interface Sci.* **2012**, *380*, 8 – 15.

[117] Y. Yang, W. Yan, C. Jing, *Langmuir* **2012**, *28*, 14588 – 14597.

Dateiname: A306709e
Pfad: L:/daten/Verlage/VCH/ACH/Hefte/1425/
Status Neusatz
Datum: 24 KW., 11. Juni 2014 (Mittwoch)

Pagina: 6353
Seite: 32 te von 35
Umfang (Seiten): 35
Zeit: 9:23:11 Uhr

[118] N. Lee, D. R. Hummer, D. A. Sverjensky, T. Rajh, R. M. Hazen, A. Steele, G. D. Cody, *Langmuir* **2012**, *28*, 17322 – 17330.
[119] E. Amstad, A. U. Gehring, H. Fischer, V. V. Nagaiyanallur, G. Hähner, M. Textor, E. Reimhult, *J. Phys. Chem. C* **2011**, *115*, 683 – 691.
[120] a) S. J. Hurst, H. C. Fry, D. J. Gosztola, T. Rajh, *J. Phys. Chem. C* **2011**, *115*, 620 – 630; b) P. Tarakeshwar, D. Finkelstein-Shapiro, S. J. Hurst, T. Rajh, V. Mujica, *J. Phys. Chem. C* **2011**, *115*, 8994 – 9004; c) A. Musumeci, D. Gosztola, T. Schiller, N. M. Dimitrijevic, V. Mujica, D. Martin, T. Rajh, *J. Am. Chem. Soc.* **2009**, *131*, 6040 – 6041.
[121] a) J. L. Dalsin, L. Lin, S. Tosatti, J. Vörös, M. Textor, P. B. Messersmith, *Langmuir* **2005**, *21*, 640 – 646; b) G. S. Tulevski, Q. Miao, M. Fukuto, R. Abram, B. Ocko, R. Pindak, M. L. Steigerwald, C. R. Kagan, C. Nuckolls, *J. Am. Chem. Soc.* **2004**, *126*, 15048 – 15050.
[122] R. Rodríguez, M. A. Blesa, A. E. Regazzoni, *J. Colloid Interface Sci.* **1996**, *177*, 122 – 131.
[123] Q. Chen, Y. Jia, S. Liu, G. Mogilevsky, A. Kleinhammes, Y. Wu, *J. Phys. Chem. C* **2008**, *112*, 17331 – 17335.
[124] H. Lee, N. F. Scherer, P. B. Messersmith, *Proc. Natl. Acad. Sci. USA* **2006**, *103*, 12999 – 13003.
[125] S.-C. Li, J.-g. Wang, P. Jacobson, X. Q. Gong, A. Selloni, U. Diebold, *J. Am. Chem. Soc.* **2009**, *131*, 980 – 984.
[126] S.-C. Li, L.-N. Chu, X.-Q. Gong, U. Diebold, *Science* **2010**, *328*, 882 – 884.
[127] S. Verma, P. Kar, A. Das, D. K. Palit, H. N. Ghosh, *Chem. Eur. J.* **2010**, *16*, 611 – 619.
[128] a) J. Hoecker, R. Liffert, P. Burch, R. Wehlauch, K. Gademann, *Org. Biomol. Chem.* **2013**, *11*, 3314 – 3321; b) R. Wehlauch, J. Hoecker, K. Gademann, *ChemPlusChem* **2012**, *77*, 1071 – 1074; c) E. Amstad, J. Kohlbrecher, E. Müller, T. Schweizer, M. Textor, E. Reimhult, *Nano Lett.* **2011**, *11*, 1664 – 1670; d) Z. Shafiq, J. Cui, L. Pastor-Pérez, V. San Miguel, R. A. Gropeanu, C. Serrano, A. del Campo, *Angew. Chem.* **2012**, *124*, 4408 – 4411; *Angew. Chem. Int. Ed.* **2012**, *51*, 4332 – 4335.
[129] a) T. Gillich, C. Acikgöz, L. Isa, A. D. Schlüter, N. D. Spencer, M. Textor, *ACS Nano* **2013**, *7*, 316 – 329; b) T. Gillich, E. M. Benetti, E. Rakhmatullina, R. Konradi, W. Li, A. Zhang, A. D. Schlüter, M. Textor, *J. Am. Chem. Soc.* **2011**, *133*, 10940 – 10950.
[130] a) J. Gomes, A. Grunau, A. K. Lawrence, L. Eberl, K. Gademann, *CHIMIA Int. J. Chem.* **2013**, *67*, 275 – 278; b) S. Zürcher, D. Wäckerlin, Y. Bethuel, B. Malisova, M. Textor, S. Tosatti, K. Gademann, *J. Am. Chem. Soc.* **2006**, *128*, 1064 – 1065.
[131] a) D. Dahlhaus, S. Franzka, E. Hasselbrink, N. Hartmann, *Nano Lett.* **2006**, *6*, 2358 – 2361; b) T. Balgar, S. Franzka, N. Hartmann, *Appl. Phys. A* **2006**, *82*, 689 – 695; c) H. Urch, S. Franzka, D. Dahlhaus, N. Hartmann, E. Hasselbrink, M. Epple, *J. Mater. Chem.* **2006**, *16*, 1798 – 1802; d) B. Klingebiel, L. Scheres, S. Franzka, H. Zuilhof, N. Hartmann, *Langmuir* **2010**, *26*, 6826 – 6831; e) L. Scheres, B. Klingebiel, J. t. Maat, M. Giesbers, H. de Jong, N. Hartmann, H. Zuilhof, *Small* **2010**, *6*, 1918 – 1926.
[132] a) M. Rosso, M. Giesbers, A. Arafat, K. Schroën, H. Zuilhof, *Langmuir* **2009**, *25*, 2172 – 2180; b) M. Rosso, A. Arafat, K. Schroen, M. Giesbers, C. S. Roper, R. Maboudian, H. Zuilhof, *Langmuir* **2008**, *24*, 4007 – 4012; c) A. Arafat, K. Schroën, L. C. P. M. de Smet, E. J. R. Sudhölter, H. Zuilhof, *J. Am. Chem. Soc.* **2004**, *126*, 8600 – 8601.
[133] a) F. Roccaforte, F. La Via, V. Raineri, P. Musumeci, L. Calcagno, G. G. Condorelli, *Appl. Phys. A* **2003**, *77*, 827 – 833; b) U. Starke, *Phys. Status Solidi B* **1997**, *202*, 475 – 499.
[134] J. ter Maat, R. Regeling, M. Yang, M. N. Mullings, S. F. Bent, H. Zuilhof, *Langmuir* **2009**, *25*, 11592 – 11597.
[135] T. K. Mischki, R. L. Donkers, B. J. Eves, G. P. Lopinski, D. D. M. Wayner, *Langmuir* **2006**, *22*, 8359 – 8365.
[136] B. Li, R. Franking, E. C. Landis, H. Kim, R. J. Hamers, *ACS Appl. Mater. Interfaces* **2009**, *1*, 1013 – 1022.
[137] R. Franking, E. C. Landis, R. J. Hamers, *Langmuir* **2009**, *25*, 10676 – 10684.
[138] R. Franking, H. Kim, S. A. Chambers, A. N. Mangham, R. J. Hamers, *Langmuir* **2012**, *28*, 12085 – 12093.
[139] R. Franking, R. J. Hamers, *J. Phys. Chem. C* **2011**, *115*, 17102 – 17110.
[140] a) Y. Li, H. Zuilhof, *Langmuir* **2012**, *28*, 5350 – 5359; b) Y. Li, M. Giesbers, M. Gerth, H. Zuilhof, *Langmuir* **2012**, *28*, 12509 – 12517.
[141] R. E. Ruther, R. Franking, A. M. Huhn, J. Gomez-Zayas, R. J. Hamers, *Langmuir* **2011**, *27*, 10604 – 10614.
[142] R. J. Hamers, S. A. Chambers, P. E. Evans, R. Franking, Z. Gerbec, P. Gopalan, H. Kim, E. C. Landis, B. Li, M. W. McCoy, T. Ohsawa, R. Ruther, *Phys. Status Solidi C* **2010**, *7*, 200 – 205.
[143] a) M. C. Benson, R. E. Ruther, J. B. Gerken, M. L. Rigsby, L. M. Bishop, Y. Tan, S. S. Stahl, R. J. Hamers, *ACS Appl. Mater. Interfaces* **2011**, *3*, 3110 – 3119; b) S. Shah, M. C. Benson, L. M. Bishop, A. M. Huhn, R. E. Ruther, J. C. Yeager, Y. Tan, K. M. Louis, R. J. Hamers, *J. Mater. Chem.* **2012**, *22*, 11561 – 11567.
[144] S. U. Schwarz, V. Cimalla, G. Eichapfel, M. Himmerlich, S. Krischok, O. Ambacher, *Langmuir* **2013**, *29*, 6296 – 6301.
[145] J. M. Alonso, A. K. Trilling, L. Scheres, M. C. R. Franssen, H. Zuilhof, unpublished results.
[146] S. P. Pujari, L. Scheres, B. van Lagen, H. Zuilhof, *Langmuir* **2013**, *29*, 10393 – 10404.
[147] a) L. Scheres, M. Giesbers, H. Zuilhof, *Langmuir* **2010**, *26*, 4790 – 4795; b) L. Scheres, M. Giesbers, H. Zuilhof, *Langmuir* **2010**, *26*, 10924 – 10929; c) A. Ng, S. Ciampi, M. James, J. B. Harper, J. J. Gooding, *Langmuir* **2009**, *25*, 13934 – 13941.
[148] M. Giesbers, A. T. M. Marcelis, H. Zuilhof, *Langmuir* **2013**, *29*, 4782 – 4788.
[149] J. ter Maat, R. Regeling, C. J. Ingham, C. A. G. M. Weijers, M. Giesbers, W. M. de Vos, H. Zuilhof, *Langmuir* **2011**, *27*, 13606 – 13617.
[150] S. P. Pujari, L. Scheres, T. Weidner, J. E. Baio, M. A. C. Stuart, C. J. M. van Rijn, H. Zuilhof, *Langmuir* **2013**, *29*, 4019 – 4031.
[151] A. Debrassi, A. Ribbera, W. M. de Vos, T. Wennekes, H. Zuilhof, *Langmuir* **2014**, *30*, 1311 – 1320.
[152] a) T. Vong, J. ter Maat, T. A. van Beek, B. van Lagen, M. Giesbers, J. C. M. van Hest, H. Zuilhof, *Langmuir* **2009**, *25*, 13952 – 13958; b) T. Vong, S. Schoffelen, S. F. M. van Dongen, T. A. van Beek, H. Zuilhof, J. C. M. van Hest, *Chem. Sci.* **2011**, *2*, 1278 – 1285.
[153] E. Faure, E. Halusiak, F. Farina, N. Giamblanco, C. Motte, M. Poelman, C. Archambeau, C. Van De Weerdt, J. Martial, C. Jérôme, A.-S. Duwez, C. Detrembleur, *Langmuir* **2012**, *28*, 2971 – 2978.
[154] S. Chen, L. Li, C. Zhao, J. Zheng, *Polymer* **2010**, *51*, 5283 – 5293.
[155] a) E. M. Sletten, C. R. Bertozzi, *Angew. Chem.* **2009**, *121*, 7108 – 7133; *Angew. Chem. Int. Ed.* **2009**, *48*, 6974 – 6998; b) R. Manova, T. A. van Beek, H. Zuilhof, *Angew. Chem.* **2011**, *123*, 5540 – 5542; *Angew. Chem. Int. Ed.* **2011**, *50*, 5428 – 5430.
[156] a) A. Calloni, A. Brambilla, G. Berti, G. Bussetti, E. V. Canesi, M. Binda, A. Petrozza, M. Finazzi, F. Ciccacci, L. Duò, *Langmuir* **2013**, *29*, 8302 – 8310; b) E. V. Canesi, M. Binda, A. Abate, S. Guarnera, L. Moretti, V. D'Innocenzo, R. S. S. Kumar, C. Bertarelli, A. Abrusci, H. Snaith, A. Calloni, A. Brambilla, F. Ciccacci, S. Aghion, F. Moia, R. Ferragut, C. Melis, G. Malloci, A. Mattoni, G. Lanzani, A. Petrozza, *Energy Environ. Sci.* **2012**, *5*, 9068 – 9076.
[157] J. J. Benítez, S. Kopta, D. F. Ogletree, M. Salmeron, *Langmuir* **2002**, *18*, 6096 – 6100.
[158] J. J. Benítez, S. Kopta, I. Díez-Pérez, F. Sanz, D. F. Ogletree, M. Salmeron, *Langmuir* **2003**, *19*, 762 – 765.

Dateiname: A306709e
Pfad: L:/daten/Verlage/VCH/ACH/Hefte/1425/
Status Neusatz
Datum: 24 KW., 11. Juni 2014 (Mittwoch)

Pagina: 6354
Seite: 33 te von 35
Umfang (Seiten): 35
Zeit: 9:23:11 Uhr

[159] I. V. Chernyshova, K. H. Rao, A. Vidyadhar, A. V. Shchukarev, *Langmuir* **2000**, *16*, 8071 – 8084.
[160] J. J. Benítez, M. A. San-Miguel, S. Domínguez-Meister, J. A. Heredia-Guerrero, M. Salmeron, *J. Phys. Chem. C* **2011**, *115*, 19716 – 19723.
[161] S. Gangarapu, A. T. M. Marcelis, H. Zuilhof, *ChemPhysChem* **2012**, *13*, 3973 – 3980.
[162] Y. Feng, S. Chen, J. You, W. Guo, *Electrochim. Acta* **2007**, *53*, 1743 – 1753.
[163] a) K. F. Khaled, N. Hackerman, *Mater. Chem. Phys.* **2003**, *82*, 949 – 960; b) C. Jeyaprabha, S. Sathiyanarayanan, G. Venkatachari, *Appl. Surf. Sci.* **2005**, *246*, 108 – 116.
[164] N. Belman, K. Jin, Y. Golan, J. N. Israelachvili, N. S. Pesika, *Langmuir* **2012**, *28*, 14609 – 14617.
[165] F. Xu, K. Chen, R. D. Piner, C. A. Mirkin, J. E. Ritchie, J. T. McDevitt, M. O. Cannon, D. Kanis, *Langmuir* **1998**, *14*, 6505 – 6511.
[166] J. Zhu, C. A. Mirkin, R. M. Braun, N. Winograd, *J. Am. Chem. Soc.* **1998**, *120*, 5126 – 5127.
[167] S. Hosseinpour, J. Hedberg, S. Baldelli, C. Leygraf, M. Johnson, *J. Phys. Chem. C* **2011**, *115*, 23871 – 23879.
[168] Ž. Petrović, M. Metikoš-Huković, R. Babić, *Prog. Org. Coat.* **2008**, *61*, 1 – 6.
[169] J. Chen, R. E. Ruther, Y. Tan, L. M. Bishop, R. J. Hamers, *Langmuir* **2012**, *28*, 10437 – 10445.
[170] J. Denayer, J. Delhalle, Z. Mekhalif, *J. Electrochem. Soc.* **2011**, *158*, P100 – P108.
[171] T. Tüken, N. Kıcır, N. T. Elalan, G. Sığırcık, M. Erbil, *Appl. Surf. Sci.* **2012**, *258*, 6793 – 6799.
[172] A. Ikegami, M. Suda, T. Watanabe, Y. Einaga, *Angew. Chem.* **2010**, *122*, 382 – 384; *Angew. Chem. Int. Ed.* **2010**, *49*, 372 – 374.
[173] J. Chen, R. Franking, R. E. Ruther, Y. Tan, X. He, S. R. Hogendoorn, R. J. Hamers, *Langmuir* **2011**, *27*, 6879 – 6889.
[174] P. Paoprasert, S. Kandala, D. P. Sweat, R. Ruther, P. Gopalan, *J. Mater. Chem.* **2012**, *22*, 1046 – 1053.
[175] B. Chatterjee, *Coord. Chem. Rev.* **1978**, *26*, 281 – 303.
[176] J. Yang, P. J. Bremer, I. L. Lamont, A. J. McQuillan, *Langmuir* **2006**, *22*, 10109 – 10117.
[177] a) W. R. McNamara, R. C. Snoeberger III, G. Li, C. Richter, L. J. Allen, R. L. Milot, C. A. Schmuttenmaer, R. H. Crabtree, G. W. Brudvig, V. S. Batista, *Energy Environ. Sci.* **2009**, *2*, 1173 – 1175; b) W. R. McNamara, R. L. Milot, H.-e. Song, R. C. Snoeberger III, V. S. Batista, C. A. Schmuttenmaer, G. W. Brudvig, R. H. Crabtree, *Energy Environ. Sci.* **2010**, *3*, 917 – 923; c) M. Hemgesberg, S. Schütz, C. Müller, M. Schlörholz, H. Latzel, Y. Sun, C. Ziegler, W. R. Thiel, *Appl. Surf. Sci.* **2012**, *259*, 406 – 415.
[178] A. Agarwala, T. Subramani, A. Goldbourt, D. Danovich, R. Yerushalmi, *Angew. Chem.* **2013**, *125*, 7563 – 7566; *Angew. Chem. Int. Ed.* **2013**, *52*, 7415 – 7418.
[179] N. Millot, A. Cox, C. C. Santini, Y. Molard, J.-M. Basset, *Chem. Eur. J.* **2002**, *8*, 1438 – 1442.
[180] Y.-J. Wanglee, J. Hu, R. E. White, M.-Y. Lee, S. M. Stewart, P. Perrotin, S. L. Scott, *J. Am. Chem. Soc.* **2012**, *134*, 355 – 366.
[181] a) N. A. LaFranzo, J. A. Maurer, *Adv. Funct. Mater.* **2013**, *23*, 2415 – 2421; b) R. Yerushalmi, J. C. Ho, Z. Fan, A. Javey, *Angew. Chem.* **2008**, *120*, 4512 – 4514; *Angew. Chem. Int. Ed.* **2008**, *47*, 4440 – 4442; c) C. Zhou, G. Nagy, A. V. Walker, *J. Am. Chem. Soc.* **2005**, *127*, 12160 – 12161; d) C. C. A. Ng, A. Magenau, S. H. Ngalim, S. Ciampi, M. Chockalingham, J. B. Harper, K. Gaus, J. J. Gooding, *Angew. Chem.* **2012**, *124*, 7826 – 7830; *Angew. Chem. Int. Ed.* **2012**, *51*, 7706 – 7710; e) I. Kaminska, W. Qi, A. Barras, J. Sobczak, J. Niedziolka-Jonsson, P. Woisel, J. Lyskawa, W. Laure, M. Opallo, M. Li, R. Boukherroub, S. Szunerits, *Chem. Eur. J.* **2013**, *19*, 8673 – 8678; f) I. Levine, S. M. Weber, Y. Feldman, T. Bendikov, H. Cohen, D. Cahen, A. Vilan, *Langmuir* **2012**, *28*, 404 – 415; g) D. Zigah, C. Herrier, L. Scheres, M. Giesbers, B. Fabre, P. Hapiot, H. Zuilhof, *Angew. Chem.* **2010**, *122*, 3225 – 3228; *Angew. Chem. Int. Ed.* **2010**, *49*, 3157 – 3160; h) W. Li, B. J. Worfolk, P. Li, T. C. Hauger, K. D. Harris, J. M. Buriak, *J. Mater. Chem.* **2012**, *22*, 11354 – 11363; i) G. Dubey, F. Rosei, G. P. Lopinski, *Chem. Commun.* **2011**, *47*, 10593 – 10595.
[182] K. R. Williams, K. Gupta, M. Wasilik, *J. Microelectromech. Syst.* **2003**, *12*, 761 – 778.
[183] a) S. A. A. Ahmad, L. S. Wong, E. ul-Haq, J. K. Hobbs, G. J. Leggett, J. Micklefield, *J. Am. Chem. Soc.* **2009**, *131*, 1513 – 1522; b) J. J. Cras, C. A. Rowe-Taitt, D. A. Nivens, F. S. Ligler, *Biosens. Bioelectron.* **1999**, *14*, 683 – 688.
[184] H. Han, J. Wu, C. W. Avery, M. Mizutani, X. Jiang, M. Kamigaito, Z. Chen, C. Xi, K. Kuroda, *Langmuir* **2011**, *27*, 4010 – 4019.
[185] H. Lee, K. D. Lee, K. B. Pyo, S. Y. Park, H. Lee, *Langmuir* **2010**, *26*, 3790 – 3793.
[186] S. Dhar, O. Seitz, M. D. Halls, S. Choi, Y. J. Chabal, L. C. Feldman, *J. Am. Chem. Soc.* **2009**, *131*, 16808 – 16813.
[187] D. K. Bhowmick, S. Linden, A. Devaux, L. De Cola, H. Zacharias, *Small* **2012**, *8*, 592 – 601.
[188] M. Auernhammer, S. J. Schoell, M. Sachsenhauser, K. C. Liao, J. Schwartz, I. D. Sharp, A. Cattani-Scholz, *Appl. Phys. Lett.* **2012**, *100*, 101601 – 101604.
[189] a) See Ref. [150]; b) A. Dey, C. J. van den Hoogen, M. Rosso, N. Lousberg, M. M. R. M. Hendrix, H. Friedrich, J. Ramírez-Rico, H. Zuilhof, G. de With, N. A. J. M. Sommerdijk, *ChemPlusChem* **2012**, *77*, 694 – 699.
[190] A. M. M. Jani, I. M. Kempson, D. Losic, N. H. Voelcker, *Angew. Chem.* **2010**, *122*, 8105 – 8109; *Angew. Chem. Int. Ed.* **2010**, *49*, 7933 – 7937.
[191] L. N. Mitchon, J. M. White, *Langmuir* **2006**, *22*, 6549 – 6554.
[192] G. Tzvetkov, G. Koller, Y. Zubavichus, O. Fuchs, M. B. Casu, C. Heske, E. Umbach, M. Grunze, M. G. Ramsey, F. P. Netzer, *Langmuir* **2004**, *20*, 10551 – 10559.
[193] W. O. Yah, H. Xu, H. Soejima, W. Ma, Y. Lvov, A. Takahara, *J. Am. Chem. Soc.* **2012**, *134*, 12134 – 12137.
[194] A. G. Thomas, K. L. Syres, *Chem. Soc. Rev.* **2012**, *41*, 4207 – 4217.
[195] a) H. J. Martin, K. H. Schulz, J. D. Bumgardner, K. B. Walters, *Langmuir* **2007**, *23*, 6645 – 6651; b) G. Zorn, J. E. Baio, T. Weidner, V. Migonney, D. G. Castner, *Langmuir* **2011**, *27*, 13104 – 13112.
[196] a) J. Das, C.-H. Huh, K. Kwon, S. Park, S. Jon, K. Kim, H. Yang, *Langmuir* **2009**, *25*, 235 – 241; b) V. M. Bermudez, A. D. Berry, H. Kim, A. Piqué, *Langmuir* **2006**, *22*, 11113 – 11125.
[197] a) M. Chockalingam, N. Darwish, G. Le Saux, J. J. Gooding, *Langmuir* **2011**, *27*, 2545 – 2552; b) M. Gliboff, H. Li, K. M. Knesting, A. J. Giordano, D. Nordlund, G. T. Seidler, J.-L. Brédas, S. R. Marder, D. S. Ginger, *J. Phys. Chem. C* **2013**, *117*, 15139 – 15147.
[198] T. J. Gardner, C. D. Frisbie, M. S. Wrighton, *J. Am. Chem. Soc.* **1995**, *117*, 6927 – 6933.
[199] C. E. J. Cordonier, A. Nakamura, K. Shimada, A. Fujishima, *Langmuir* **2011**, *27*, 3157 – 3165.
[200] W. Guo, J. Zhu, Z. Cheng, Z. Zhang, X. Zhu, *ACS Appl. Mater. Interfaces* **2011**, *3*, 1675 – 1680.
[201] A. Raman, M. Dubey, I. Gouzman, E. S. Gawalt, *Langmuir* **2006**, *22*, 6469 – 6472.
[202] C.-M. Ruan, T. Bayer, S. Meth, C. N. Sukenik, *Thin Solid Films* **2002**, *419*, 95 – 104.
[203] M. Anil, M. J. Dave, N. P. Devang, D. F. Marc, A. A. Arturo, A. C. Mauli, *Nanomed. Nanotech. Biol. Med.* **2006**, *2*, 182 – 190.
[204] M. L. Manesse, R. Sanjines, V. Stambouli, C. Jorel, B. Pelissier, M. Pisarek, R. Boukherroub, S. Szunerits, *Langmuir* **2009**, *25*, 8036 – 8041.

Dateiname: A306709e
Pfad: L:/daten/Verlage/VCH/ACH/Hefte/1425/
Status Neusatz
Datum: 24 KW., 11. Juni 2014 (Mittwoch)

Pagina: 6355
Seite: 34te von 35
Umfang (Seiten): 35
Zeit: 9:23:11 Uhr

[205] R. De Palma, W. Laureyn, F. Frederix, K. Bonroy, J.-J. Pireaux, G. Borghs, G. Maes, *Langmuir* **2007**, *23*, 443 – 451.
[206] D. Costenaro, F. Carniato, G. Gatti, C. Bisio, L. Marchese, *J. Phys. Chem. C* **2011**, *115*, 25257 – 25265.
[207] F. H. Li, J. D. Fabbri, R. I. Yurchenko, A. N. Mileshkin, J. N. Hohman, H. Yan, H. Yuan, I. C. Tran, T. M. Willey, M. Bagge-Hansen, J. E. P. Dahl, R. M. K. Carlson, A. A. Fokin, P. R. Schreiner, Z.-X. Shen, N. A. Melosh, *Langmuir* **2013**, *29*, 9790 – 9797.
[208] S. Pasche, S. M. De Paul, J. Vörös, N. D. Spencer, M. Textor, *Langmuir* **2003**, *19*, 9216 – 9225.

Dateiname: A306709e
Pfad: L:/daten/Verlage/VCH/ACH/Hefte/1425/
Status Neusatz
Datum: 24 KW., 11. Juni 2014 (Mittwoch)

Pagina: 6356
Seite: 35 te von 35
Umfang (Seiten): 35
Zeit: 9:23:12 Uhr